Dyes and Pigments

Highly efficient unbridged D-A+(D) chromophores based on the quinolizinium cation for nonlinear optical (NLO) applications

--Manuscript Draft--

Manuscript Number:	DYPI-D-21-02182R2
Article Type:	Research paper
Keywords:	quinolizinium cation; D-A+(D) unbridged chromophores; nonlinear optical application; first hyperpolarizability
Corresponding Author:	Ana M. Cuadro Alcala University Madrid, Alcala de Henares Spain
First Author:	Ana M. Cuadro, Prof. Dr.
Order of Authors:	Ana M. Cuadro, Prof. Dr.
	Esmeralda Sánchez-Pavón, Dr.
	Javier Recio, Dr.
	Marco Antonio Ramirez, Dr.
	Belen Batanero, Prof. Dr.
	Koen Clays, Prof. Dr.
	Francisco Mendicuti, Prof. Dr.
	Gema Marcelo, Dr.
	Thais Carmona, Dr.
	Obis Castaño, Prof. Dr.
	Silvia Angelova, Dr.
	Jose L. Andres, Dr.
	Juan J. Vaquero, Prof. Dr.
Abstract:	Novel charged D-A + chromophores based on quinolizinium cations as acceptor unit have been prepared by treating haloquinolizinium salts with N -heteroarylstannanes under Stille reaction conditions. This approach provides an easy access to potential one-dimensional D-A + and two-dimensional D-A + -D chromophores in which the acceptor moiety (A +) is the simple azonia cation and the donors are different π-rich N -heterocycles. The first hyperpolarizabilities (β) were measured by hyper-Rayleigh scattering experiments and the experimental data confirmed that the inherent polarization between donor and acceptor fragments modulates the NLO properties. The electronic structures and properties (including both the linear and nonlinear optical properties) of the quinolizinium chromophores were examined by theoretical (DFT, HF and MP2) calculations. A promising strategy for the rational design of D-A building blocks to create new organic-based NLO materials is proposed.
Suggested Reviewers:	Jürgen Heck, Prof. University of Hamburg: Universitat Hamburg juergen.heck@chemie.uni-hamburg.de Expert in: Organic Synthesis -Pd chemistry/Nonlinear optical materials /materials and nanochemistry/Theoretical Chemistry
	Javier Perez-Moreno, Prof. Skidmore College jperezmo@skidmore.edu Expert in: theoretical and experimental data from nonlinear organic molecules/ Applycation sum rules to interpret experimental data from nonlinear molecules
	Bouchata Shahraoui, Prof.

	Université d'Angers: Universite d'Angers bouchta.sahraoui@univ-angers.fr Expert in: Photonics, Nanophotonics, Nonlinear Optical and Energy Applications.
Response to Reviewers:	

Universidad de Alcalá

DEPARTAMENTO DE QUIMICA ORGANICA
Y QUIMICA INORGANICA
Ctra. Madrid – Barcelona, km. 33,600
28871 Alcalá de Henares (Madrid)
Telf.: (91) 885 46 28
Fax. : (91) 885 46 86
e-mail: ana.cuadro@uah.es

ELSEVIER

Professor B.M. Heron
Editor, Dyes and Pigments
University of Huddersfield,
Huddersfield, UK

Subject: Manuscript submission to Dyes & Pigments

Dear Prof. Heron,

On behalf of my co-authors and myself, I would like to submit the manuscript entitled ***"Highly efficient unbridged D-A+ (D) chromophores based on quinolizinium cation for nonlinear optical (NLO) applications"***, for consideration for publication as a regular Research Article in Dyes & Pigments. The present study investigates the role of the quinolizinium as acceptor unit in simple charged dipolar chromophores, directly connected to electron donor (D) unit(s) that generates D-A$^+$ and D-A$^+$-D unbridged chromophores. The results surprisingly reveal that the absence of a bridge between the donor and acceptor fragments enhances and modulates NLO properties by inherent polarization between donor and acceptor, and provide an attractive strategy in guiding the design of new NLO materials. An absolutely new generation of second-order nonlinear materials with enhanced first hyperpolarizability can be based on the quinolizinium systems. The promising performance of the proposed quinolizinium cation based D-A+(D) unbridged chromophores has a potential for stimulating further research and discussion on D-A- building blocks in organic–based materials.

Being fundamental in its essence, this work has a high translational potential. The results presented in the manuscript are expected to impact the design of new materials and appeal to the broad and multidisciplinary audience of Dyes & Pigments.

This work has not been submitted for publication nor has been published in whole or in part elsewhere.

All authors have seen and approved the submission of the manuscript.

Sincerely,

Prof. Ana M. Cuadro

(corresponding author)

06-April-2022

Professor Denis Jacquemin
Editor
Dyes and Pigments

Manuscript Number: DYPI-D-21-02182R1
TITLE: Highly efficient unbridged D-A+(D) chromophores based on the quinolizinium cation for nonlinear optical (NLO) applications

Dear Prof. Jacquemin,

Thank you very much for your message.

Thank you for giving us the opportunity to submit a revised draft (R2) of our manuscript. We appreciate the time and effort that you and the reviewers have dedicated to providing your valuable feedback on my manuscript. Revised manuscript file which addresses the Reviewer 1' additional comments is submitted. Please, find below the Reviewer 1' comments repeated in *italics* and point-by-point responses inserted after each comment. The changes/additions are in blue. Page numbers refer to the revised (R2) manuscript.

In addition, I would like to include a brief dedication to Prof. Dr. Carolina Burgos, who recently passed away.

Reviewer #1

Reviewer #1: In general, the authors tried to give convincing replies and complements to the point raised in my initial report. Regarding my first point, the sentence which mentions that "cationic acceptors were introduced only recently" sounded like a little weird and approximative statement to me, although it is true that, contrary to what I told, pyridinium derivatives were clearly mentioned in the text. Sorry for that!

The same goes for the number of carbons of compound 5f, I totally realized that the Cs point group to which it belongs should give 25 shifts for the carbon, but I probably looked at the wrong line when counting (probably that of 6b) because I remember thinking that only half of the carbon were reported. For 6b, however, when I mention "11 C founds while 12 are expected" I am actually taking into account the fact that two C are pseudo-isochrones, as only 10 chemical shifts are reported.

Authors' reply: For the described product **6b**, 10 signals are reported in the 13C-NMR spectrum. However, 11 signals should be seen, since two of the carbons are pseudo-isochrones. This last carbon, which was not reported by mistake, has a chemical shift of 117.7 ppm. Although it cannot be observed in the usual ^{13}C spectrum, it is perfectly observable in the HMBC experiment, where the protons located in positions 1 and 3 provide an additional correlation with a signal at 117.7 ppm. Additionally, the broad signal

corresponding to the hydrogen nuclei of the pyrazole ring shows a single correlation with this same signal at 117.7ppm.

These data, together with the high-resolution mass experiments and elemental analysis, provide additional evidence to conclude that compound **6b**, is indeed, the molecule described.

All this evidence can be seen below and has been entered into the ESI.

^{1}H NMR (500 MHz, DMSO)

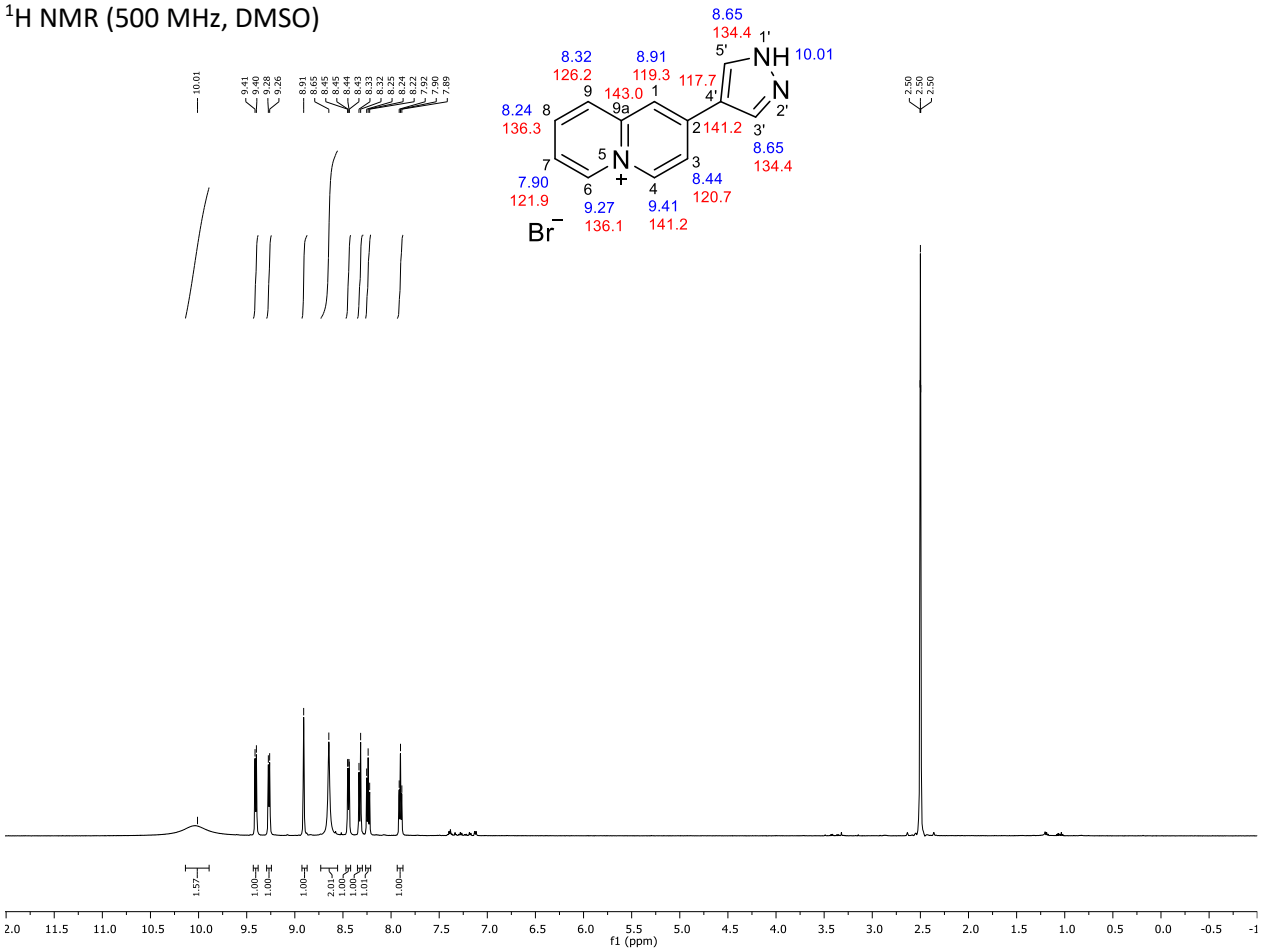

^{13}C NMR (126 MHz, DMSO)

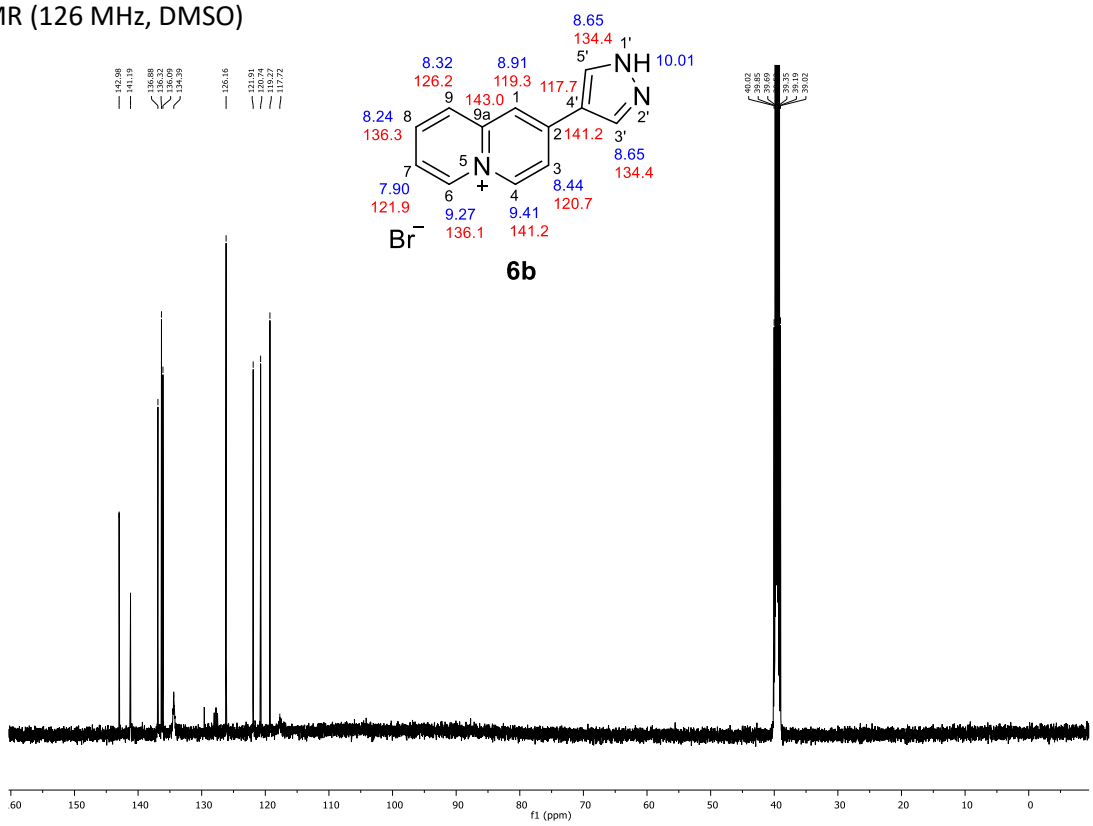

gCOSY NMR (500 MHz, DMSO)

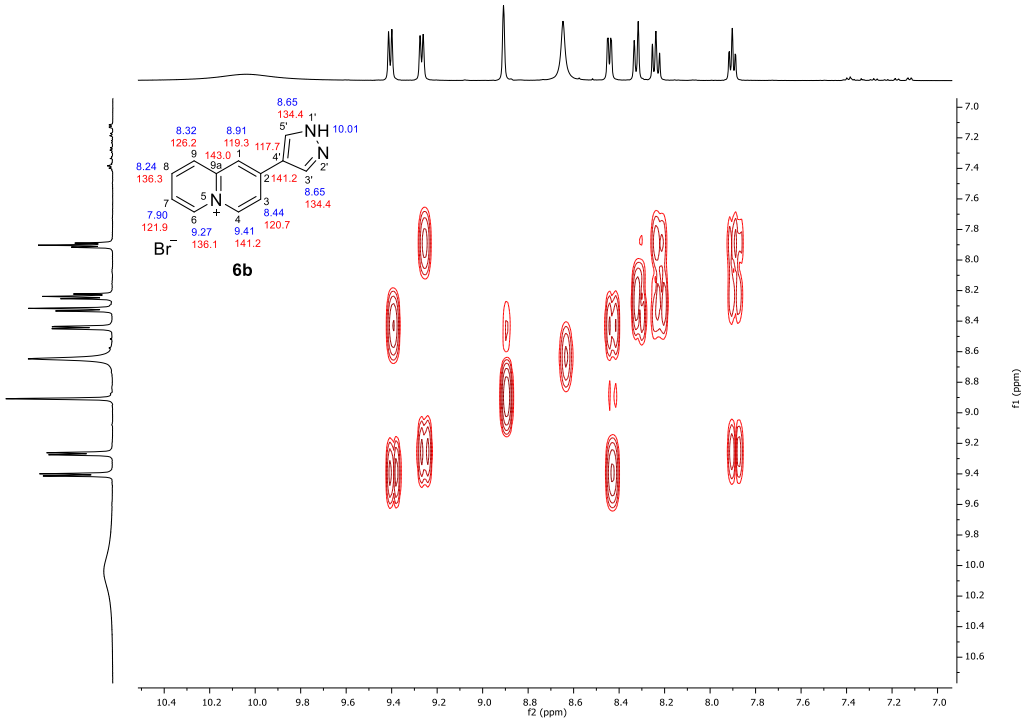

TOCSY NMR (500 MHz, DMSO)

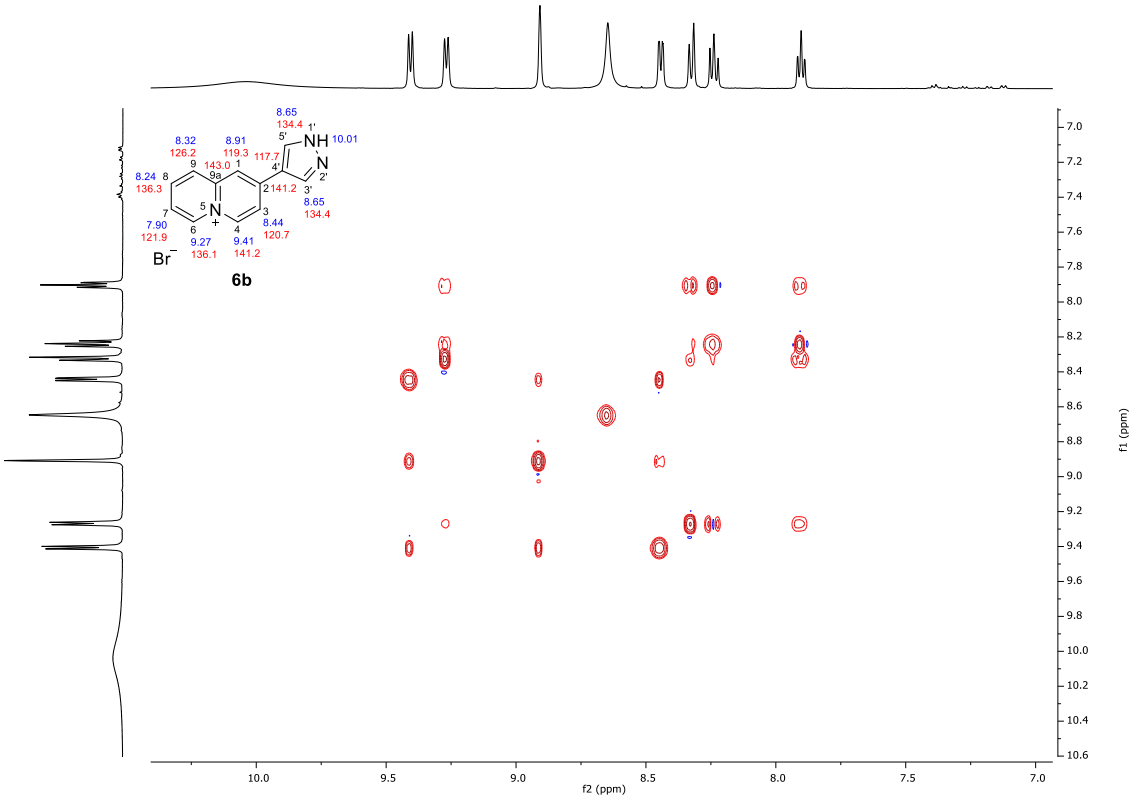

gHSQC NMR (500 MHz, DMSO)

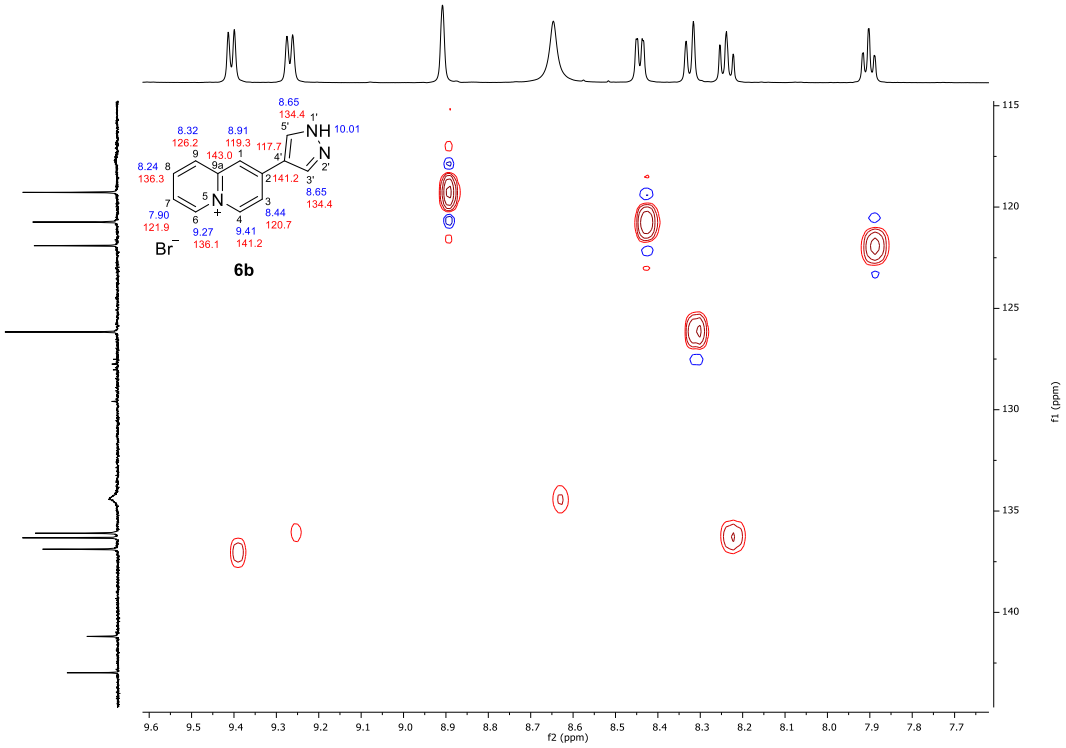

gHMBC NMR (500 MHz, DMSO)

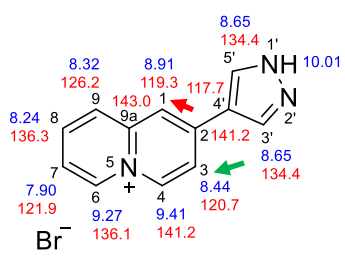

6b

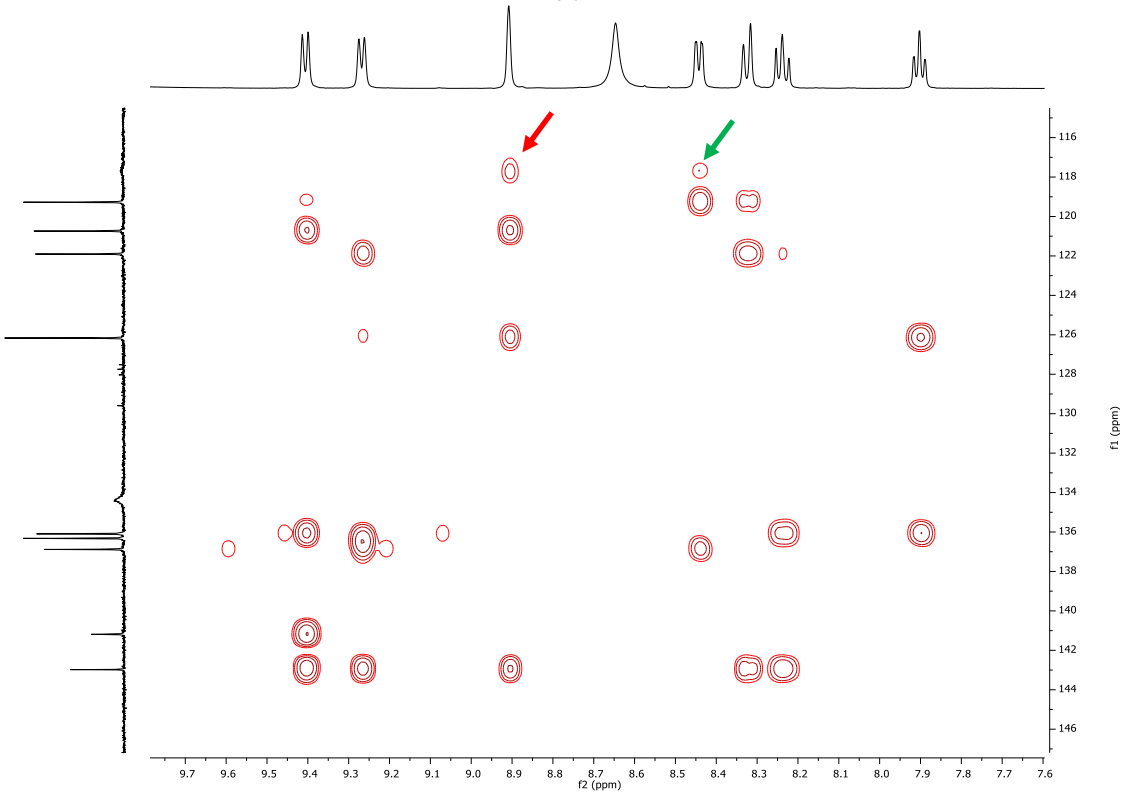

gHMBC RMR (in detail) (500 MHz, DMSO)

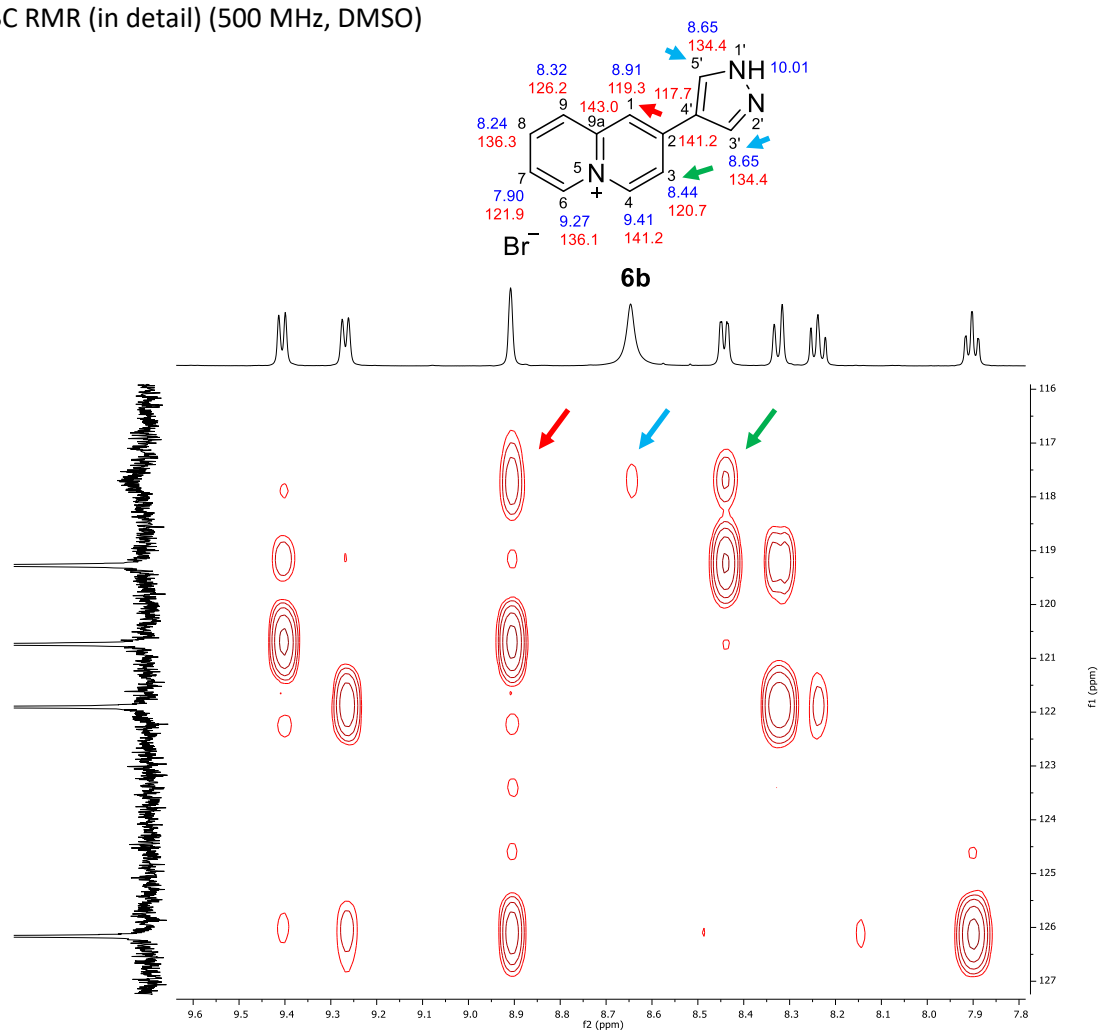

Regarding the calculations of kr and knr the authors are right. Yet, from the reported data, it is not clear whether significant differences are found between the short and long lifetimes and to what extent each participate in the calculated weighed lifetime (if the short one has a negligible contribution, it could perhaps be neglected). Globally, one can question the interest in providing these weighed lifetime values in the manuscript if almost nothing is concluded from those.

Authors' reply: Based on the analysis of the fluorescence intensity decay profiles, it is clear to us that two lifetime components were observed and that the short one cannot be disregarded without considerably increasing the chi-square. The short component cannot be attributed to the scattering of the sample solutions either. Furthermore, the contributions of the fast components to the weighted average lifetimes for most of the compounds are similar or even larger than the slow ones.

We agree that not much information can be gained from the collected weighted average lifetimes, but we believe that a photophysical study should always include lifetimes or weighted average lifetimes, even if we cannot rationalize the results.

"Disubstituted cationic quinolizinium systems (D-A+-D) are expected to have lower βHRS values than for theirmonosubstituted counterparts (D-A+): second order optical nonlinearity in organic compounds derives from a highly polarizable charge asymmetry of a π-conjugated system capped with groups of different electron affinities (D and A). "
I perfectly agree with that

"This is true for the 2c/5c, 2f/5f, 6d/7d couples, but not for other compounds" .The theoretically predicted β values for these couples follow the trend"
The problem, precisely, is that theoretical calculations nicely match theoretical predictions, but that measurements appear in 2 out of the 5 cases where comparison is possible in stark contraction : when comparing compound 7b and 6b (and not only the betaHRS but also the betazero) and also 5b and 2b.

This is not necessarily a problem that can be easily addressed, but the claim that theory and experimental values are in good agreement and that "Both theoretical approaches (HF and MP2) used to compute the first hyperpolarizabilities in this study reproduce the trends in the experimental βHRS data presented in Table 5 reasonably well, except for compounds 2a and 2d, the values of which are more strongly underestimate" is in my opinion wrong because if it was the case, it should be possible, based on these calculations to provide a reasonable explanation to the "exception to the rules" which is not the case here. Where it becomes more problematic is that the conclusions use these calculated values to claim the superiority of the reported systems to existing ones "Indeed, the βHRS values predicted at the MP2 level for a model pyrrole-substituted cationic quinolizinium system (2c, Table 7, Figure S3) are higher (βHRS,800 =100×10−30 esu) than those calculated for a model 2-methylpyridinium (B), 3-methylpyridinium(C) and 4-methylpyridinium cationic system (D) (βHRS,800 values of 32×10−30, 29×10−30 and66×10−30 esu, respectively)" which, given the observed experimental discrepancies measured here seems very optimistic and not fully supported

This does not, however, precludes publication in D&P but conclusions should be more balanced and exceptions/surprising trends clearly mentioned in the discussion

Authors' reply: We agree with the reviewer that the theory did not fully succeed in predicting the experimental β_{HRS} values of the series of differently substituted protected/unprotected compounds and some discrepancies remain unexplained. To compare the model pyrrole-substituted cationic quinolizinium and 4-methylpyridinium cationic systems is not so problematic because of the structural similarity of the systems. As suggested by the Reviewer, the text has been modified (p.27 and pp.32-33) to reflect the discrepancies between theory and experiment. We thank the reviewer for pointing this out.

Highly efficient unbridged D-A$^+$(D) chromophores based on the quinolizinium cation for nonlinear optical (NLO) applications

Esmeralda Sánchez-Pavón,[a†] Javier Recio,[a♯] Marco Antonio Ramirez,[a≠] Belen Batanero,[a] Koen Clays,[b] Francisco Mendicuti,[c] Gema Marcelo,[c] Thais Carmona,[c±] Obis Castaño,[c] Silvia Angelova,[c‡] Jose L. Andres,[d] Juan J. Vaquero[a*] and Ana M. Cuadro[a*]

Research highlights

- Quinolizinium cation is efficient acceptor unit in new D-A$^+$ and D-A$^+$(D) unbridged chromophores.
- Inherent polarization between donor and acceptor fragments modulates NLO properties.
- The *N*-protecting groups in the heterocyclic donors strongly affect the β_{HRS} values.
- Quinolizinium systems in comparison with pyridinium ones appear to perform better in terms of NLO properties.
- Valuable hints for the rational design of D-A building blocks with potential application in NLO devices.

Graphical Abstract

Highly efficient unbridged D-A$^+$(D) chromophores based on the quinolizinium cation for nonlinear optical (NLO) applications

Esmeralda Sánchez-Pavón,[a†] Javier Recio,[a#] Marco Antonio Ramirez,[a≠] Belen Batanero,[a] Koen Clays,[b] Francisco Mendicuti,[c] Gema Marcelo,[c] Thais Carmona,[c±] Obis Castaño,[c] Silvia Angelova,[c‡] Jose L. Andres,[d] Juan J. Vaquero[a]* and Ana M. Cuadro[a]*

Quinolozinium cation as a new efficient acceptor unit in D-A$^+$ and D-A$^+$-D unbridged chromophores with different π-excessive *N*-heterocycles is proposed. Experimental and theoretical data confirm that inherent polarization between donor and acceptor fragments modulates NLO properties.

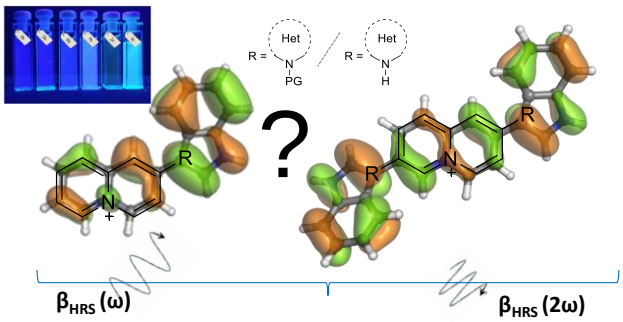

Highly efficient unbridged D-A^{+}(D) chromophores based on the quinolizinium cation for nonlinear optical (NLO) applications

Esmeralda Sánchez-Pavón,[a†] Javier Recio,[a♯] Marco Antonio Ramirez,[a≠] Belen Batanero,[a] Koen Clays,[b] Francisco Mendicuti,[c] Gema Marcelo,[c] Thais Carmona,[c±] Obis Castaño,[c] Silvia Angelova,[c‡] Jose L. Andres,[d] Juan J. Vaquero[a*] and Ana M. Cuadro[a*]

[a] Departamento de Química Orgánica y Química Inorgánica, Universidad de Alcalá, (IRYCIS); 28871-Alcalá de Henares, Madrid, Spain

[b] Department of Chemistry, University of Leuven, Celestijnenlaan 200 D,3001 Leuven, Belgium

[c] Departamento de Química Analítica, Química Física e Ingeniería Química, Universidad de Alcalá, 28871 Alcalá de Henares, Madrid, Spain

[d] IES Matarraña, 44580 Valderrobres, Teruel, Spain

[†] E. Sanchez-Pavon (permanent address): Facultad de Ciencias Químicas UV, Orizaba, Mexico

[♯] J. Recio (current address): Centro de Investigaciones Biológicas Margarita Salas-CSIC, 28040, Madrid, Spain

[≠] M.A. Ramirez (permanent address): Departamento de Farmacia, Universidad de Guanajuato, Mexico

± T. Carmona (permanent address): Center for the Development of Nanoscience and Technology (CEDENNA), Universidad de Santiago de Chile, 9170022 Santiago de Chile

[‡] S. Angelova (permanent address): Institute of Optical Materials and Technologies, Bulgarian Academy of Sciences, 1113, Sofia, Bulgaria

* Corresponding author: Ana M. Cuadro, e-mail: ana.cuadro@uah.e

Dedicated to the memory of Prof. Dr. Carolina Burgos

Abstract: Novel charged D-A$^+$ chromophores based on quinolizinium cations as acceptor unit have been prepared by treating haloquinolizinium salts with *N*-heteroarylstannanes under Stille reaction conditions. This approach provides an easy access to potential one-dimensional D-A$^+$ and two-dimensional D-A$^+$-D chromophores in which the acceptor moiety (A$^+$) is the simple azonia cation and the donors are different π-rich *N*-heterocycles. The first hyperpolarizabilities (β) were measured by hyper-Rayleigh scattering experiments and the experimental data confirmed that the inherent polarization between donor and acceptor fragments modulates the NLO properties. The electronic structures and properties (including both the linear and nonlinear optical properties) of the quinolizinium chromophores were examined by theoretical (DFT, HF and MP2) calculations. A promising strategy for the rational design of D-A building blocks to create new organic-based NLO materials is proposed.

Keywords: quinolizinium cation, D-A$^+$(D) unbridged chromophores, nonlinear optical application, first hyperpolarizability

Graphical abstract:

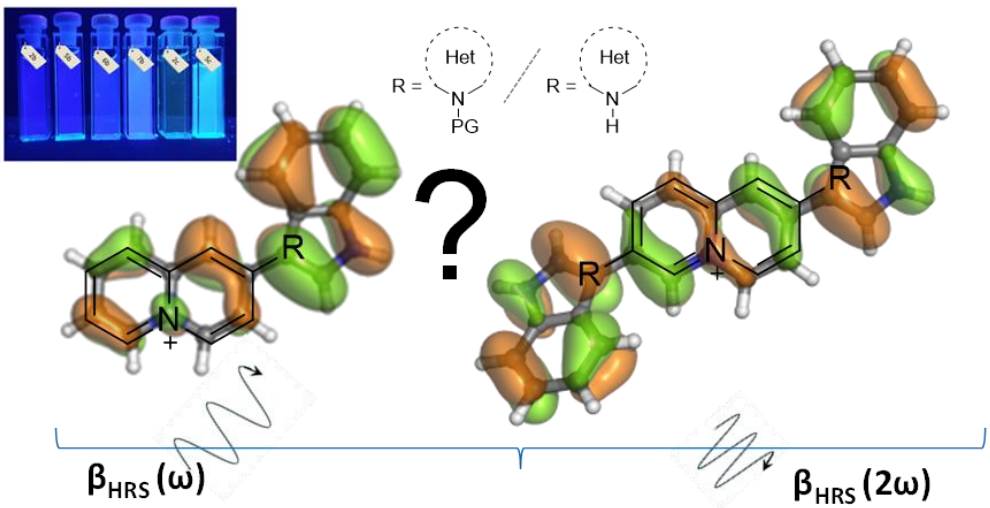

Research highlights

- Quinolizinium cation is efficient acceptor unit in new D-A$^+$ and D-A$^+$(D) unbridged chromophores
- Inherent polarization between donor and acceptor fragments modulates NLO properties
- The N-protecting groups in the heterocyclic donors strongly affect the β_{HRS} values
- Quinolizinium systems in comparison with pyridinium ones appear to perform better in terms of NLO properties
- Valuable hints for the rational design of D-A building blocks with potential application in NLO devices

1. Introduction

In recent years, the design and synthesis of conjugated donor-acceptor (D-A) organic molecules with nonlinear optical (NLO) [1] properties has been of considerable interest due to their applications in areas such as optoelectronics [2], all-optical data processing [3], biological imaging [4], dye-sensitized solar cells [5] and photodynamic therapy [6], amongst others, as well as for the understanding [7] of the structural requirements needed to achieve large second-order polarizabilities, related to an electronic intramolecular charge transfer (ICT) effect [8], excellent thermal and chemical stabilities [9] and easy tuning of the D-A properties for various applications [10].

Although a wide range of materials has been studied over the past few decades, the cationic acceptors have only recently been introduced. Amongst the cationic chromophores reported, charged acceptor units are restricted to benzothiazolium [11] and azinium salts [12]. The latter have received significant attention as 1D(D-π-A$^+$) and 2D(D-π-A$^+$-π-D) pyridinium-based chromophores, including DAST(4-(N,N-dimethylamino)-4´-N´-methylstilbazolium tosylate) /DSTMS(4-N,N´-dimethylamino-4´-N´-methylstilbazolium-2,4,6-trimethyl benzenesulfonate) [13] and diquats/helquats [14] for the design of stable redox-active organic materials (ROMs),

switching materials and chiral NLO chromophores [15]. However, azonia aromatic heterocycles (AZAH) [16] have not been explored to date as an acceptor unit, except by us, as a marker in nonlinear optical bioimaging, where they were found to exhibit a large two-photon absorption (2PA), and as push-pull cationic chromophores (D-π-A+-π-D) [17]. Furthermore, some derivatives of these azonia salts have been found to be useful in important applications, for example as highly fluorescent lysosomotropic probes and photosensitizer [18] (Figure 1).

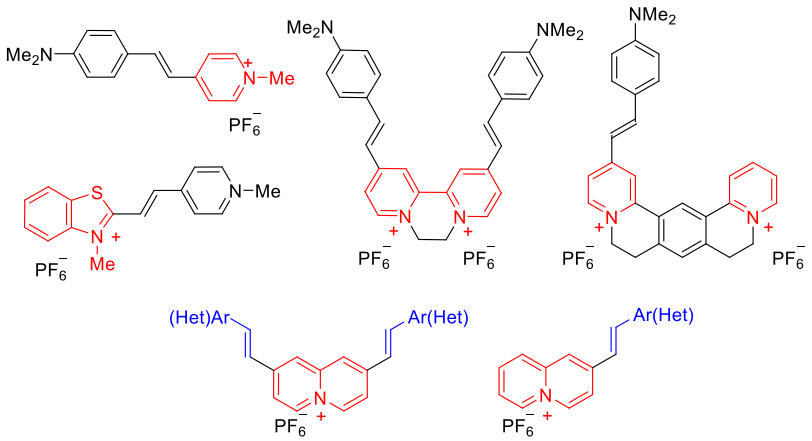

Figure 1. Representative examples of nonlinear optical chromophores based on azolium, pyridinium and quinolizinium cations as acceptor units.

As a result of our research on the applications of heteroaromatic cations in the NLO field [19], we recently showed that chromophores generated by direct coupling of a quinolizinium fragment to an aryl donor [19a] or a pyridinium cation to a π-rich heterocycle [19b], a kind of molecule that rarely appears in the NLO literature [20], may exhibit better nonlinear optical properties than other heteroaromatic cations tested to date, such as azinium [21] and azolium [22] salts. When connected directly, these chromophores have been shown to be useful for guiding the design of new NLO materials, thus contributing to the development of new β enhancement strategies [23] as alternatives to traditional π-conjugated chromophores in applications for nonlinear optical materials.

Herein we report the synthesis of a series of dipolar D-A$^+$ and quadrupolar D-A$^+$-D charged chromophores (Figure 2), which are synthesized by way of a Stille cross-coupling reaction

[24], to give push-pull molecules that combine quinolizinium cations as acceptor units (A^+) with π-rich N-heterocycles as donor units to achieve higher polarizability.

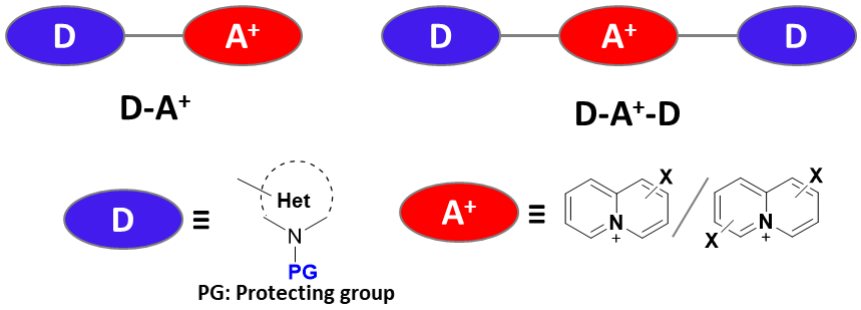

Figure 2. D–A^+(D) chromophores created by coupling a quinolizinium-based π-deficient charged heteroaromatic cation to a π-rich heteroarenes

From literature is known that the absence of a conjugated bridge ensures a higher chemical stability with respect to standard D-π-A systems [20b], and the introduction of multiple D units gives rise to multi-dimensional (MD) structures that can offer increased β responses by extending the charge transfer to higher dimensions. The photophysical properties of the resulting D-A+ and D-A+-D chromophores were studied by means of UV-visible and hyper-Rayleigh scattering (HRS) spectroscopy, as well as by performing quantum-chemical calculations at different levels of theory, including density functional theory (DFT), Hartree-Fock (HF) and post-HF ab initio methods (MP2). In addition, the redox activity was evaluated by cyclic voltammetry and the results of the theoretical calculations were compared with those obtained for known pyridinium-based systems to illustrate the influence of quinolizinium as acceptor unit and to establish the relevant structure-activity relationships.

2. Results and Discussion

2.1. Synthesis

Chromophores with the general structure D-A^+ (Figure 2) were synthesised starting from 2-bromoquinolizinium (**1**) using previously described conditions for palladium-promoted coupling reactions with quinolizinium salts [25], adapted and optimized for **1** using two

different catalytic systems, namely palladium tetrakis(triphenylphosphine)/copper iodide [$Pd(PPh_3)_4$/CuI] (Method A) or tri(ortho-tolyl)phosphine/tris(dibenzylideneacetone) dipalladium [$Pd_2(dba)_3$/P(*o*-Tol)$_3$] (Method B), both in DMF as solvent. Initially, starting from **1** and 3-tributylstannanyl-(toluen-4-sulfonyl)-1*H*-indole, with $Pd(PPh_3)_4$ (5% mol) and CuI as co-catalyst (10% mol) in DMF (Method **A**), the coupled compound **2a** was obtained in 97% yield after 4 h at 70 °C (Scheme 1). As such, method **A** was applied to produce a variety of coupling products (Table 1). The data collected showed that conditions **A** lead to the corresponding coupling products (**2a-j**) in good yields (except for ferrocenylstannanes Fc-$SnBu_3$ [26]). Compounds 2**f** and **2i** (entries 6 in Table 1, and entry 9 Table S1 in SI) were therefore synthesised using Method **B**, in good yields.

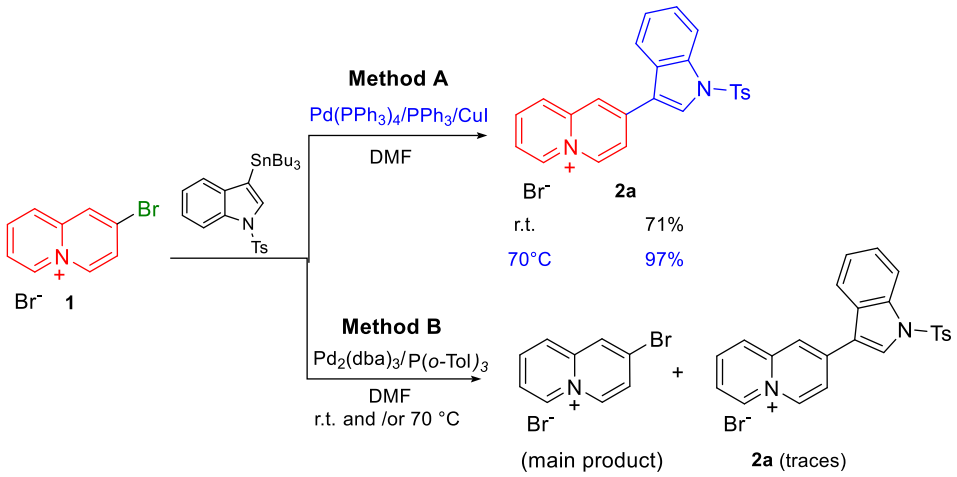

Scheme 1. Stille reaction of 2-bromoquinolizinium with heteroarylstannanes

The coupling with stannane pyrrole and indole derivatives, protected with TIPS (entry 3) and TBDMS (entry 6), respectively, led to coupling products **2c** and **2f,** respectively, with loss of the protecting groups.

Coupling with electron-deficient pyrazine, pyrimidine and pyridine stannanes proved possible without protecting the NH_2 group, obtaining moderate to good yields (see SI, Table S1, compounds **2g**, **2h**, **2i**).

In light of the approach outlined in the introduction and considering the results of the couplings to afford D-A$^+$ chromophores, we examined the coupling of 2,7-dibromo quinolizinium (**3**) with similar stannanes under Stille reaction conditions, using Methods **A** or **B**, to synthesise the D-A$^+$-D chromophores.

The study of reactivity of **3** with tributylstannylpyrazole was carried out first using one equivalent of stannane and $Pd(PPh_3)_4$/CuI as catalyst in DMF (Method **A**). Under these conditions, after 22 h at 70 °C, mono-coupling at the C-2 position furnished product **4b** along with unreacted starting material. Subsequently, coupling with 2-2.5 equivalents of tributylstannanyl-1-trityl-1*H*-pyrazole, under the reaction conditions outlined above, afforded di-coupling product **5b** in 52% yield (Scheme 3), although under these conditions the mono-coupling product **4b** was also formed. An evaluation of the process with all stannanes (2-2.5 equiv.), using methods **A** and **B**, can be found in Table 2.

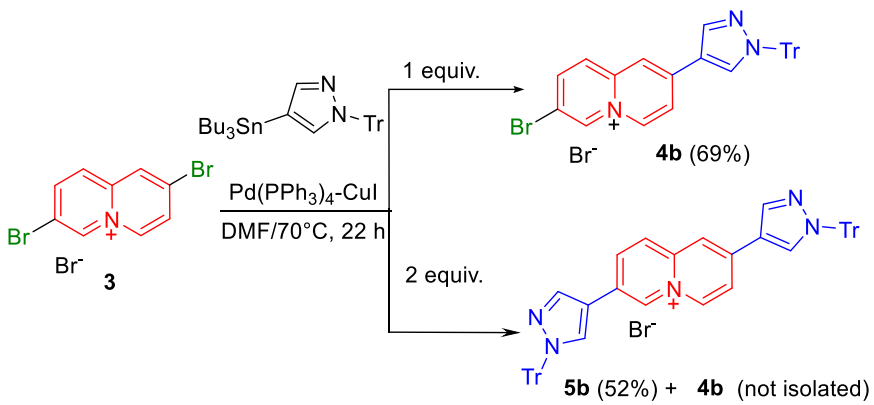

Scheme 2. Stille reaction of 2,7-bromoquinolizinium with heteroarylstannanes.

Based on the results, it should be noted that, generally, when protected tributylstannylpyrrol (R = TMS or TIPS) was used in a temperature range of 70-75 °C for 8 or 24 h, a mixture of mono-coupling product **4c** (not isolated) and di-coupling product **5c** (61%), with removal of the protecting group, was observed by ^{1}H NMR spectroscopy.

Table 1. Stille reaction of 2-Bromoquinolizinium salt

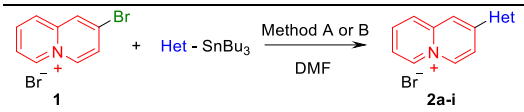

Table 2. Stille reaction of 2,7-Bromo quinolizinium salt

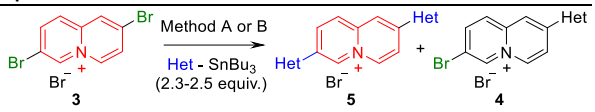

Entry	Het-SnBu3	Mono-coupling Product 2	Reac. Conds. Meth/T(°C)/ t(h)	Yield (%)	Di-coupling product 5	Reac. Conds. T(°C)/t(h)/Meth/ equiv. Het-SnBu3	Yield % 5	Yield % 4
1	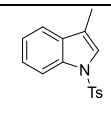	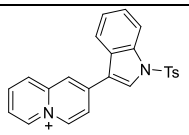 **2a**	**A**/70 /4	97				
2	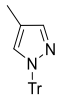	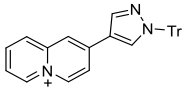 **2b**	**A**/65 /8	94[1]	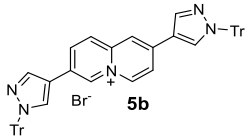 **5b**	70 /22/ **A**/1 70 /22/ **A**/2	69	52
3		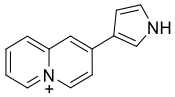 **2c**	**A**/70 /24	74[1]	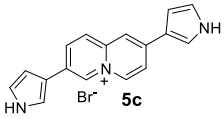 **5c**	70-75/8 or 24/**A**/2.3	61 (R=H))	
4	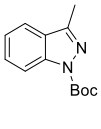	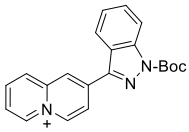 **2d**	**A**/r.t/24	70	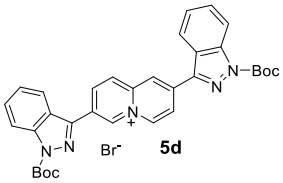 **5d**	70 /24/**A**/2.3 rt /7/**A**/2.3	15 30	13 25
5	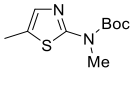	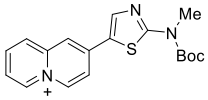 **2e**	**A**/r.t/24	93	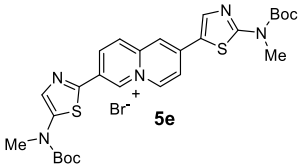 **5e**	70 /22/**A**/2.8	36	
6	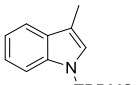	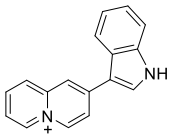 **2f**	**B**/75 /20	(X^-= Br) 94	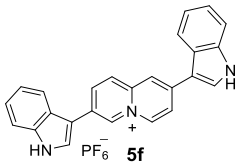 **5f**	70 /24/**B**/2.5	(X^-= Br^-) 60	

TMS: Trimethylsilyl; TIPS: Triisopropylsilyl; TBS: tert-Butyldimethylsilyl; Tr: Trityl; Boc: tert-Butoxycarbonyl; Ts: Tosyl.
Table 1. Method A: $Pd(PPh_3)_4$/CuI/rt or 70 °C/DMF; Method B: $Pd_2(dba)_3$/P(*o*-Tol)$_3$/70-75 °C/DMF.
Table 2. Method A: $Pd(PPh_3)_4$/CuI/rt or 70-75 °C/DMF; Method B: $Pd_2(dba)_3$/P(*o*-Tol)$_3$/75 °C/DMF.

The coupling reaction between **3** and stannylindazole at room temperature for 7 h afforded **5d** and **4d** (30% and 25%, respectively). This result is in agreement with the conditions applied for the coupling between **1** and tributylstannylindazole, for which the best results were obtained at room temperature (see Table 1, entry 5). Under standard conditions, the coupling of **3** with

the tributylstannylthiazole derivative (entry 4, Table 2) leads to the di-coupling compound **5e** in 36% yield as the only product.

The coupling of **3** with tributylstannylindole (entry 5, Table 2), protected as the TBDMS derivative, using the catalytic system [$Pd_2(dba)_3$/P(o-Tol)$_3$] in DMF at 70 °C for 24 h, gave **5f** (deprotected) in 60% yield (Table 2, entry 5). Under these reaction conditions, indole deprotection is observed as in the case for pyrrole.

In light of these results for the coupling reactions of 2-bromoquinolizinium **1** and 2,7-dibromoquinolizinium **3** with different stannanes (Table 1 and 2), we were unable to establish a relationship between the nature of the stannane and the reaction yields (medium or high) because of the low solubility of the coupling compounds in common organic solvents. Another obstacle was the difficulties encountered during the purification process as the mono- and di-coupled systems have similar *Rf* (retention factor) values, with both being lower than for the starting compound **3**.

Finally, having obtained unprotected quinolizinium derivatives D-A$^+$ (**2c, 2f**) and D-A$^+$-D (**5c**, **5f**) directly upon loss of the protecting group during Stille coupling with pyrrole and indole, we then investigated the reaction conditions for deprotection of chromophores **2b**(Tr), **2d**(Boc), **5b**(Tr) and **5d**(Boc) (Scheme 3 and SI), with the aim of analyzing the effect of the presence/absence of a protecting group on the linear and nonlinear optical properties of 1D and 2D chromophores (see Figure 5 and/or Figure 8).

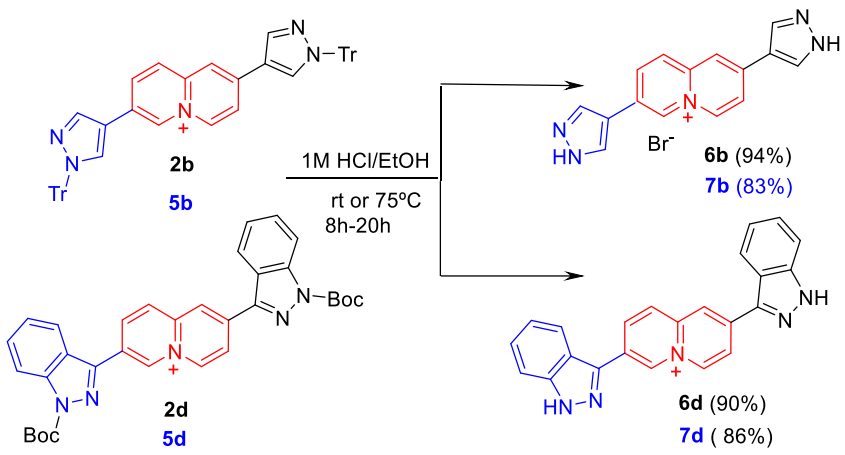

Scheme 3. Reaction conditions for unprotected chromophores

The isolation of functionalized unprotected quinolizinium systems will allow us to direct our research towards generating structures with high charge delocalization between the two rings upon abstraction of a proton from the donor group, thus generating a heterobetainic system as a new organic material. As mentioned above, most of the hyperpolarizability studies reported in the literature have involved traditional π-electron conjugated systems, with only a few unbridged D-A systems being reported as good alternatives [19a,b] for applications as nonlinear optical materials. A deeper understanding of their fundamental structure-property relationships must therefore be acquired by evaluating their linear and NLO properties.

2.2 Linear optical properties

The UV/Vis spectra (see Figure 3) for all 2-mono- and 2,7-disubstituted selected quinolizinium derivatives (see Figure 5) exhibit an absorption below 500 nm. The band with a maximum at the longest wavelength was assigned to the transition to a π–π* excited state prior to the formation of a stable intramolecular charge transfer (ICT) excited state from which emission occurs. Band position ($\lambda_{abs,max}$) is usually quite sensitive to the ring conjugation and the electron-donating character of the heterocycle substituted at the acceptor, in this case the

quinolizinium moiety. The ICT bands for all the derivatives studied exhibit a sharp cut-off, with no broadening of this absorption band to the red. A weak broadening, attributed to the n–π* transition due to the presence of N heteroatoms, was observed previously for some other cationic acceptors, such as pyridinium cations, containing the same substituents [19b,c]. A comparison of $\lambda_{abs,max}$ for the C-2 substituted quinolizinium acceptor derivatives with those containing pyridinium moieties with the same electron-donating substituents linked in the activated positions (C2/C4) [19b] revealed bathochromic shifts in the 10-45 nm range, which were attributed to an increase in the degree of conjugation for the quinolizinium derivatives. Similarly, a comparison of $\lambda_{abs,max}$ for the unprotected 2-mono substituted derivatives containing indole, pyrazole, indazole and pyrrole groups (**2f**, **6b**, **6d** and **2c** respectively) indicated that the compound containing the weakest donor pyrazole substituent (**6b**) absorbed at the shortest wavelength (354 nm). The $\lambda_{abs,max}$ for indole- and indazole-substituted compounds (good donors), as well as their pyrrole counterpart, appeared at 396, 366 and 370 nm, respectively. Similar findings were obtained when comparing the protected monosubstituted **2a** (364 nm) with **2b** (357 nm), the unprotected **2f** (396 nm) with **6b** (400 nm), as well as the disubstituted **5c** (395 nm) with **7b** (377 nm) derivatives. Those containing weak pyrazole donors (**2b, 6b** and **7b**) exhibited shorter $\lambda_{abs,max}$ than their counterparts (**2a**, **2f** and **5c**). The greater electron-withdrawing character of the tosyl group, compared to the trityl one, probably reduces the difference between $\lambda_{abs,max}$ for **2a** and **2b**. As expected, moving from mono- to disubstituted protected (**2b** to **5b**) or non-protected (**6b** to **7b**) compounds resulted in a shift of the absorption maxima to the red (357 to 378 nm and 354 to 377 nm). The addition of a second heterocyclic of even the weakest pyrazole donor to the quinolizinium acceptor moiety at C(7) contributes to extending the π-delocalization, thus inducing a bathochromic displacement in the π-π* transitions. Something similar could be inferred for mono- and

disubstituted **2c** and **5c** pyrrole derivatives, which showed $\lambda_{abs,max}$ at 370 and 395 nm, respectively.

The $\lambda_{abs,max}$ for derivative **2a** (364 nm) was shifted to the blue by 32 nm compared to the non-protected **2f** (396 nm). Adding an electron-withdrawing tosyl group to the indole donor decreases its electron donating ability resulting in a diminishing of the charge transfer efficiency and hence a higher energy is associated to the transition. However, no apparent correlation was found between $\lambda_{abs,max}$ for **2b** substituted at C-2 with a pyrazole ring protected with a trityl group, which exerts a slight electron-withdrawing effect, and unprotected **6b**, the maxima for which appear at 357 and 354 nm respectively. A similar situation was found for pyrazole-disubstituted compounds **5b** and **7b**, whose maxima appear at 378 and 377 nm. In general, molar absorptivities at $\lambda_{abs,max}$ (ε_{max}) for quinolizinium acceptor derivatives (Table 3) are larger than for their pyridinium-containing counterparts [19b], with values ranging from approximately 1.1×10^4 to 3.7×10^4 $M^{-1}cm^{-1}$. However, no correlation was found between the ε_{max} values and the number of substituents on the different derivatives, their electron-donating character, or whether they were protected or not.

The emission spectra for all compounds were structureless (see Figure 4), showing maxima whose locations can be explained in a very similar manner to those of the absorption spectra. Thus, the unprotected mono-substituted derivatives **2f**, **6b**, **6d** and **2c** exhibit $\lambda_{em,max}$ at 496, 400, 451 and 485 nm, respectively. The pyrazole-containing compound (**6b**, weakest donor) emits at 400 nm, with the indole (**2f**), indazole (**6d**) and pyrrole (**2c**) counterparts being significantly shifted to the red by 96, 51 and 85 nm, respectively.

The changes in $\lambda_{em,max}$ upon moving from the protected 2-monosubstituted **2a** (448 nm) to **2b** (398 nm) and from the unprotected **2f** (496 nm) to **6b** (354 nm) and from the disustituted unprotected **5c** (463 nm) to **7b** (412 nm) can also be explained in a similar manner. The pyrazole-containing derivatives exhibited the smallest $\lambda_{em,max}$. As was also the case for the

absorption maxima, a comparison of $\lambda_{em,max}$ for mono- and disubstituted pyrazole-containing derivatives protected **2b** (398 nm) and **5b** (409 nm) or unprotected **6b** (400 nm) and **7b** (412 nm) revealed a displacement to the red, in this case by about 12 nm. However, the opposite behavior was observed when comparing mono- and disubstituted **2c** (485 nm) and **5c** (463 nm) compounds with pyrrole donor groups. The high degree of electronic asymmetry of a good donor substituent and central accepting moiety in the monosubstituted derivatives compared to the disubstituted ones should increase the extent of ICT. As a result, the emission of **2c** is displaced to higher wavelengths relative to the disubstituted derivatives **5c**.

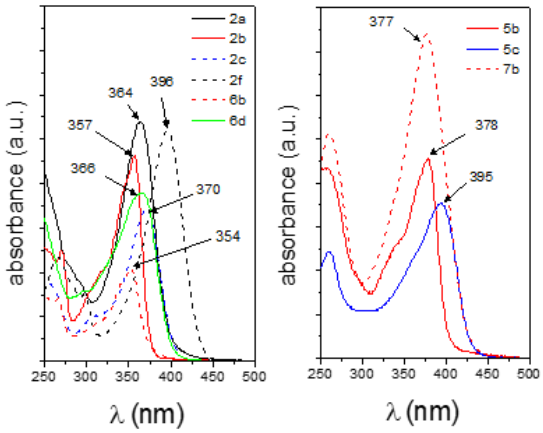

Figure 3. Electronic UV-Vis absorption spectra for 2-substituted quinolizinium derivatives 2a, 2b, 2c, 2f, 6b and 6d (left) and 2,7-disubstituted derivatives 5b, 5c and 7b in methanol at 25 °C (right). Values at the absorption maxima (depicted) are proportional to the molar absorptivities.

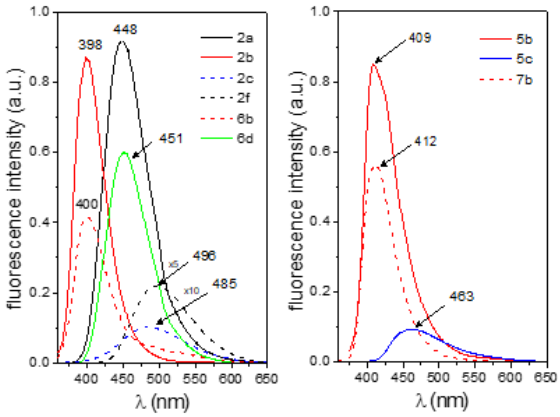

Figure 4. Emission spectra for 2-monosubstituted quinolizinium derivatives 2a, 2b, 2c, 2f, 6b and 6d (left) and 2,7-disubstituted derivatives 5b, 5c and 7b in methanol at 25 °C (right). Values at the emission maxima (depicted) are proportional to their fluorescence quantum yields.

The $\lambda_{em,max}$ for the electron-withdrawing tosyl protecting group at the indole ring of **2a** (448 nm) was, as expected, displaced to the blue compared to its unprotected counterpart **2f** (496 nm). This effect was smaller for pyrazole protected with a trityl group **5b** (409 nm) and its unprotected counterpart **7b** (412 nm) in the case of 2,7-quinolizinium derivatives. A similar situation was found for the C2-monosubstituted compounds **2b** (398 nm) and **6b** (400 nm), protected with a trityl group and unprotected, respectively.

An interesting observation was that the Stokes shifts ($\Delta\bar{\nu}$) for most derivatives were in the 5300-6575 cm^{-1} range. However, the series of mono- and disubstituted pyrazole derivatives **2b**, **6b**, **5b** and **7b** showed significantly smaller $\Delta\bar{\nu}$ values (2125-3435 nm) than the other compounds studied. Upon photoexcitation, the excited state reached quickly transfers its energy to the excited ICT state, from which emission occurs. As stated previously, the stability of ICT excited states depends strongly on the donating character of the substituent at the quinolizinium acceptor. Obviously, the small Stokes shifts observed for **2b**, **6b**, **5b** and **7b** are due to the low stabilization of the ICT complexes when the substituent was the weak donor pyrazole. In contrast, C-2 monosubstituted derivatives **2c**, **2f** and **6d**, which contain unprotected pyrrole, indole and indazole moieties, seemed to exhibit larger Stokes shifts as a consequence of a better ICT stabilization [27]. When comparing monosubstituted **2b**, **2c** and **6b** derivatives with their disubstituted **5b**, **5c** and **7b** partners, smaller Stokes shift were observed for the latter ones. As stated, pseudo-quadripolar structures (disubstituted derivatives), which hardly exhibit change in dipole moments upon electronic transition in polar solvents, usually exhibit smaller Stokes shifts than monosubstituted ones.

Table 3. Photophysical properties of selected quinolizinium derivatives (Fig. 5)

Comp	$\lambda_{abs,max}$ nm	λ_{exc} nm	$\lambda_{em,max}$ nm	$\Delta\bar{\nu}$ cm^{-1}	ϕ	$\varepsilon_{max}\times10^{-3}$ M^{-1} cm^{-1}	<τ> (ns)
2a	364	366	448	5300	0.59±0.10[a]	26.7±1.7	3.6(3.0)
2b	357	354	398	2885	0.88±0.03[a]	23.6±0.5	2.6(2.5)
2c	370	373	485	6575	0.01±0.01[a]	17.4±1.3	1.0(0.8)
2f	396	395	496	5450	0.04±0.0 [b]	26.1±0.5	3.6(3.5)
5b	378	373	409	2125	0.85±0.03[b]	21.5±0.1	2.0(1.9)
5c	395	373	463	3855	0.09±0.01[b]	17.6±0.1	1.7(1.7)
6b	354	354	400	3435	0.42±0.04[a]	2.10.5±0.04	3.4(3.4)
6d	366	366	451	5345	0.60±0.08[a]	19.0±2.1	3.0(3.4)
7b	377	373	412	2370	0.57±0.06[b]	37.0±1.7	2.8(2.9)

Maximum absorption wavelength (λ_{max}), excitation wavelength (λ_{exc}) used for fluorescence quantum yield (ϕ) measurements, maximum emission wavelength ($\lambda_{em,max}$), Stokes Shift ($\Delta\bar{\nu}$), molar absorptivity at $\lambda_{abs,max}$ (ε_{max}) and weighted average lifetimes upon excitation at 335 and 370 nm (in parentheses) by fixing the emission at $\lambda_{em,max}$. For fluorescence quantum yields: (a) using quinine sulfate in H_2SO_4 0.1M (ϕ=0.546) or (b) perylene in ethanol (ϕ=0.93) as standard [28].

Fluorescence quantum yields (ϕ) are shown in Table 3. In general, most of the quinolizinium-containing derivatives exhibit high quantum yields that are larger than for their counterparts containing pyridinium acceptors[19a,b]. Compounds **2b**, **6b**, **5b** and **7b**, which contain the weak donor pyrazole substituent with low ICT and exhibit the smallest Stokes shifts, present large ϕ values. The opposite was found for **2f**, **2c** and **5c** (with pyrrole or indazole donors), which exhibited the lowest ϕ values, $\lambda_{em,max}$ clearly displaced to the red, and relatively high Stokes shifts. In general, fluorescence quantum yields tend to decrease with the electron-donating ability of the substituent [19a].

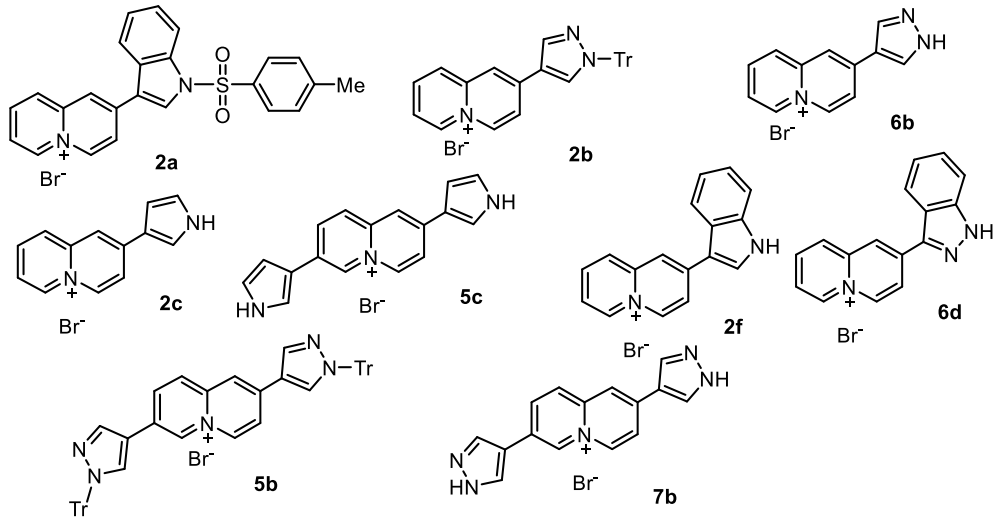

Figure 5. Selected chromophores for the study of linear optical properties and cyclic voltammetry (Tables 3 and 4). Tr: Trityl group

Fluorescence decay profiles were obtained upon excitation with monochromatic nanoleds emitting at 335 and 370 nm by fixing the fluorescence emission at $\lambda_{em,max}$. Irrespective of the excitation wavelength, all profiles could be reasonably fitted to double exponential decay functions. Weighted average lifetimes (<τ>), which depended slightly on the donor nature, exhibited similar values upon excitation at 335 or 370 nm, ranging from approximately 1.0 to 3.6 ns (Table 3 and Table S1). Rather low <τ> values were obtained for derivatives **2c** and **5c**, which contain pyrrole substituents; they also exhibited low fluorescence quantum yields. We

were unable to find any plausible correlation between the quantitative values for <τ> or lifetime component contributions and substituent donor features of the different derivatives.

2.3. Electrochemical properties

The electrochemical behaviour of selected quinolizinium salts (Figure 5) was studied by cyclic voltammetry (CV) (see Figure S1 in SI and Figure 6 in text) in dry acetonitrile/$LiClO_4$ (**5c** and **7b** in DMF-acetonitrile (1:1)/$LiClO_4$) as SSE (solvent-supporting electrolyte) system. The cathodic and anodic peak potentials, measured at a scan rate of 100 mV/s, and summarized in Table 4, are quoted relative to the Ag/Ag^+ ($AgCl_{sat}$) reference electrode.

The redox abilities of the above-mentioned quinolizinium salts were investigated, focusing on the first oxidation-reduction potentials, since these values correspond (tentatively) to the HOMO and LUMO energies, respectively. These cationic chromophores are electroactive at the cathode, to give the corresponding stabilized radicals, in the same potential range (E*pc* = -1.35 ± 0.15 V) due to the positive charge at the nitrogen atom in the quinolizinium ring. A similar electron-acceptor ability was recently described for aza-quinolizinium perchlorates [29].

The relationship between the energy of the highest occupied molecular orbital (HOMO) and the voltammetric oxidation potential values of a molecular organic semiconductor was described by Forrest *et al*. [30]. Table 4 includes the estimation of this energy (-IP, eV) and the energy gap (eV) for each compound.

Compound **2c**, which is substituted at the C2-position with a 3-pyrrolyl ring, has an Epa value of + 0.480 V, which correlates with the expected higher ability of this compound to be oxidized in comparision with the homologous 3-indolyl **2f** (Epa = +0.551 V). The loss of stability for **2c**, when oxidized to its cation radical, is energetically favoured compared with **2f** (Scheme 4). The same occurs for **6d** in comparison with **6b** (see Scheme S1 in SI).

Table 4. Experimental values of the peak potentials E (V, vs Ag/Ag+) (± 0.03V) of selected D-A$^+$ chromophores (Figure 5). *Epa* is the anodic peak potential, *Epc* is the cathodic peak potential. Scan rate: 100 mV/s. Ionization potentials (IP) and electron affinities (EA) and fundamental gap (Efund=IP – EA) (eV).

Comp.	*Epa1*	*Epa2*	*Epc*	-IP^1 (eV)^a	-IP^2 (eV)	-EA (eV)	Energy band gap (eV)
2a	+0.643	+0.834	-1.231	-5.50	-5.77	-2.88	2.62
2b	+0.737	+0.982	-1.351	-5.63	-5.97	-2.71	2.92
2c	+0.480	+0.798	-1.478	-5.27	-5.72	-2.53	2.74
2f	+0.551	+0.822	-1.440	-5.37	-5.75	-2.58	2.79
5b	+0.574	+0.99	-1.238	-5.40	-5.99	-2.87	2.53
5c	+0.610	+0.89	-1.407	-5.45	-5.85	-2.63	2.82
6b	+0.607	+0.836	-1.36	-5.45	-5.77	-2.70	2.75
6d	+0.726	+1.00	-1.292	-5.62	-6.0	-2.80	2.82
7b	+ 0.530	+0.96	-1.282	-5.34	-5.94	-2.79	2.55

IP and EA: Estimated from CV data (E*pa1* or E*pa2* values) by applying the relationship proposed by Forrest [30].

When comparing structures **6b** and **2c**, the latter is expected to be easier to oxidize (lower E*pa*) than **6b** as the pyrazole ring is less π-rich than the pyrrole ring. This argument can also be applied to the experimental E*pa* values for **2f** and **6d.** Thus, larger energy gaps are found for **2f** and **6d**, respectively, than for **2c** and **6b**, and the Epa values are also less positive compared with **2f** and **6d** (Figure S6 see SI).

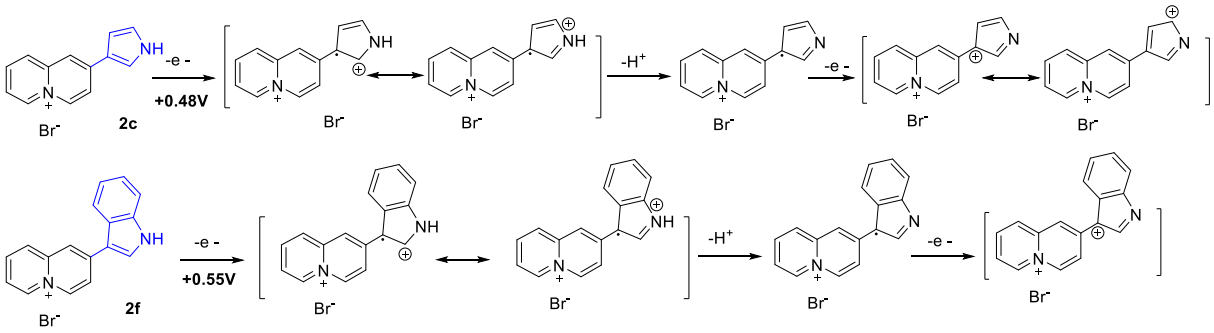

Scheme 4. Comparative Epa values for D-A$^+$ chromophores **2c** and **2f**.

For compounds **2a** and **2f**, a less negative E*pc* value can be expected for **2a** because the electron-withdrawing tosyl group increases the charge deficiency of the quinolizinium ring, which is therefore more easily reduced. However, when anodic potentials are compared for

2a and **2f**, the first E*pa* value for **2a** is more positive than that for **2f**, as expected due to the above-mentioned influence of the tosyl group.

Compound **2b**, which is substituted at C-2 with an *N*-triphenylmethyl (trityl) pyrazole ring, should be compared with its homologue **6b**. The trityl group (weak electron-withdrawing character) makes **2b** slightly more difficult to be oxidized than **6b**, as confirmed by the cyclic voltammetry data. The E*pa* value for **2b** is +0.737 V, compared with +0.607 V for **6b**, which correlates with the expected results.

When the E*pc* values of disubstituted compounds **5b**, **5c** and **7b** at the cathode are compared, it can be seen that the effect of two pyrazole rings in **7b**, instead of two pyrrole rings in **5c**, results in an easier reduction, similar to that already mentioned for **6b** compared to **2c.** However, for **5b** (*N*-substituted with a trityl group), the reduction potential is even less negative compared with unsubstituted **7b**, thus meaning that **5b** is easier to reduce.

With regard to the voltammetric oxidation scan of these two molecules, it is surprising that the E*pa* values for the first and second peaks are quite similar for **5b**, **5c** and **7b**, probably due to the compensation of electronic effects.

A final comparison of the pairs **2b/5b, 2c/5c** and **6b/7b** was performed (Figure 7). For 2,7-disubstituted quinolizinium bromides, the E*pc* values appear only to be affected by electronic effects. Thus, at the C2-position, both inductive and conjugative effects are important, whereas at the C7-position, only inductive effects are seen. As such, the cathodic discharge potentials (E*pc* values) are less negative when a second heterocyclic ring is introduced at the C7-position. i.e. the disubstituted compounds are reduced more easily than the monosubstituted ones.

The oxidation tendencies for C2- and C7-disubstituted quinolizinium salts, in comparison with their monosubstituted counterparts (Figure 7 SI), depend on the stability of cationic intermediates and oxidation products. Thus, the pyrazole ring at the C7-position in **5b** and

7b is easier to oxidize than that at the C2-position (Scheme 5) because the positive charge on quinolizinium cannot be delocalized by the C7-position, thus meaning that the C7-pyrazole ring has a higher electronic density. In **7b**, after losing $2e^-$ and $2H^+$ (or 2e- and $2Tr^+$ in **5b**), a stable, highly conjugated and symmetric new quinolizinium bromide is formed. For this reason, compounds **5b**/**7b** are more easily oxidized than their monosubstituted counterparts **2b**/**6b**, respectively. The oxidation proceeds as follows:

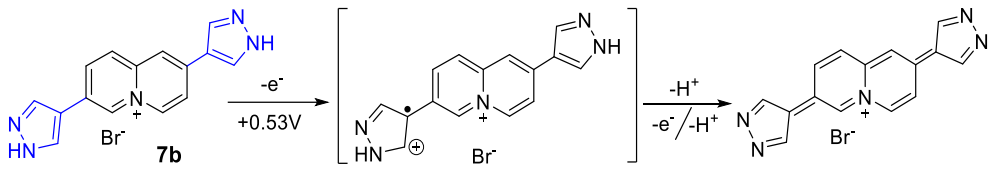

Scheme 5. Oxidation process for D-A+-D chromophore **7b**

However, in contrast to the former disubstituted salts, compound **5c** (Epa = +0.610 V) is slightly more difficult to oxidize than monosubstituted **2c** (Epa = +0.48 V). A plausible explanation is as follows.

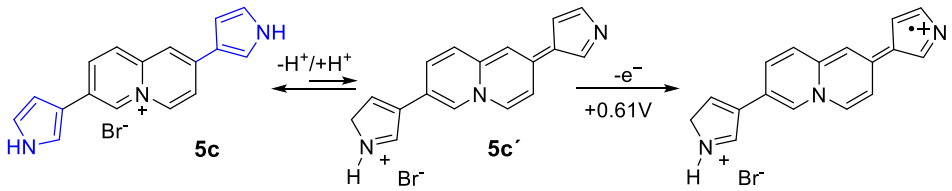

Scheme 6. Oxidation process for D-A+-D chromophore **5c**

Compound **5c** delocalizes the positive charge on the quinolizinium over the pyrrole ring at C2 but not that at C7 position. The latter heterocycle (at C7) is therefore more easily oxidized as it is more electron-rich. However, an internal acid-base equilibrium prior to the oxidative step can be proposed, as indicated in Scheme 6. When this occurs, the oxidation potential E*pa* of cation **5c´** increases as the heterocycle at C7 is protonated, which means that oxidation of the C2 ring is more difficult.

These electrochemical results show that double substitution at both the C2 and C7 positions in quinolizinium salts by weakly electron-donating heterocycles clearly decreases the HOMO-LUMO gap (in comparison to C2 monosubstitution).

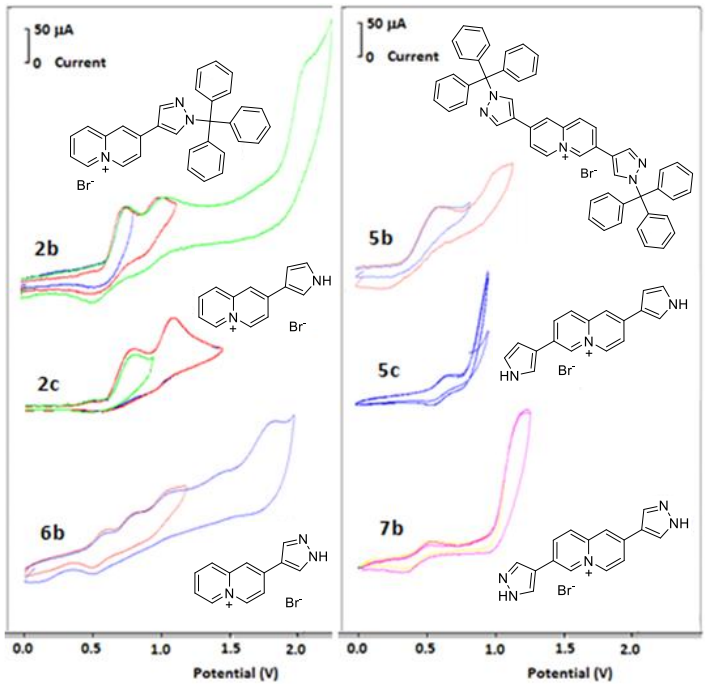

Figure 6. Cyclic voltammograms of **2b/5b**, **2c/5c** and **6b/7b** in dry acetonitrile/$LiClO_4$ (0.1M) (**2b**, **2c** and **6b**) or DMF/$LiClO_4$ (0.1M) (**5b**, **5c** and **7b**) as SSE, at Pt working and auxiliary electrodes. Ag/Ag^+ (sat) as reference electrode. Scan rate: 100 mV/s.

Another interesting conclusion is that, in contrast to electronic effects, steric hindrance does not seem to affect the electrochemical response (**7b**→**5b** or **6b**→**2b**).

Thus, the presence of a highly electrodonating ring at C7, where conjugation is blocked (**5c**), seems to cause destabilization in the D-A^+ system, which behaves as an amphoteric molecule before being oxidized.

2.4. Nonlinear optical properties: Hyper-Rayleigh Scattering (HRS) measurements

Femtosecond hyper-Rayleigh scattering (HRS) measurements were performed at a wavelength of 800 nm to study the potential of these relatively small ionic compounds for second-order nonlinear optical applications. The results of these HRS experiments are given in Table 5 both

in terms of dynamic hyperpolarizability (measured at 800 nm) and of static values, derived from the two-level model (TLM). The second-order nonlinear optical properties reflect the observations already made for linear optical properties as regards the nature of the conjugation at C-2 in relation to disubstitution at the C2 and C7 positions of the chromophores, thus confirming that the best conjugation and charge transfer from the donor to the acceptor is achieved at position C2.

The largest first hyperpolarizability values were found for protected indole-substituted compound **2a** (β_{HRS}= 674×10^{-30} esu), and **5b** (393x10^{-30} esu), followed by indazole derivatives **6d** (β_{HRS}=356×10^{-30} esu) and **2d** (β_{HRS}= 250×10^{-30} esu). In agreement with the greater influence of the donor substituent at the C2-position of the quinolizinium acceptor, the relative electron-donating strength characteristics, and better conjugation and stabilization, the largest β values correspond to indole and indazole derivatives (relatively good donors), which can be explained by a more efficient charge transfer between frontier orbitals in these non-bridged systems.

Table 5. Experimental nonlinear optical properties of D–A+ and D-A+-D

Comp.	λ_{max}	β_{HRS}	β_{zzz}	$\beta_{zzz,0}$	β_0	τ
2a	364	674±34	1629±83	222±11	33±1.6	4.21±0.73
2b	357	68±5	165±13	27±2	4±0.3	2.94±0.36
2c	370	91±6	220±15	25±2	3±0.2	0.92±0.18
2d	360	250±10	606±25	91±4	13.7±0.55	3.48±0.44
2f	399	129±52	312±127	1.1±0.5	0.16±0.06	----
5b	365	393±13	951±32	126±4	18.7±0.61	1.93±0.19
5c	392	49±17	120±42	25±2	0.49±0.17	1.91±0.70
5f	423	87±5	210±14	18±1.2	2.35±0.13	6.14±3.09
6b	350	45±2	109±6	21±1.1	3.16±0.14	3.41±0.51
6d	371	356±16	860±40	94±4	13.8±0.62	3.55±0.44
6e	416	95±11	231±28	14±1.7	1.82±0.21	----
7b	364	203±9	492±22	67±3	9.95±0.44	3.19±0.45
7d	397	171±17	415±43	5±05	0.64±0.06	2.18±0.37

Wavelength of maximum absorbance λmax (nm), resonance-enhanced HRS experimental first hyperpolarizability β_{HRS} (10^{-30} esu), resonance-enhanced diagonal component of the molecular first hyperpolarizability βzzz (10^{-30} esu), off-resonance diagonal component of the molecular first hyperpolarizability βzzz,0 (10 $^{-30}$ esu), dispersion-free hyperpolarizability β_0 (10^{-30} esu) .
The values of the fluorescence lifetime, τ (ns) are also included for molecules exhibiting demodulation.

The effects of the *N*-protecting groups were also evaluated. Thus, compound **2a**, which bears a strongly electron-withdrawing substituent that is expected to increase intramolecular charge transfer and, thus, the first hyperpolarizability, shows a higher β_{HRS} value. *N*-substitution stabilizes the ground and excited state upon *N*-*p*-toluensulfonyl substitution at indole [32]. The HOMO and LUMO energies are stabilized for the electron-withdrawing group due to the delocalization of π electrons from indole to the sustituent [32]. Compound **2a**, which bears a strongly electron-attracting substituent, exhibits higher charge transfer compared to **2f**.

N-Boc substitution in indazole **2d** (β_{HRS}=250×10^{-30} esu) was also studied and measured in the absence of the protecting group (**6d**, β_{HRS}=356×10^{-30} esu), exhibiting a large increase in β_{HRS}. In contrast, the *N*-Tr group is a slightly sigma-withdrawing (inductive -I effect) and therefore has less effect on delocalization onto the pyrazole ring, which is a less π-rich system. Interestingly, chromophores bearing an *N*-Tr protecting group give β values that are twice those for the corresponding unprotected C2 and C2/C7 quinolizinium derivatives.

Similar absorption maxima and first hyperpolarizabilities approximately 50% lower are observed for compounds with double substitution at the C2/C7 positions, (**2f**/**5f** and **6d/7d**). However, the absorption maxima for compounds **7b** and **5b** are similar (364/365 nm), whereas the chromophore substituted with a trityl protecting group (**5b**) exhibits a large β value (393 × 10^{-30} esu) that is nearly twice that measured for **7b**. A similar trend is observed for **6d**/**7d.**

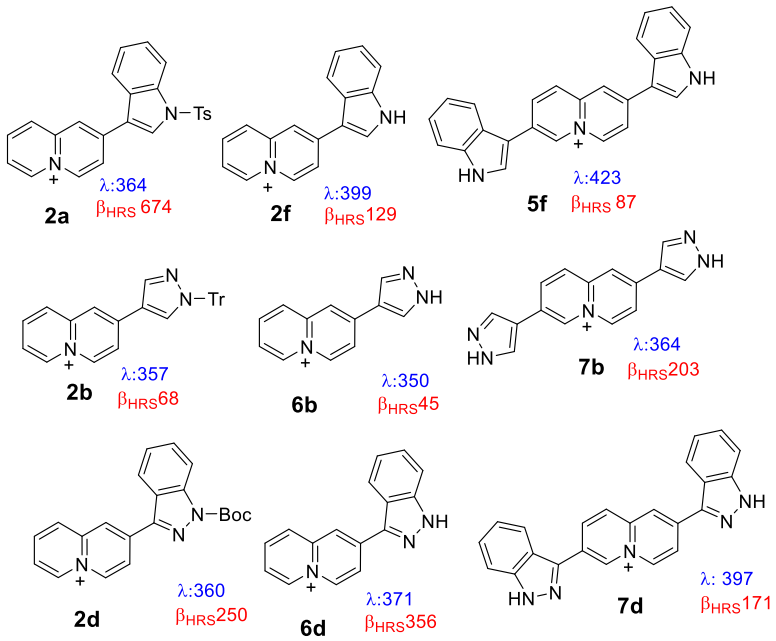

Figure 8. Selected chromophores for the study of nonlinear optical properties

A comparison of monosubstituted chromophores **2f** and **6d** and disubstituted compounds **5f** and **7d**, which contain indole and indazole moieties, respectively, lacking a protecting group, allows us to conclude that the disubstituted compounds exhibit a beta value half that of the C2-functionalized chromophore.

For the series of charged dipolar (D-A$^+$) and quadrupolar (D-A$^+$-D) chromophores, large first hyperpolarizabilities were obtained for compounds **2a**, **2d** and **6d**, as determined by HRS. The low transition energy and high degree of CT are the decisive factors resulting in a large first hyperpolarizability in compounds substituted at the C2 position of the quinolizinium system.

In comparison to previously reported (D–π-A$^+$) molecules [19c], the lack of a conjugated bridge in pyridinium-containing (D–A$^+$) chromophores [19b] results in higher β values. Consequently, the common assumption that β can be maximized by using a conjugated bridge to link D and A units does not hold in general [19b].

The experimental results reported here for quinolizinium chromophores (D-A$^+$) or (D-A$^{+\prime}$-D) reveal the highest hyperpolarizability for the unbridged geometry. Furthemore, the β value

obtained for D-A$^+$ chromophores with a quinolizinium acceptor are larger than for their pyridinium counterparts. These results for non-bridged azonia systems allow a remarkable degree of control by supression of the linker and N-substitution at the donor heterocycle unit.

2.5 Computational studies

To understand the electronic reorganizations that occur upon excitation and the microscopic NLO properties of the synthesized quinolizinium chromophores, theoretical (DFT and HF) calculations were performed using the Gaussian 09 program package [33]. As a first step, a geometry optimization of the molecular structures was performed at the B3LYP/6-31+G(d,p) level of theory for all cations studied, in the gas phase and in methanol, except the bulky compound **5b**, the geometry of which was optimized at the B3LYP/6-31G(d,p) level of theory. The gas phase optimized low-energy isomers for protected and deprotected 1D (compounds **2** and **6**) and 2D chromophores (compounds **5** and **7**) are shown in Figure S1 in the Supporting Information. Time-dependent density functional theory (TDDFT) calculations were used to probe the electronic reorganizations of the cationic systems studied upon excitation in methanol. The data reported in Table 6 show that the TDDFT method with a hybrid Perdew–Burke–Ernzerhof exchange-correlation functional (PBE0) is able to fully reproduce the linear optical properties, with the theoretically predicted wavelength values differing from the experimental ones by up to 7%. The TDDFT/PBE0/6-311+G(2d,p) absorption maxima, oscillator strengths and frontier orbital energies for the compounds studied (with/without protecting group) in methanol are reported in Table 6.

The band positions and intensities predicted by TDDFT are consistent with the experimentally observed values. For all compounds, the first excited states are determined by HOMO → LUMO transitions. The HOMO-LUMO gaps range from 3.44 (**5e**) to 4.46 eV (**6b**) for the compounds in methanol.

In all compounds shown in Figure 9, the HOMO orbitals were found to be populated over the entire molecular system, except for the protecting groups. Similarly, the LUMOs were found to be delocalized over the quinolizinium and, to a lesser extent, over the substituents (indole, pyrazole and indazole fragments). It is known that the gap, defined as the difference between the ionization potential (IP) and electron affinity (EA) (E_{fund} = IP - EA), is only approximately given by the difference between the calculated HOMO and LUMO energy levels [34]. The computational methodology we have adopted, more specifically the hybrid functional (PBE0) with 25% exact Hartree–Fock exchange, reproduces the experimental cyclic voltammetry-based ionization potentials relatively well (with errors of about 1 eV) and the electron affinities very well.

Table 6. Calculated TDDFT/PBE0/6-311+G(2d,p) absorption maxima λmax (nm), oscillator strengths (f), HOMO and LUMO energies, and difference between the calculated FMOs energies, HLG, (eV).

Comp.	λ_{max}	f	HOMO	LUMO	HLG
2a	373	0.61	-6.73	-2.76	3.98
2b	337	0.81	-7.00	-2.66	4.34
2c	357	0.32	-6.69	-2.55	4.14
2d	360	0.56	-7.08	-2.99	4.09
2e	384	0.87	-6.67	-2.87	3.80
2f	385	0.42	-6.42	-2.57	3.85
2g	372	0.97	-6.66	-2.80	3.86
2h	352	0.82	-6.88	-2.75	4.14
2i	376	0.75	-6.54	-2.68	3.86
5b	371	1.32	-6.49	-2.74	3.75
5c	388	0.46	-6.35	-2.50	3.85
5d	387	1.00	-6.97	-3.14	3.83
5e	432	1.38	-6.40	-2.96	3.44
5f	418	0.63	-6.14	-2.54	3.60
5g	412	1.49	-6.40	-2.86	3.54
5h	379	1.20	-6.68	-2.79	3.89
5i	404	1.14	-6.33	-2.69	3.65
6b	329	0.57	-7.13	-2.67	4.46
6d	367	0.60	-6.80	-2.81	3.98
7b	357	0.76	-6.83	-2.70	4.13
7d	397	0.94	-6.60	-2.88	3.72

The largest experimental β_{HRS} values were found for compounds **2a** (674 × 10^{-30} esu), **2d** (250 × 10^{-30} esu), **5b** (393 × 10^{-30} esu) and **6d** (356 × 10^{-30} esu). Both theoretical approaches (HF and MP2) predict higher β_{HRS} values for deprotected mono- and disubstituted quinolizinium cationic systems in comparison with the values calculated for the Ts- and Boc-protected ones. The calculated β_{HRS} values for Tr-protected systems (**2b** and **5b**) are higher than those calculated for the corresponding deprotected ones (**6b** and **7b**, respectively).

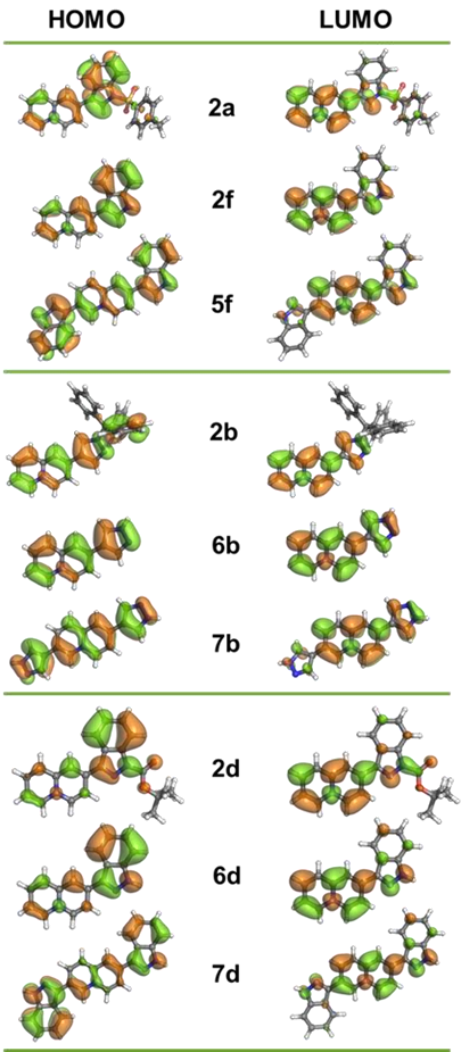

Figure 9. Graphical representation of the frontier orbitals (isodensity plot, isovalue = 0.02 a.u.) for the cationic fragments of the triads protected monosubstituted/deprotected monosubstituted/disubstituted cationic quinolizinium systems **2a/2f/5f**; **2b/6b/7b**; **2d/6d/7d**.

Disubstituted cationic quinolizinium systems are characterized by lower β_{HRS} values than their monosubstituted counterparts (**2f**/**5f**; **6b**/**7b**; **6d**/**7d**). Similar trends are observed for the static

($\beta_{HRS,0}$) and dynamic (evaluated at 800 nm, $\beta_{HRS,800}$) molecular first hyperpolarizabilities. It should be noted that the theory (both theoretical approaches - HF and MP2) did not fully succeed in predicting the experimental β_{HRS} values of the series of differently substituted protected/unprotected compounds (Table 7). Further investigations based on both representative and reliable experimental data and computational approaches are needed to address this issue.

Table 7. HF-calculated β_{HRS} values ($\beta_{HRS,0}$ and $\beta_{HRS,800}$) for selected compounds **2**, **5-7**. MP2-calculated β_{HRS} values are given in parentheses.

Comp.	$\boldsymbol{\beta_{HRS,0}}$ ($\times 10^{-30}$ esu)	$\boldsymbol{\beta_{HRS,800}}$ ($\times 10^{-30}$ esu)
2a	35 (70)	61 (122)
2b	38 (65)	59 (101)
2c	44 (71)	62(100)
2d	16 (35)	26 (57)
2f	48 (100)	93 (194)
5b*	11 (98)	10 (125)
5c	18 (35)	25 (47)
5f	28 (38)	58 (79)
6b	29 (44)	37 (56)
6d	37 (68)	58 (107)
7b	13 (24)	20 (35)
7d	19 (27)	34 (48)

In comparison with the previously investigated pyridinium systems [19b], the newly proposed cationic quinolizinium systems appear to perform better in terms of applications related to nonlinear optics. Indeed, the β_{HRS} values predicted at the MP2 level for a model pyrrole-substituted cationic quinolizinium system (**2c**, Table 7, Figure S3) are higher ($\beta_{HRS,800}$ = 100×10^{-30} esu) than those calculated for a model 2-methylpyridinium (**B**), 3-methylpyridinium (**C**) and 4-methylpyridinium cationic system (**D**) ($\beta_{HRS,800}$ values of 32×10^{-30}, 29×10^{-30} and 66×10^{-30} esu, respectively). The representatives with the smallest substituents in the methylpyridinium/quinolizinium cationic systems were compared and the electron densities for both substituted cations (quinolizinium and methylpyridinium) found to be quite similar (Figure S3).

3. Experimental section

3.1 Materials and Methods (See SI)

3.2. *Synthesis of D–A$^+$ and D-A$^+$-D Quinolizinium chromophores.*

The structures of all new chromophores were unambiguously confirmed by their analytical and spectral data. Details are provided in the supplementary information (ESI). Only General Procedures and selected chromophores are given here.

Synthesis of D–A+ quinolizinium salts (2). ***General procedure. Stille Reaction***. *A flame-dried flask was charged under argon with 1 equiv. of bromoquinolizinium bromide or hexafluorophosphate (1 mmol), 5 mol % $Pd(PPh_3)_4$ (**Method A**) or 5 mol % $Pd_2(dba)_3$ and 5 mol % $P(o\text{-}Tol)_3$ (**Method B**) in dry DMF (5 mL). The corresponding stannyl heterocycle (1.3-1.4 mmol or 1.1 mmol) was then added. After stirring at room temperature or heating at 65-75 °C for 15-20 h, the solution was filtered through a small pad of celite and washed with methanol. The solution was then concentrated and the solid purified by flash chromatography on silica gel using CH_2Cl_2/MeOH (9:1) as eluent.*

2-(*N*-Tosylindol-3'-yl)quinolizinium bromide (2a). General procedure A, from 2-bromoquinolizinium bromide **1** (0.10 g, 0.35 mmol) and 3-tributylstannyl-*N*-(toluen-4-sulfonyl)-1-*H*-indole (0.21 g, 0.38 mmol). Heating the reaction mixture for 4 h at 70 °C afforded **2a** (0.16 g, 97%) as a pale-brown solid: M.p. 265–266 °C (CH_3CN); IR (KBr) $\nu_{máx}$ (cm^{-1}): 1647, 1173, 1146, 1552; ^{1}H NMR (500 MHz, DMSO-d_6) δ (ppm): 9.41 (d, *J* = 7.2 Hz, 1H), 9.31 (d, *J* = 6.8 Hz, 1H), 8.99 (s, 1H), 8.92 (s, 1H), 8.67 (dd, *J* = 7.2, 2.2 Hz, 1H), 8.64 (d, *J* = 8.7 Hz, 1H), 8.37 (t, *J* = 8.0 Hz, 1H), 8.33 (d, *J* = 7.8 Hz, 1H), 8.08 (d, *J* = 8.1 Hz, 1H), 8.07 – 8.01 (m, 3H), 7.53 (t, *J* = 7.7 Hz, 1H), 7.49 (t, *J* = 7.5 Hz, 1H), 7.44 (d, *J* = 8.0 Hz, 2H), 2.33 (s, 3H); ^{13}C NMR (126 MHz, DMSO-d_6) δ (ppm): 146.3, 142.9, 140.4, 136.9, 136.6, 136.4, 134.8, 133.5, 130.5, 129.5, 127.1, 127.0, 126.6, 126.0, 124.7, 123.0, 122.1, 121.8, 121.0, 117.4, 113.6, 21.1.; MS (ESI$^+$, *m/z*): 399 (M$^+$). Anal. Calcd for $C_{24}H_{19}N_2SO_2Br$ (479 g/mol) C,

60.12; H, 3.97; N, 5.84 S, 6.68. Found: C, 60.52; H, 4.35; N, 6.16, S, 7.06. HRMS (ESI-TOF) m/z calcd for $C_{24}H_{19}N_2O_2S$ $[M + H]^+$ 399.11618, found: 399.11597.

2-(*N*-Trityl-1*H*-pyrazol-4-yl)quinolizinium bromide (2b). General procedure A, from 2-bromoquinolizinium bromide **1** (0.10 g, 0.35 mmol) and 4-tributylstannyl-1-tritylpyrazole (0.27 g, 0.45 mmol). Heating the reaction mixture for 8 h at 65 °C afforded **2b** (0.17 g, 94%) as a pale-brown solid: M.p. 256–258 °C (CH_3CN); IR (KBr) $\nu_{máx}$ (cm^{-1}): 1647, 1458, 1072, 1028. ^1H NMR (500 MHz, CD_3OD) δ 9.09 (d, *J* = 7.3 Hz, 1H), 9.06 (d, *J* = 6.5 Hz, 1H), 8.62 (d, *J* = 2.1 Hz, 1H), 8.43 (d, *J* = 0.8 Hz, 1H), 8.40 (d, *J* = 0.8 Hz, 1H), 8.31 (d, *J* = 8.5 Hz, 1H), 8.23 (dd, *J* = 7.2, 2.1 Hz, 1H), 8.19 (ddd, *J* = 8.6, 7.1, 1.2 Hz, 1H), 7.84 (td, *J* = 7.0, 1.5 Hz, 1H), 7.42 – 7.33 (m, 9H), 7.25 – 7.17 (m, 6H). ^{13}C NMR (75 MHz, CD_3OD) δ (ppm): 146.3, 145.0, 144.1, 141.2, 139.1, 138.8, 138.5, 135.3, 132.5, 130.5, 130.3, 129.1, 124.7, 123.6, 122.5, 120.0, 82.5. MS (ESI^+, *m/z*): 438 (M^+). Anal. Calcd for $C_{31}H_{24}N_3Br$ (518 g/mol) C, 71.82; H, 4.67; N, 8.10. Found: C, 71.67; H, 4.71; N, 8.32. HRMS (ESI-TOF) m/z calcd for $C_{31}H_{24}N_3$ $[M + H]^+$ 438.19647, found: 438.19668.

Synthesis of D-A⁺-D Quinolizinium Salts 5. General Procedure. Stille Reaction. *A flame-dried flask (two necks, 25 ml) was charged under argon with 1 equiv. of 2,7-dibromoquinolizinium bromide **3** (1 mol), 14 mol% of CuI in DMF (2ml), the corresponding stannyl heterocycle (2.3-2.5 mmol), then 7 mol% of $Pd(PPh_3)_4$ (**Method A**) or 5 mol % $Pd_2(dba)_3$ and 10 mol % $P(o\text{-}Tol)_3$ (**Method B**) in dry DMF (3-5 mL). The corresponding stannyl heterocycle (2.3-2.5 mmol) in DMF (3 ml) 1.1 mmol) was then added. After stirring at room temperature or heating at 70-75 °C for 18-24 h, the solution was filtered through a small pad of celite and washed with methanol. The solution was concentrated and the solid purified by flash chromatography on silica gel using CH_2Cl_2/MeOH (9:1) as eluent.*

2,7-*bis*-(*N*-Tritylpyrazol-4'-yl)quinolizinium bromide (5b). From 2,7-dibromoquinolizinium bromide **3** (0.1 g, 0.27 mmol) and 4-tributylstannyl-1-trityl-1*H*-

pyrazole (0.38 g, 0.63 mmol) following the general procedure A , heating the mixture at 70 °C for 22 h. The solution was concentrated and treated with CH_2Cl_2, then the precipitate was isolated by filtration and washed with CH_2Cl_2 and MeOH to afford **5b** (0.116 g, 52%) as a pale-brown solid. M.p. 331–335 °C (d) (CH_3CN/EtOH). IR (KBr) $\nu_{máx}$ (cm^{-1}): 1641, 1555, 1489, 1442, 746. ^{1}H NMR (300 MHz, DMSO-d_6) δ (ppm): 9.50 (s, 1H), 8.97 (d, *J* = 7.3 Hz, 1H), 8.69 (s, 1H), 8.55 (dd, *J* = 8.9, 1.7 Hz, 1H), 8.48 (s, 1H), 8.46 (s, 1H), 8.41 – 8.32 (m, 2H), 8.28 (s, 1H), 8.23 (d, *J* = 9.1 Hz, 1H), 7.48 – 7.34 (m, 18H), 7.22 – 7.06 (m, 12H). ^{13}C NMR (75 MHz, DMSO) δ 142.1 (3C), 142.0 (3C), 140.6, 138.8, 138.4, 137.4, 135.8, 134.1, 132.4, 130.8, 130.7, 129.3, 127.7, 127.7, 126.5, 126.0, 120.9, 119.5, 117.2, 115.3. EM (ESI)$^+$ (*m/z)* 746 (M)$^+$. Anal. Calcd for $C_{53}H_{40}N_5Br$ (826 g/mol) C, 77.0; H, 4.84; N, 8.47. Found: C, 77.38; H, 5.25; N, 8.17. HRMS (ESI-TOF) m/z calcd for $C_{53}H_{40}N_5$ [M + H]$^+$ 746.32782, found: 746.32753.

2,7-bis-(1'*H*-Indol-3'-yl)-quinolizinium bromide (5f.Br$^-$). From 2,7-dibromoquinolizinium bromide **3** (0.05 g, 0.14 mmol) and 3-tributylstannyl indole (0.13 g, 0.34 mmol), following general procedure B, and heating the mixture at 70 °C for 24 h. The resulting solid was treated with AcOEt to afford **5f.Br$^-$** (0.036 g, 60%) as a brown solid: mp 249-251 °C (CH_3CN) .IR (KBr) ν_{max} 3102, 1636, 1524, 1430, 1256 cm^{-1}.^{1}H-NMR (DMSO, 300 MHz) δ (ppm) 12.25 (s, 1H, NH), 11.94 (s, 1H, NH), 9.38-9.34 (m, 2H), 8.72-8.24 (m, 8H), 7.59-7.46 (m, 2H), 7.4-7.12 (m, 4H).^{13}C-NMR (DMSO, 75 MHz) δ (ppm) 141.7, 140.1, 137.0, 136.5, 135.1, 134.1, 129.8, 128.9, 128.3, 126.8, 125.5, 123.5, 123.1, 122.3, 121.9, 120.9, 120.4, 120.1, 119.4, 119.0, 116.9, 112.2, 111.8, 110.6, 108.6. MS (ESI)$^+$ *m/z*(relative intensity) 360 (M)$^+$. Anal. Calcd for $C_{25}H_{18}BrN_3$ (440 g/mol) C, 68.18; H, 4.12; N, 9.54. Found: C, 68.59; H, 4.43; N, 9.36.

Deprotection reaction. General procedure. HCl 1M (2-7 mmol) was added to a suspension of starting salt (1 mol equiv.) in EtOH (5-8 ml) in several portions at different times. The reaction

mixture was then stirred at room temperature or heated at 75 °C for 18-30 h. It was then concentrated to dryness and the residue obtained was purified as indicated for each compound.

2-(1'*H*-Pyrazol-4'-yl)quinolizinium (6b). Following the general procedure, from **2b** (0.17 g, 0.33 mmol) and HCl 1M (0.5 ml, 0.5 mmol). After stirring at room temperature for 8 h, the solution was concentrated and the residue treated with Et_2O. The solid was filtered off to afford **6b** (0.11 g, 94%) as a pale solid: mp 230–231 °C (EtOH). IR (KBr) $\nu_{máx}$ (cm^{-1}): 3416, 1650, 1456, 1151, 839. ^1H NMR (500 MHz, CD_3OD) δ (ppm): 9.17 (d, *J* = 7.1 Hz, 1H), 9.11 (dd, *J* = 6.8, 1.1 Hz, 1H), 8.77 (bs, 2H), 8.72 (d, *J* = 2.0 Hz, 1H), 8.38 (dd, *J* = 9.0, 1.4 Hz, 1H), 8.34 (dd, *J* = 7.2, 2.0 Hz, 1H), 8.24 (ddd, *J* = 8.6, 7.1, 1.2 Hz, 1H), 7.88 (td, *J* = 7.0, 1.4 Hz, 1H). ^{13}C NMR (125 MHz, DMSO-d_6) δ (ppm): 143.0, 141.2, 136.9, 136.3, 136.1, 134.4 (2C), 126.2, 121.9, 120.7, 119.3, 117.7. MS (ESI^+, *m/z*): 196 $(M)^+$. Anal. Calcd for $C_{12}H_{10}BrN_3$ (276 g/mol) C, 52.20; H, 3.65; N, 15.22. Found: C, 52.63, H, 3.12, N, 15.90. HRMS (ESI-TOF) m/z calcd for $C_{12}H_{10}N_3$ $[M + H]^+$ 196.08692, found: 196.08707.

2,7-*bis*(1'*H*-Pyrazol-4'-yl)quinolizinium bromide (7b). . Following the general procedure, from **5b** (0.038 g, 0.046 mmol) and HCl 1M (0.17 ml, 0.17 mmol). Heating the mixture for 24 h afforded a crude residue, which was treated with a mixture of CH_2Cl_2:AcOEt (95:5). The solid was then filtered off and washed twice with EtOH:AcOEt to give **8b** (0.013 g, 83%) as a pale-brown solid. M.p. 312–313 °C (MeOH:EtOH). IR (KBr) $\nu_{máx}$ (cm^{-1}): 3089, 1641, 1561, 1438. ^1H NMR (500 MHz, DMSO-d_6, 80 °C) δ (ppm):9.49 (s, 1H), 9.42 – 8.73 (m, 5H), 8.64 (s, 1H), 8.51 (d, *J* = 8.6 Hz, 1H), 8.36 – 8.25 (m, 2H). MS (ESI^+, *m/z*) 262 $(M)^+$. Anal. Calcd. for $C_{15}H_{12}N_5Br$ (342 g/mol) C, 52.65; H, 3.53; N, 20.47. Found: C, 52.95, H, 3.88, N, 20.19. HRMS (ESI-TOF) m/z calcd for $C_{15}H_{12}N_5$ $[M + H]^+$ 262.10872, found: 262.10858.

4. Conclusions

A series of azonia cation derivatives has been synthesized and investigated for the first time as D-A$^+$ and D-A$^+$-D chromophores. The structure–property relationship of the studied chromophores may contribute to the recent interest in β enhancement strategies and to be used as an alternative to traditional azinium π-conjugated chromophores in nonlinear optics. We attribute this cooperative enhancement to the cationic strong acceptor, along with the increasing electron-donating ability of the donor, thus revealing the crucial role played by inherent polarization between both fragments to modulate NLO properties.

The photophysical and electrochemical properties of dipolar D-A$^+$ chromophores were investigated and compared with the corresponding D-A$^+$-D chromophores on the basis of UV–vis absorption/fluorescence spectroscopy and cyclic voltammetry to evaluate the intramolecular electronic interactions between the donor and acceptor and *N*-substitution at the donor unit.

The first hyperpolarizabilities of charged chromophores (D-A$^+$) and (D-A$^+$-D) were determined by HRS. Candidates with high β values were identified and the key factors governing the enhancement of the NLO responses determined. The low transition energy and high degree of CT are the decisive factors that confer a large first hyperpolarizability on compounds substituted at C2 of the quinolizinium system. The NLO response depends on the nature of the protecting group: β_{HRS} increases when removing the Ts and Boc protecting groups, whereas Tr-protected systems have higher values than their unprotected counterparts. It can therefore be concluded that Tr group deprotection does not result in quinolizinium systems with improved NLO properties.

The experimental linear/nonlinear optical and electrochemical measurements are compared with values calculated by the electronic structure methods (DFT and/or *ab initio*). The comparison sheds light on the structure-property relationship for these new D-A$^+$(D)

chromophores, although the theory did not fully succeed in predicting the experimental NLO properties. The structure-property relationships obtained will be used in ongoing studies focused on heterobetaines based on quinolizinium as cation for D-A- building blocks in organic–based materials. Overall, this study provides an insight into the promising D-A^+ and D-A^+-D architectures based on quinolizinium cation as an acceptor fragment. Our results suggest that materials based on this quinolizinium system have a great potential for application in integrated NLO devices. These findings also provide an intriguing area for future research into quinolizinuim building blocks and structure-directing constituents that may help to tune the NLO properties of these systems. It is expected that the present study that demonstrates the synthesis and properties of quinolizinium based D-A^+ and D-A^+-D architectures paves the way for the development of new organic NLO materials.

Acknowledgements

Financial support from the Spanish Ministerio de Ciencia y Competitividad (MINECO/ CTQ2017-85263-R), Instituto de Salud Carlos III (MINEC0/ RD16/0009/0015). J.R gratefully acknowledges the funding of the FEDER funds and Comunidad de Madrid (CAM, project B2017/BMD-3688 MULTI-TARGET&VIEW-CM FEDER FUNDS). E.S-P and M.A.R.M are gratefully acknowledged for CONACYT grants 93389 and 144234/192425. S. A. gratefully acknowledges support from the "GINER DE LOS RIOS" program of the Universidad de Alcalá and B. B. gratefully acknowledges financial support from the Universidad de Alcala (project CCG19/CC-033).

Author information

Corresponding Author

*E-mail for AMC: ana.cuadro@uah.es.

ORCID https://orcid.org/0000-0002-8077-6938

Conflicts of interest

The authors declare no competing interest.

References

[1] (a) Popczyk A, Grabarz A, Cheret Y, El-Ghayoury A, Myśliwiec J, Sahraoui B. Tailoring the acceptor moiety of novel thiophene-based chromophores: Conjoined experimental and theoretical study on the nonlinear optical properties. Dyes Pigments 2021; 196: 109789. https://doi.org/10.1016/j.dyepig.2021.109789.
(b) Rajeshirke M, Sekar N. Multi-stimuli responsive emissive NLOphoric colorants – A recent trend in research, Dyes Pigments 2019; 163: 675-683. https://doi.org/10.1016/j.dyepig.2018.12.063.
(c) Gao W, Liu J, Kityk IV. The Progress in the Field Auxiliary Donors and their Application in Novel Organic Second-Order Nonlinear Optical Chromophores, Mini-Rev. Org. Chem 2019; 16: 228-235. https://doi.org/10.2174/1570193X15666180627150155.
(d) Dini D, Calvete MJF, Hanack M. Nonlinear Optical Materials for the Smart Filtering of Optical Radiation. Chem. Rev. 2016; 116: 13043-13233. ttps://doi.org/10.1021/acs.chemrev.6b00033.
(e) Cambre S, Campo J, Beirnaert C, Verlackt C, Cool P, Wenseleers W. Asymmetric dyes align inside carbon nanotubes to yield a large nonlinear optical response. Nat. Nanotechnol. 2015; 10: 248-252. https://doi.org/10.1038/nnano.2015.1.
(f) Taboukhat S, Akdas-Kilig H, Fillaut JL, Karpierz M, Sahraoui B. Tuning the nonlinear optical properties of BODIPYs by functionalization with dimethylaminostyryl substituents. Dyes Pigments 2017; 137: 507-511. https://doi.org/10.1016/j.dyepig.2016.10.045.
(g) Szukalski A, Parafiniuk K, Haupa K, Goldeman W, Sahraoui B, Kajzar F, Mysliwiec J. Synthesis and nonlinear optical properties of push-pull type stilbene and pyrazoline based chromophores. Dyes Pigments 2017; 142: 507-515. https://doi.org/10.1016/j.dyepig.2017.04.009.
(h) Kulyk B, Taboukhat S, Akdas-Kilig H, Fillaut J-L, Karpierz M, Sahraoui B. Tuning the nonlinear optical properties of BODIPYs by functionalization with dimethylaminostyryl substituents. Dyes Pigments 2017; 137:507-511. https://doi.org/10.1016/j.dyepig.2016.10.045
(i) Spiridon MC, Iliopoulos K, Jerca FA, Jerca VV, Vuluga DM, Vasilescu DS, Gindre D, Sahraoui B. Novel pendant azobenzene/polymer systems for second harmonic generation and optical data storage. Dyes Pigments 2015; 114:2-32. https://doi.org/10.1016/j.dyepig.2014.10.010

[2] (a) Yang X, Lin X, Zhao YS, Yan D. Recent Advances in Micro-/Nanostructured Metal–Organic Frameworks towards Photonic and Electronic Applications. Chem. Eur. J. 2018; 24: 6484-6493. https://doi.org/10.1002/chem.201704650.
(b) Xin H, Ge C, Jiao X, Yang X, Rundel K, McNeill CR, Gao X. Incorporation of 2,6-Connected Azulene Units into the Backbone of Conjugated Polymers: Towards High-Performance Organic Optoelectronic Materials. Angew. Chem. Int. Ed. 2018; 57: 1322-1326. https://doi.org/10.1002/anie.201711802.
(c) Kalinin AA, Smirnov MA, Islamova LN, Fazleeva GM, Vakhonina TA, Levitskaya AI, Fominykh OD, Ivanova NV, Khamatgalimov AR, Nizameev IR, Balakina MY. Synthesis and characterization of new second-order NLO chromophores containing the isomeric indolizine moiety for electro-optical materials. Dyes Pigments 2017; 147: 444-454. https://doi.org/10.1016/j.dyepig.2017.08.047.
(d) Ostroverkhova O. Organic Optoelectronic Materials: Mechanisms and Applications. Chem. Rev. 2016; 116: 13279- 13412. https://doi.org/10.1021/acs.chemrev.6b00127.
(e) Dalton LR, Sullivan PA, Bale DH. Electric Field Poled Organic Electro-optic Materials: State of the Art and Future Prospects. Chem. Rev. 2010; 110: 25-55. https://doi.org/10.1021/cr9000429.

[3] (a) Yu S, Wu X, Wang Y, Guo X, Tong L. 2D Materials for Optical Modulation: Challenges and Opportunities. Adv. Mater. 2017; 29: 1606128. https://doi.org/10.1002/adma.201606128.
(b) Hales JM, Barlow S, Kim H, Mukhopadhyay S, Bredas J, Perry JW, Marder SR. Design of Organic Chromophores for All-Optical Signal Processing Applications. Chem. Mater. 2014; 26; 549-560. https://doi.org/10.1021/cm402893s.

(c) Gieseking RL, Mukhopadhyay S, Risko C, Marder SR, Bredas J. 25th Anniversary Article: Design of Polymethine Dyes for All-Optical Switching Applications: Guidance from Theoretical and Computational Studies. Adv. Mater. 2014; 26: 68-84.
https://doi.org/10.1002/adma.201302676.
(d) He GS, Zhu J, Baev A, Samoc M, Frattarelli DL, Watanabe N, Facchetti A, Agren H, Marks TJ, Prasad PN. Twisted π-System Chromophores for All-Optical Switching. J. Am. Chem. Soc. 2011; 133: 6675-6680.
https://doi.org/10.1021/ja1113112.

[4] (a) Fu Q, Zhu R, Song J, Yang H, Chen X. Photoacoustic Imaging: Contrast Agents and Their Biomedical Applications. Adv. Mater. 2019; 31: 1805875.
https://doi.org/10.1002/adma.201805875.
(b) Mei J, Huang Y, Tian H. Progress and Trends in AIE-Based Bioprobes: A Brief Overview. ACS Appl. Mater. Interfaces 2018; 10: 12217-12261.
https://doi.org/10.1021/acsami.7b14343.
(c) Klymchenko AS. Solvatochromic and Fluorogenic Dyes as Environment-Sensitive Probes: Design and Biological Applications. Acc. Chem. Res. 2017; 50: 366-375.
https://doi.org/10.1021/acs.accounts.6b00517.
(d) Qi J, Qiao W, Wang ZY. Advances in Organic Near-Infrared Materials and Emerging Applications. Chem. Rec. 2016; 16: 1531-1548.
https://doi.org/10.1002/tcr.201600013.

[5] (a) Ding L, Ou Y, Sun A, Li H, Wu T, Zhang D, Xu P, Zhao R, Zhu L, Wang R, Xu B, Hua Y. Developing D-π-D hole-transport materials for perovskite solar cells: The effect of π-bridge on device performance. Mater. Chem. Front. 2021; 5: 876-884.
https://doi.org/10.1039/D0QM00719F.
(b) Chen F. Emerging Organic and Organic/Inorganic Hybrid Photovoltaic Devices for Specialty Applications: Low-Level-Lighting Energy Conversion and Biomedical Treatment. Adv. Opt. Mater. 2019; 7: 1800662 (24p).
https://doi.org/10.1002/adom.201800662.
(c) Benesperi I, Michaels H, Freitag M. The researcher's guide to solid-state dye-sensitized solar cells. J. Mater. Chem. C 2018; 6: 11903-11942.
https://doi.org/10.1039/C8TC03542C.
(d) Prachumrak N, Sudyoadsuk T, Thangthong A, Nalaoh P, Jungsuttiwong S, Daengngern R, Namuangruk S, Pattanasattayavong P, Promarak V. Improvement of D–π–A organic dye-based dye-sensitized solar cell performance by simple triphenylamine donor substitutions on the π-linker of the dye. Mater. Chem. Front. 2017; 1: 1059-1072.
https://doi.org/10.1039/C6QM00271D.
(e) Eom YK, Kang SH, Choi IT, Yoo Y, Kim J, Kim HK. Significant light absorption enhancement by a single heterocyclic unit change in the π-bridge moiety from thieno[3,2-b]benzothiophene to thieno[3,2-b]indole for high performance dye-sensitized and tandem solar cells. J. Mater. Chem. A 2017; 5: 2297-2308.
https://doi.org/10.1039/C6TA09836C.
(f) Lee CP, Lin RY, Lin L, Li C, Chu T, Sun S, Lin JT, Ho K. Recent progress in organic sensitizers for dye-sensitized solar cells. RSC Adv. 2015; 5: 23810-23825.
https://doi.org/10.1039/C4RA16493H.
(g) Malytskyi V, Simon J, Patrone L, Raimundo J. Thiophene-based push–pull chromophores for small molecule organic solar cells (SMOSCs). RSC Adv. 2015; 5: 354-397.
https://doi.org/10.1039/C4RA11664J.

[6] (a) Beharry AA. Next-Generation Photodynamic Therapy: New Probes for Cancer Imaging and Treatment. Biochemistry 2018; 57: 173-174.
https://doi.org/10.1021/acs.biochem.7b01037.
(b) Zhao J, Chen K, Hou Y, Che Y, Liu L, Jia D. Recent progress in heavy atom-free organic compounds showing unexpected intersystem crossing (ISC) ability. Org. Biomol. Chem. 2018; 16: 3692-3701.
https://doi.org/10.1039/C8OB00421H.
(c) Lucky SS, Soo KC, Zhang Y, Nanoparticles in Photodynamic Therapy. Chem Rev. 2015; 115: 1990-2042.
https://doi.org/10.1021/cr5004198.
(d) Ji S, Ge J, Escudero D, Wang Z, Zhao J, Jacquemin D. Molecular Structure–Intersystem Crossing Relationship of Heavy-Atom-Free BODIPY Triplet Photosensitizers. J. Org. Chem. 2015; 80: 5958-5963.
https://doi.org/10.1021/acs.joc.5b00691.

[7] (a) Wu K, Pan S. A review on structure-performance relationship toward the optimal design of infrared nonlinear optical materials with balanced performances. Coord. Chem. Rev. 2018; 377: 191-208.
https://doi.org/10.1016/j.ccr.2018.09.002.
(b) Lv X, Li W, Ouyang M, Zhang Y, Wright DS, Zhang C. Polymeric electrochromic materials with donor–acceptor structures. J. Mater. Chem. C 2017; 5: 12-28.
https://doi.org/10.1039/C6TC04002K.
(c) Ok KM. Toward the Rational Design of Novel Noncentrosymmetric Materials: Factors Influencing the Framework Structures. Acc. Chem. Res. 2016; 49: 2774-2785.
https://doi.org/10.1021/acs.accounts.6b00452.

(d) Wu J, Wilson BA, Smith DW, Nielsen SO. Towards an understanding of structure-nonlinearity relationships in triarylamine-based push-pull electro-optic chromophores: the influence of substituent and molecular conformation on molecular hyperpolarizabilities. J. Mater. Chem. C 2014; 2: 2591-2599. https://doi.org/10.1039/C3TC32510E.

[8] (a) Wang L, Ye JT, Wang H, Xie H, Qiu Y. Self-Assembled Donor–Acceptor Chromophores: Evident Layer Effect on the First Hyperpolarizability and Two-Dimensional Charge Transfer Character. J. Phys. Chem. C 2017; 121: 21616-21626. https://doi.org/10.1021/acs.jpcc.7b07053.

(b) Vijayalakshmi S, Kalyanaraman S. Role of charge transfer on the nonlinear optical properties of donor-π-acceptor (D-π-a) conjugated schiffbases with DFT approach. J. Phys. Org. Chem. 2016; 29: 436-442. https://doi.org/10.1002/poc.3556.

(c) List NH, Zalesny R, Murugan NA, Kongsted J, Bartkowiak W, Aagren H. Relation between Nonlinear Optical Properties of Push–Pull Molecules and Metric of Charge Transfer Excitations. J. Chem. Theory Comput. 2015; 11: 4182-4188. https://doi.org/10.1021/acs.jctc.5b00538.

(d) Mallia AR, Salini PS, Hariharan M. Nonparallel Stacks of Donor and Acceptor Chromophores Evade Geminate Charge Recombination. J. Am. Chem. Soc. 2015; 137: 15604-15607. https://doi.org/10.1021/jacs.5b08257.

[9] (a) Xu H, Zhou Z, Wang J, Zhang X, Li Z, Deng G, Liu F. Synthesis, characterization and comparative studies of nonlinear optical chromophores with rod-like, Y-shaped and X-shaped configurations. Dyes Pigments 2019; 164: 54-61. https://doi.org/10.1016/j.dyepig.2019.01.008.

(b) Chen P, Zhang H, Han M, Cheng Z, Peng Q, Li Q, Li Z. Janus molecules: large second-order nonlinear optical performance, good temporal stability, excellent thermal stability and spherical structure with optimized dendrimer structure. Mater. Chem. Front. 2018; 2: 1374-1382. https://doi.org/10.1039/C8QM00128F.

(c) Hu C, Chen Z, Xiao H, Zhen Z, Liu X, Bo S. Synthesis and characterization of a novel indoline based nonlinear optical chromophore with excellent electro-optic activity and high thermal stability by modifying the π-conjugated bridges. J. Mater. Chem. C 2017; 5: 5111-5118. DOI https://doi.org/10.1039/C7TC00735C.

(d) Yang Y, Liu J, Xiao H, Zhen Z, Bo S. The important role of the isolation group (TBDPS) in designing efficient organic nonlinear optical FTC type chromophores, Dyes Pigments 2017; 139: 239-246. https://doi.org/10.1016/j.dyepig.2016.12.003.

(e) Chen P, Yin X, Xie Y, Li S, Luo S, Zeng H, Guo G, Li Q, Li Z. FTC-containing molecules: large second-order nonlinear optical performance and excellent thermal stability, and the key development of the "Isolation Chromophore" concept. J. Mater. Chem. C 2016; 4: 11474-11481. https://doi.org/10.1039/C6TC04282A.

[10] Bures F. Fundamental aspects of property tuning in push–pull molecules. RSC Adv. 2014; 4: 58826-58851. https://doi.org/10.1039/C4RA11264D.

[11] (a) Sulatskaya AI, Sulatsky MI, Povarova OI, Rodina NP, Kuznetsova IM, Lugovskii AA, Voropay ES, Lavysh AV, Maskevich AA, Turoverov KK. Trans-2-[4-(dimethylamino) styryl]-3-ethyl-1,3-benzothiazolium perchlorate - New fluorescent dye for testing of amyloid fibrils and study of their structure. Dyes Pigments. 2018; 157: 385-395. https://doi.org/10.1016/j.dyepig.2018.05.006.

(b) Wen L, Fang Y, Yang J, Han Y, Song Y. Third-order nonlinear optical properties and ultrafast excited-state dynamics of benzothiazolium salts: Transition in absorption and refraction under different time regimes. Dyes Pigments 2018; 156: 26-32. https://doi.org/10.1016/j.dyepig.2018.03.065.

(c) Cigan M, Gaplovsky A, Sigmundova I, Zahradnik P, Dedic R, Hromadova M. Photostability of D–π–A nonlinear optical chromophores containing a benzothiazolium acceptor. J. Phys. Org. Chem. 2011; 24: 450-459. https://doi.org/10.1002/poc.1782.

(d) Coe BJ, Harris JA, Hall JJ, Brunschwig BS, Hung S, Libaers W, Clays K, Coles SJ, Horton PN, Light ME, Hursthouse MB, Garin J, Orduna J. Syntheses and Quadratic Nonlinear Optical Properties of Salts Containing Benzothiazolium Electron-Acceptor Groups. Chem. Mater. 2006; 18: 5907-5918. https://doi.org/10.1021/cm061594t.

[12] (a) Tang Y, Liu H, Zhang H, Li D, Su J, Zhang S, Zhou H, Li S, Wu J, Tian Y. A series of stilbazolium salts with A-π-A model and their third-order nonlinear optical response in the near-IR region. Spectrochim. Acta Part A 2017; 175: 92-99. https://doi.org/10.1016/j.saa.2016.12.017.

(b) Bures F, Cvejn D, Melanova K, Benes L, Svoboda J, Zima V, Pytela O, Mikysek T, Ruzickova Z, Kityk IV, Wojciechowski A, AlZayed N. Effect of intercalation and chromophore arrangement on the linear and nonlinear optical properties of model aminopyridine push–pull molecules. J. Mater. Chem. C 2016; 4: 468-478. https://doi.org/10.1039/C5TC03499J.

(c) Hao WH, Yan P, Li G, Wang ZY. Short-conjugated zwitterionic cyanopyridinium chromophores: Synthesis, crystal structure, and linear/nonlinear optical properties. Dyes Pigments 2014; 111: 145-155. https://doi.org/10.1016/j.dyepig.2014.06.005.

(d) Li L, Cui H, Yang Z, Tao X, Lin X, Ye N, Yang H. Synthesis and characterization of thienyl-substituted pyridinium salts for second-order nonlinear optics. CrystEngComm 2012; 14: 1031-1037. https://doi.org/10.1039/C1CE06177A.
(d) Coe BJ, Fielden J, Foxon SP, Harris JA, Helliwell M, Brunschwig BS, Asselberghs I, Clays K, Garin J, Orduna J. Diquat Derivatives: Highly Active, Two-Dimensional Nonlinear Optical Chromophores with Potential Redox Switchability. J. Am. Chem. Soc. 2010; 132: 10498-10512. https://doi.org/10.1021/ja103289a.
(e) Coe BJ, Harper CE, Clays K, Franz E. The synthesis of chiral, cationic nonlinear optical dyes based on the 1,1′-binaphthalenyl unit. Dyes Pigments 2010; 87: 22-29. https://doi.org/10.1016/j.dyepig.2010.01.018.
[13] (a) Somma C, Folpini G, Gupta J, Reimann K, Woerner M, Elsaesser T. Ultra-broadband terahertz pulses generated in the organic crystal DSTMS, Opt Lett 2015; 40: 3404-3407. https://doi.org/10.1364/OL.40.003404.
(b) Teng B, Wang S, Feng K, Cao L, Zhong D, You F, Jiang X, Hao L, Sun Q. Crystal growth, quality characterization and THz properties of DAST crystals. Cryst. Res. Technol. 2014; 49: 943-947. https://doi.org/10.1002/crat.201400147.
[14] (a) Jeong C, Kang BJ, Lee S, Lee S, Kim WT, Jazbinsek M, Yoon W, Yun H, Kim D, Rotermund F, Kwon O. Yellow-Colored Electro-Optic Crystals as Intense Terahertz Wave Sources. Adv. Funct. Mater. 2018; 28: 1801143. https://doi.org/10.1002/adfm.201801143.
(b) Lee S, Kang BJ, Shin M, Lee S, Lee S, Jazbinsek M, Yun H, Kim D, Rotermund F, Kwon O. Efficient Optical-to-THz Conversion Organic Crystals with Simultaneous Electron Withdrawing and Donating Halogen Substituents. Adv. Opt. Mater. 2017; 6; 1700930 (12p). https://doi.org/10.1002/adom.201700930.
(c) Dhillon SS, Vitiello MS, Linfield EH, Davies AG, Hoffmann MC, Booske J, Paoloni C et al. The 2017 terahertz science and technology roadmap. J. Phys. D: Appl. Phys. 2017; 50: 043001 (49p). https://doi.org/10.1088/1361-6463/50/4/043001.
[15] (a) Huang J, Yang Z, Murugesan V, Walter E. Spatially Constrained Organic Diquat Anolyte for Stable Aqueous Flow Batteries. ACS Energy Letters 2018; 3: 2533-2538. https://doi.org/10.1021/acsenergylett.8b01550.
(b) Yang NN, Fang JJ, Sui Q, Gao EQ. Incorporating Electron-Deficient Bipyridinium Chromorphores to Make Multiresponsive Metal–organic Frameworks. ACS Appl. Mater. Interfaces 2018; 10: 2735-2744. https://doi.org/10.1021/acsami.7b17381.
(c) Buckley LE, Coe BJ, Rusanova D, Sanchez S, Jirasek M,. Joshi VD, Vavra J, Khobragade D, Pospisil L, Ramesova S, Cisarova I, Saman D, Pohl R, Clays K, Van Steerteghem N, Brunschwig BS, Teply F. Ferrocenyl helquats: unusual chiral organometallic nonlinear optical chromophores, Dalton Trans. 2017; 46: 1052-1064. https://doi.org/10.1039/C6DT04347J.
(d) Coe BJ, Rusanova D, Joshi VD, Sanchez S, Vavra J, Khobragade D, Severa L, Cisarova I, Saman D, Pohl R, Clays K, Depotter G, Brunschwig BS, Teply F. Helquat Dyes: Helicene-like Push–Pull Systems with Large Second-Order Nonlinear Optical Responses. J. Org. Chem. 2016; 81: 1912-1920. https://doi.org/10.1021/acs.joc.5b02692.
[16] Sucunza D, Cuadro AM, Alvarez-Builla J, Vaquero JJ. Recent Advances in the Synthesis of Azonia Aromatic Heterocycles. J. Org. Chem. 2016; 81: 10126-10135. https://doi.org/10.1021/acs.joc.6b01092.
[17] (a) Marcelo G, Pinto S, Caneque T, Mariz IFA, Cuadro AM, Vaquero JJ, Martinho JMG, Maçôas E. Nonlinear Emission of Quinolizinium-Based Dyes with Application in Fluorescence Lifetime Imaging. J. Phys. Chem. A 2015; 119: 2351-2362. https://doi.org/10.1021/jp507095b.
(b) Maçôas E, Marcelo G, Pinto S, Cañeque T, Cuadro AM, Vaquero JJ, Martinho JMG. A V-shaped cationic dye for nonlinear optical bioimaging. Chem. Commun. 2011; 47: 7374-7376. https://doi.org/10.1039/C1CC12163D.
(c) Caneque T, Cuadro AM, Alvarez-Builla J, Perez-Moreno J, Clays K, Castano O, Andres JL, Vaquero JJ. Novel charged NLO chromophores based on quinolizinium acceptor units. Dyes Pigments 2014; 101: 116-121. https://doi.org/10.1016/j.dyepig.2013.09.031.
[18] (a) Zacharioudakis E, Caneque T, Custodio R, Muller S, Cuadro AM, Vaquero JJ, Rodriguez R. Quinolizinium as a new fluorescent lysosomotropic probe. Bioorg. Med. Chem. Lett. 2017; 27: 203-207. https://doi.org/10.1016/j.bmcl.2016.11.074.
(b) Suarez RM, Bosch P, Sucunza D, Cuadro AM, Domingo A, Mendicuti F, Vaquero JJ. Targeting DNA with small molecules: a comparative study of a library of azonia aromatic chromophores. Org. Biomol. Chem. 2015; 13: 527-538. https://doi.org/10.1039/C4OB01465K.
(c) Mariz IFA, Pinto SN, Santiago AM, Martinho JMG, Recio J, Vaquero JJ, Cuadro AM, Maçôas E. Two-photon activated precision molecular photosensitizer targeting mitocondria, Commun. Chem. 2021; 4: 142. https://doi.org/10.1038/s42004-021-00581-4.
[19] (a) Cañeque T, Cuadro AM, Custodio R, Alvarez-Builla J, Batanero B, Gómez-Sal P, Pérez-Moreno J, Clays K, Castaño O, Andrés JL, Carmona T, Mendicuti F, Vaquero JJ. Azonia aromatic heterocycles as

a new acceptor unit in D-π-A+ vs D-A+ nonlinear optical chromophores. Dyes Pigments 2017; 144: 17-31.
https://doi.org/10.1016/j.dyepig.2017.05.005.
(b) Ramirez MA, Custodio R, Cuadro AM, Alvarez-Builla J, Clays K, Asselberghs I, Mendicuti F, Castaño O, Andrés JL, Vaquero JJ. Synthesis of charged bis-heteroaryl donor–acceptor (D–A+) NLO-phores coupling (π-deficient–π-excessive) hetero aromatic rings. Org Biomol Chem. 2013; 11: 7145-7154.
https://doi.org/10.1039/C3OB41159A
(c) Ramirez MA, Cuadro AM, Alvarez-Builla J, Castano O, Andres JL, Mendicuti F, Clays K, Asselbergh I, Vaquero JJ. Donor-(π-bridge)-azinium as D-π-A+ one-dimensional and D-π-A+-π-D multidimensional V-shaped chromophores, Biomol Chem. 2012; 10: 1659-1669.
https://doi.org/10.1039/C2OB06427H.
(d) M. A. Ramirez, T. Caneque, A. M. Cuadro, F. Mendicuti, K. Clays , I. Asselbergh and J. J. Vaquero, Novel linear and V-shaped D-pi-A+-pi-D chromophores by Sonogashira reaction, *ARKIVOC*. 2011, 140-155.
(e) Caneque T, Cuadro AM, Alvarez-Builla J, Perez-Moreno J, Clays K, Marcelo G, Mendicuti F, Castaño O, Andrés JL, Vaquero JJ. Heteroaromatic Cation-Based Chromophores: Synthesis and Nonlinear Optical Properties of Alkynylazinium Salts. Eur. J. Org. Chem. 2010; 33: 6323-6330.
https://doi.org/10.1002/ejoc.201000816.
[20] (a) Chen X, Zhang N, Cai L, Li P, Wang M, Guo G. N-Methyl-4-pyridinium Tetrazolate Zwitterion-Based Photochromic Materials. Chem. Eur. J. 2017; 23: 7414-7417.
https://doi.org/10.1002/chem.201700677.
(b) Beverina L, Sanguineti A, Battagliarin G, Ruffo R, Roberto D, Righetto S, Soave R, Lo Presti L, Ugo R Pagani G. A. UV absorbing zwitterionic pyridinium-tetrazolate: exceptional transparency/optical nonlinearity trade-off. Chem. Commun. 2011; 47: 292-294.
https://doi.org/10.1039/C0CC01652G.
(c) Marder SR. Themed issue: nonlinear optics. The evolving field of nonlinear optics—a personal perspective. J. Mater. Chem. 2009; 19: 7392-7393.
https://doi.org/10.1039/B916810A.
(d) Nerenz H, Meier M, Grahn W, Reisner A, Schmälzlin E, Stadler S, Meerholtz K, Bräuchle C, Jones PG. Nonlinear optical chromophores with isoquinolines, thieno[2,3-c]-pyridines and 2-(2'-thienyl)pyridines as inherently polarized π-electron bridges. J. Chem. Soc., Perkin Trans. 2 1998; 2: 437–448.
https://doi.org/10.1039/A703325G.
[21] (a) Jeong JH, Kim J, Campo J, Lee SH, Jeon WY, Wenseleers W, Jazbinsek M, Yun H, Kwon OP. N-Methyl quinolinium derivatives for photonic applications: Enhancement of electron-withdrawing character beyond that of the widely-used N-methylpyridinium. Dyes Pigments 2015; 113: 8-17.
https://doi.org/10.1016/j.dyepig.2014.07.016.
(b) Lee SH, Jazbinsek M, Yun H, Kim JT, Lee YS, Kwon OP. New quiolinium polymorph with optimal packing for maximal off-diagonal nonlinear optical response. Dyes Pigments 2013; 96: 435-439.
https://doi.org/10.1016/j.dyepig.2012.08.022
(c) Coe BJ, Beljonne D, Vogel H, Garin J, Orduna J. Theoretical Analyses of the Effects on the Linear and Quadratic Nonlinear Optical Properties of N-Arylation of Pyridinium Groups in Stilbazolium Dyes. J. Phys. Chem. A. 2005; 109: 10052-10057.
https://doi.org/10.1021/jp053721z.
[22] (a) Hrobarik P, Sigmundova I, Zahradnik P, Kasak P, Arion V, Franz E, Clays K. Molecular Engineering of Benzothiazolium Salts with Large Quadratic Hyperpolarizabilities: Can Auxiliary Electron-Withdrawing Groups Enhance Nonlinear Optical Responses?. J. Phys. Chem. C. 2010; 114: 22289-22302.
https://doi.org/10.1021/jp108623d.
(b) Quist F, Vande Velde CML, Didier D, Teshome A, Asselberghs I, Clays K, Sergeyev S. Push–pull chromophores comprising benzothiazolium acceptor and thiophene auxiliary donor moieties: Synthesis, structure, linear and quadratic nonlinear optical properties. Dyes Pigments 2009; 81: 203-210.
https://doi.org/10.1016/j.dyepig.2008.10.004.
(c) Coe BJ, Harris JA, Hall JJ, Brunschwig BS, Hung S, Libaers W, Clays K, Coles SJ, Horton PN, Light ME, Hursthouse MB, Garin J, Orduna J. Syntheses and Quadratic Nonlinear Optical Properties of Salts Containing Benzothiazolium Electron-Acceptor Groups. Chem. Mater. 2006; 18: 5907-5918.
https://doi.org/10.1021/cm061594t.
[23] (a) Cheng Q, Shi X, Li C, Jiang Y, Shi Z, Zou J, Wang X, Wang X, Cui Z. Chromophores with side isolate groups and applications in improving the poling efficiency of second nonlinear optical (NLO) materials. Dyes Pigments 2019; 162: 721-727.
https://doi.org/10.1016/j.dyepig.2018.11.001.
(b) Li M, Li Y, Zhang H, Wang S, Ao Y, Cui Z. Molecular engineering of organic chromophores and polymers for enhanced bulk second-order optical nonlinearity. J. Mater. Chem. C 2017; 5: 4111-4122.
https://doi.org/10.1039/C7TC00713B.
(c) Jia J, Li Y, Gao J. A series of novel ferrocenyl derivatives: Schiff bases-like push-pull systems with large third-order optical responses. Dyes Pigments 2017; 137: 342-351.
https://doi.org/10.1016/j.dyepig.2016.11.008.

(d) Zhang X, Yu G, Huang X, Chen W. Introducing the triangular BN nanodot or its cooperation with the edge-modification via the electron-donating/withdrawing group to achieve the large first hyperpolarizability in a carbon nanotube system. Phys. Chem. Chem. Phys. 2017; 19: 17834-17844. https://doi.org/10.1039/C7CP02327H.
(e) Ziemann EA, Freudenreich N, Speil N, Stein T, Van Steerteghem N, Clays K, Heck J. Synthesis, structure and NLO properties of a 1,3,5-substituted tricationic cobaltocenium benzene complex. J. Organomet Chem. 2016; 820: 125-129. https://doi.org/10.1016/j.jorganchem.2016.07.021
(f) Yang Y, Wang H, Liu F, Yang D, Bo S, Qiu L, Zhen Z, Liu X. The synthesis of new double-donor chromophores with excellent electro-optic activity by introducing modified bridges. Phys. Chem. Chem. Phys. 2015; 17: 5776-5784. https://doi.org/10.1039/C4CP05829A.
(g) Zhang Y, Blau WJ. Dipoles align inside a nanotube. Nat. Nanotechnol. 2015; 10: 205-206. https://doi.org/10.1038/nnano.2015.9.
(h) Beverina L, Pagani GA. π-Conjugated Zwitterions as Paradigm of Donor–Acceptor Building Blocks in Organic-Based Materials. Acc. Chem. Res. 2014; 47: 319-329. https://doi.org/10.1021/ar4000967.

[24] For Stille reaction see: (a) Heravi MM, Mohammadkhani L. Recent applications of Stille reaction in total synthesis of natural products: An update. J. Organomet. Chem. 2018; 869: 106-200. https://doi.org/10.1016/j.jorganchem.2018.05.018.
(b) Cordovilla C, Bartolome C, Martinez-Ilarduya JM, Espinet P, The Stille Reaction, 38 Years Later. ACS Catal. 2015; 5: 3040-3053. https://doi.org/10.1021/acscatal.5b00448.

[25] (a) Cañeque T, Cuadro AM, Alvarez-Builla J, Vaquero JJ, Efficient functionalization of quinolizinium cations with organotrifluorobrates in water. Tetrahedron Lett. 2009; 50: 1419-1422. https://doi.org/10.1016/j.tetlet.2009.01.040.
(b) Nuñez A, Abarca B, Cuadro AM, Alvarez-Builla J, Vaquero JJ. Ring-Closing Metathesis Reactions on Azinium Salts: Straightforward Access to Quinolizinium Cations and Their Dihydro Derivatives. J. Org. Chem. 2009; 74: 4166-4176. https://doi.org/10.1021/jo900292b.
(c) Nuñez A, Cuadro AM, Alvarez-Builla J, Vaquero JJ. A New Approach to Polycyclic Azonia Cations by Ring-Closing Metathesis. Org. Lett. 2007; 9: 2977-2980. https://doi.org/10.1021/ol070773t.
(d) García-Cuadrado D, Cuadro AM, Barchín BM, Nuñez A, Cañeque T, Alvarez-Builla J, Vaquero JJ. Palladium-Mediated Functionaliza tion of Heteroaromatic Cations: Comparative Study on Quinolizinium Cation. J. Org. Chem. 2006; 71: 7989-7995. https://doi.org/10.1021/jo060634+.
(e) García-Cuadrado D, Cuadro AM, Alvarez-Builla J, Sancho U, Castaño O, Vaquero JJ. First Synthesis of Biquinolizinium Salts: Novel Example of a Chiral Azonia Dication. *Org. Lett.* 2006; **8**: 5955-5958. https://doi.org/10.1021/ol062314i.
(f) Garcia-Cuadrado D, Cuadro AM, Alvarez-Builla J, Vaquero JJ. Sonogashira Reaction on Quinolizium Cations. Org. Lett. 2004; 6: 4175-4178. https://doi.org/10.1021/ol048368e.

[26] (a) Liu C, Zhai J, Ma Y, Liang Y. A Simple Way for the Preparation of 3-Ferrocenyl-6,8-disubstituted Quinoline. Synth. Commun. 1998; 28: 2731-2735. https://doi.org/10.1080/00397919808004844.
(b) Liu CM, Chen BH, Liu WY, Wu XL, Ma YX. Conversion of tributylstannylferrocene to a variety of heteroaryl ferrocenes. J. Organomet. Chem. 2000; 598: 348-352. https://doi.org/10.1016/S0022-328X(99)00733-0.

[27] Misra R, Bhattachraryya SP , Intramolecular Charge Transfer (ICT): Theory and Applications. 2018 Wiley-VCH Verlag GmbH & Co. KGaA.

[28] Brouver AM. Standards for photoluminescence quantum yield measurements in solution (IUPAC Technical Report). Pure Appl. Chem. 2011; 83: 2213-2228. https://doi.org/10.1351/PAC-REP-10-09-31.

[29] Toriumi N, Asano N, Miyamoto K, Muranaka A, Uchiyama M. Alkynylpyridinium Salts: Highly Electrophilic Alkyne–Pyridine Conjugates as Precursors of Cationic Nitrogen-Embedded Polycyclic Aromatic Hydrocarbons. J. Am. Chem. Soc. 2018; 140: 3858−3862. https://doi.org/10.1021/jacs.8b00356.

[30] D'Andrade BW, Datta S, Forrest SR, Djurovich P, Polikarpov E, Thompson ME. Relationship between the ionization and oxidation potentials of molecular organic semiconductors. Org. Electron. 2005; 6: 11-20. https://doi.org/10.1016/j.orgel.2005.01.002.

[31]Okamoto K, Chiba K. Electrochemical Total Synthesis of Pyrrolophenanthridone Alkaloids: Controlling the Anodically Initiated Electron Transfer Process, Organic Letters 2020; 22: 3613-3617. https://doi.org/10.1021/acs.orglett.0c01082.

[32] Kumar J, Kumar N, Kumar P. Hota, Optical properties of 3-substituted índoles. RSC Adv. 2020; 10: 28213-28224. https://doi.org/10.1039/D0RA05405D.

[33] **Gaussian 09**, Revision A.1, Frisch MJ, Trucks GW, Schlegel HB, Scuseria GE, Robb MA, Cheeseman JR, Scalmani G, Barone V, Mennucci B, Petersson GA, Nakatsuji H, Caricato M, Li X, Normand HPJ, Raghavachari K, Rendell A, Burant JC, Iyengar SS, Tomasi J, Cossi M, Rega N, Millam JM, Klene M, Knox JE, Cross JB, Bakken V, Adamo C, Jaramillo J, Gomperts R, Stratmann RE, Yazyev O, Austin AJ, Cammi R, Pomelli C, Ochterski JW, Martin RL, Morokuma K, Zakrzewski VG, Voth GA, Salvador P, Dannenberg JJ, Dapprich S, Daniels AD, Farkas Ö, Foresman JB, Ortiz JV, Cioslowski J, Fox DJ. Gaussian, Inc., Wallingford CT, 2009.

[34] Bredas JL. Mind the gap!, Mater. Horiz. 2014; 1: 17–19. https://doi.org/10.1039/C3MH00098B.

Universidad de Alcalá

DEPARTAMENTO DE QUIMICA ORGANICA
Y QUIMICA INORGANICA
Ctra. Madrid – Barcelona, km. 33,600
28871 Alcalá de Henares (Madrid)
Telf.: (91) 885 46 28
Fax. : (91) 885 46 86
e-mail: ana.cuadro@uah.es

Subject: Conflict of interest.

On behalf of my co-authors and myself, we declare that there are no conflicts of interest.

Sincerely,

Prof. Ana M. Cuadro

(corresponding author)

Contributions:

Esmeralda Sánchez-Pavón: Investigation, Methodology.

Javier Recio: Investigation, Methodology, Writing – original draft, review & editing.

Marco Antonio Ramirez: Investigation, Methodology.

Belen Batanero: Investigation, Methodology, Writing – original draft.

Koen Clays: Methodology.

Francisco Mendicuti: Methodology, Writing – original draft.

Gema Marcelo: Investigation

Thais Carmona: Investigation

Obis Castaño: Formal análisis.

Silvia Angelova: Formal análisis, Investigation, Writing – original draft.

José L. Andrés: Formal análisis.

Juan J. Vaquero: Funding acquisition, Methodology.

Ana M. Cuadro: Conceptualization, Supervision, Methodology, Writing – original draft, review & editing.

Highly efficient unbridged D-A$^+$(D) chromophores based on the quinolizinium cation for nonlinear optical (NLO) applications

Esmeralda Sánchez-Pavón,[a†] Javier Recio,[a♯] Marco Antonio Ramirez,[a≠] Belen Batanero,[a] Koen Clays,[b] Francisco Mendicuti,[c] Gema Marcelo,[c] Thais Carmona,[c±] Obis Castaño,[c] Silvia Angelova,[c‡] Jose L. Andres,[d] Juan J. Vaquero[a*] and Ana M. Cuadro[a]*

[a] Departamento de Química Orgánica y Química Inorgánica, Universidad de Alcalá, (IRYCIS); 28871-Alcalá de Henares, Madrid, Spain

[b] Department of Chemistry, University of Leuven, Celestijnenlaan 200 D,3001 Leuven, Belgium

[c] Departamento de Química Analítica, Química Física e Ingeniería Química, Universidad de Alcalá, 28871 Alcalá de Henares, Madrid, Spain

[d] IES Matarraña, 44580 Valderrobres, Teruel, Spain

[†] E. Sanchez-Pavon (permanent address): Facultad de Ciencias Químicas UV, Orizaba, Mexico

[♯] J. Recio (current address): Centro de Investigaciones Biológicas Margarita Salas-CSIC, 28040, Madrid, Spain

[≠] M.A. Ramirez (permanent address): Departamento de Farmacia, Universidad de Guanajuato, Mexico

± T. Carmona (permanent address): Center for the Development of Nanoscience and Technology (CEDENNA), Universidad de Santiago de Chile, 9170022 Santiago de Chile

[‡] S. Angelova (permanent address): Institute of Optical Materials and Technologies, Bulgarian Academy of Sciences, 1113, Sofia, Bulgaria

* Corresponding author: Ana M. Cuadro, e-mail: ana.cuadro@uah.e

Dedicated to the memory of Prof. Dr. Carolina Burgos

Abstract: Novel charged D-A$^+$ chromophores based on quinolizinium cations as acceptor unit have been prepared by treating haloquinolizinium salts with *N*-heteroarylstannanes under Stille reaction conditions. This approach provides an easy access to potential one-dimensional D-A$^+$ and two-dimensional D-A$^+$-D chromophores in which the acceptor moiety (A$^+$) is the simple azonia cation and the donors are different π-rich *N*-heterocycles. The first hyperpolarizabilities (β) were measured by hyper-Rayleigh scattering experiments and the experimental data confirmed that the inherent polarization between donor and acceptor fragments modulates the NLO properties. The electronic structures and properties (including both the linear and nonlinear optical properties) of the quinolizinium chromophores were examined by theoretical (DFT, HF and MP2) calculations. A promising strategy for the rational design of D-A building blocks to create new organic-based NLO materials is proposed.

Keywords: quinolizinium cation, D-A$^+$(D) unbridged chromophores, nonlinear optical application, first hyperpolarizability

Graphical abstract:

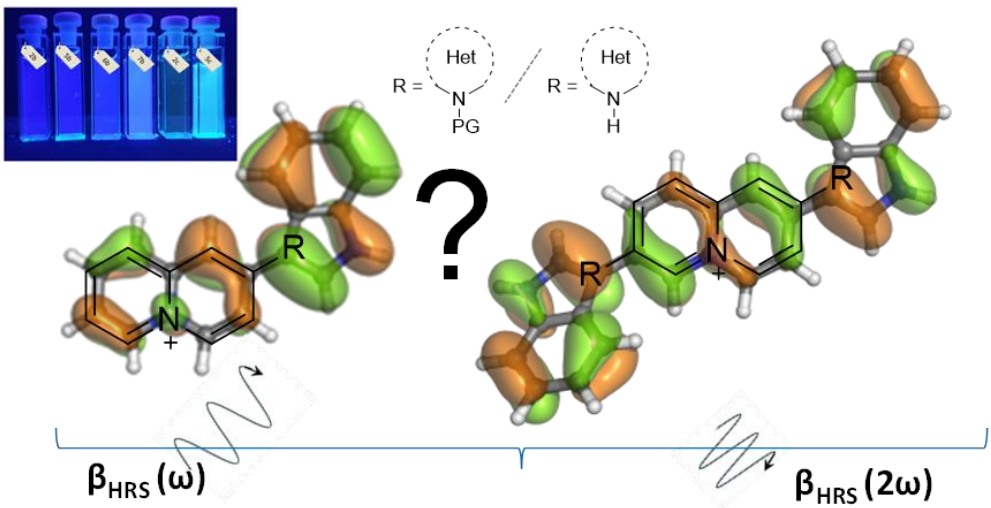

Research highlights

- Quinolizinium cation is efficient acceptor unit in new D-A^+ and D-A^+(D) unbridged chromophores
- Inherent polarization between donor and acceptor fragments modulates NLO properties
- The N-protecting groups in the heterocyclic donors strongly affect the β_{HRS} values
- Quinolizinium systems in comparison with pyridinium ones appear to perform better in terms of NLO properties
- Valuable hints for the rational design of D-A building blocks with potential application in NLO devices

1. Introduction

In recent years, the design and synthesis of conjugated donor-acceptor (D-A) organic molecules with nonlinear optical (NLO) [1] properties has been of considerable interest due to their applications in areas such as optoelectronics [2], all-optical data processing [3], biological imaging [4], dye-sensitized solar cells [5] and photodynamic therapy [6], amongst others, as well as for the understanding [7] of the structural requirements needed to achieve large second-order polarizabilities, related to an electronic intramolecular charge transfer (ICT) effect [8], excellent thermal and chemical stabilities [9] and easy tuning of the D-A properties for various applications [10].

Although a wide range of materials has been studied over the past few decades, the cationic acceptors have only recently been introduced. Amongst the cationic chromophores reported, charged acceptor units are restricted to benzothiazolium [11] and azinium salts [12]. The latter have received significant attention as 1D(D-π-A^+) and 2D(D-π-A^+-π-D) pyridinium-based chromophores, including DAST(4-(N,N-dimethylamino)-4´-N´-methylstilbazolium tosylate) /DSTMS(4-N,N´-dimethylamino-4´-N´-methylstilbazolium-2,4,6-trimethyl benzenesulfonate) [13] and diquats/helquats [14] for the design of stable redox-active organic materials (ROMs),

switching materials and chiral NLO chromophores [15]. However, azonia aromatic heterocycles (AZAH) [16] have not been explored to date as an acceptor unit, except by us, as a marker in nonlinear optical bioimaging, where they were found to exhibit a large two-photon absorption (2PA), and as push-pull cationic chromophores (D-π-A+-π-D) [17]. Furthermore, some derivatives of these azonia salts have been found to be useful in important applications, for example as highly fluorescent lysosomotropic probes and photosensitizer [18] (Figure 1).

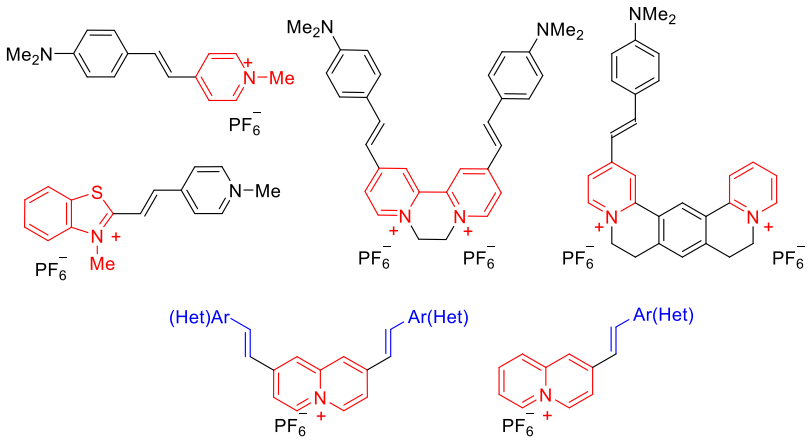

Figure 1. Representative examples of nonlinear optical chromophores based on azolium, pyridinium and quinolizinium cations as acceptor units.

As a result of our research on the applications of heteroaromatic cations in the NLO field [19], we recently showed that chromophores generated by direct coupling of a quinolizinium fragment to an aryl donor [19a] or a pyridinium cation to a π-rich heterocycle [19b], a kind of molecule that rarely appears in the NLO literature [20], may exhibit better nonlinear optical properties than other heteroaromatic cations tested to date, such as azinium [21] and azolium [22] salts. When connected directly, these chromophores have been shown to be useful for guiding the design of new NLO materials, thus contributing to the development of new β enhancement strategies [23] as alternatives to traditional π-conjugated chromophores in applications for nonlinear optical materials.

Herein we report the synthesis of a series of dipolar D-A^+ and quadrupolar D-A^+-D charged chromophores (Figure 2), which are synthesized by way of a Stille cross-coupling reaction

[24], to give push-pull molecules that combine quinolizinium cations as acceptor units (A^+) with π-rich N-heterocycles as donor units to achieve higher polarizability.

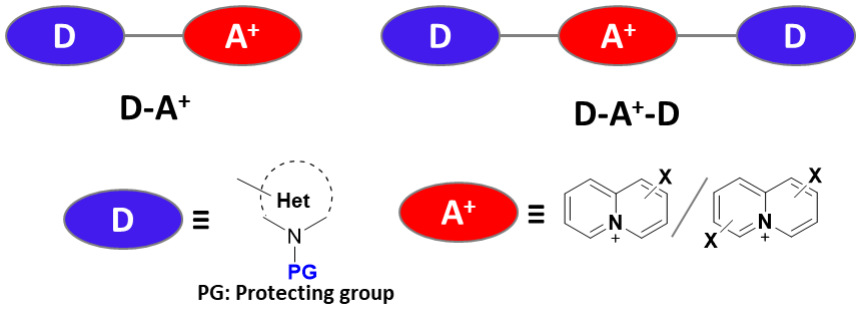

Figure 2. D–A^+(D) chromophores created by coupling a quinolizinium-based π-deficient charged heteroaromatic cation to a π-rich heteroarenes

From literature is known that the absence of a conjugated bridge ensures a higher chemical stability with respect to standard D-π-A systems [20b], and the introduction of multiple D units gives rise to multi-dimensional (MD) structures that can offer increased β responses by extending the charge transfer to higher dimensions. The photophysical properties of the resulting D-A+ and D-A+-D chromophores were studied by means of UV-visible and hyper-Rayleigh scattering (HRS) spectroscopy, as well as by performing quantum-chemical calculations at different levels of theory, including density functional theory (DFT), Hartree-Fock (HF) and post-HF ab initio methods (MP2). In addition, the redox activity was evaluated by cyclic voltammetry and the results of the theoretical calculations were compared with those obtained for known pyridinium-based systems to illustrate the influence of quinolizinium as acceptor unit and to establish the relevant structure-activity relationships.

2. Results and Discussion

2.1. Synthesis

Chromophores with the general structure D-A^+ (Figure 2) were synthesised starting from 2-bromoquinolizinium (**1**) using previously described conditions for palladium-promoted coupling reactions with quinolizinium salts [25], adapted and optimized for **1** using two

different catalytic systems, namely palladium tetrakis(triphenylphosphine)/copper iodide [$Pd(PPh_3)_4$/CuI] (Method A) or tri(ortho-tolyl)phosphine/tris(dibenzylideneacetone) dipalladium [$Pd_2(dba)_3$/P(*o*-Tol)$_3$] (Method B), both in DMF as solvent. Initially, starting from **1** and 3-tributylstannanyl-(toluen-4-sulfonyl)-1*H*-indole, with $Pd(PPh_3)_4$ (5% mol) and CuI as co-catalyst (10% mol) in DMF (Method **A**), the coupled compound **2a** was obtained in 97% yield after 4 h at 70 °C (Scheme 1). As such, method **A** was applied to produce a variety of coupling products (Table 1). The data collected showed that conditions **A** lead to the corresponding coupling products (**2a-j**) in good yields (except for ferrocenylstannanes Fc-$SnBu_3$ [26]). Compounds 2**f** and **2i** (entries 6 in Table 1, and entry 9 Table S1 in SI) were therefore synthesised using Method **B**, in good yields.

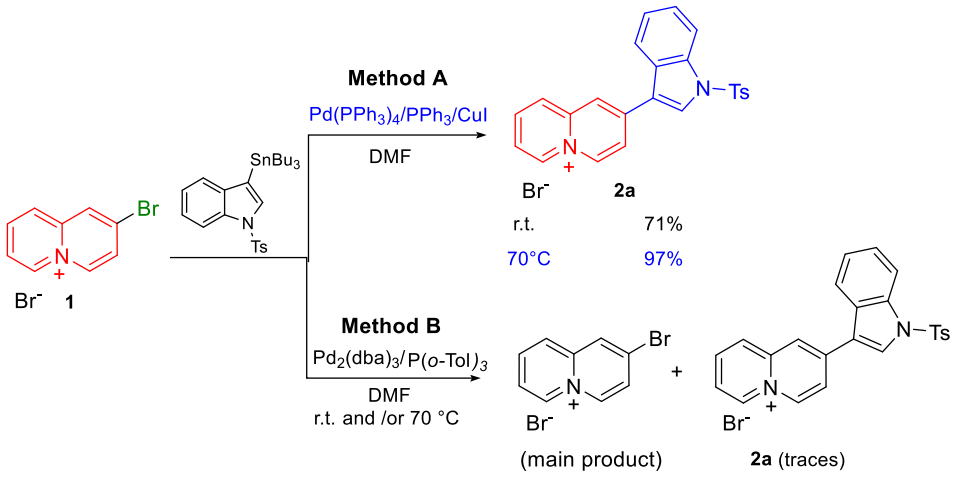

Scheme 1. Stille reaction of 2-bromoquinolizinium with heteroarylstannanes

The coupling with stannane pyrrole and indole derivatives, protected with TIPS (entry 3) and TBDMS (entry 6), respectively, led to coupling products **2c** and **2f,** respectively, with loss of the protecting groups.

Coupling with electron-deficient pyrazine, pyrimidine and pyridine stannanes proved possible without protecting the NH_2 group, obtaining moderate to good yields (see SI, Table S1, compounds **2g**, **2h**, **2i**).

In light of the approach outlined in the introduction and considering the results of the couplings to afford D-A$^+$ chromophores, we examined the coupling of 2,7-dibromo quinolizinium (**3**) with similar stannanes under Stille reaction conditions, using Methods **A** or **B**, to synthesise the D-A$^+$-D chromophores.

The study of reactivity of **3** with tributylstannylpyrazole was carried out first using one equivalent of stannane and $Pd(PPh_3)_4$/CuI as catalyst in DMF (Method **A**). Under these conditions, after 22 h at 70 °C, mono-coupling at the C-2 position furnished product **4b** along with unreacted starting material. Subsequently, coupling with 2-2.5 equivalents of tributylstannanyl-1-trityl-1*H*-pyrazole, under the reaction conditions outlined above, afforded di-coupling product **5b** in 52% yield (Scheme 3), although under these conditions the mono-coupling product **4b** was also formed. An evaluation of the process with all stannanes (2-2.5 equiv.), using methods **A** and **B**, can be found in Table 2.

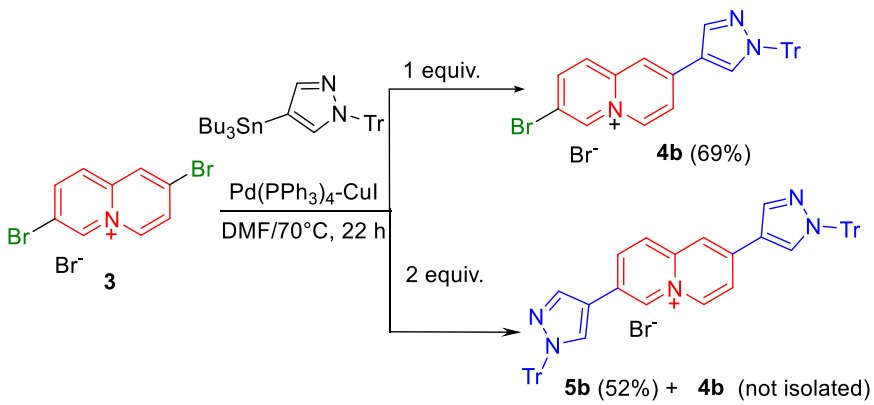

Scheme 2. Stille reaction of 2,7-bromoquinolizinium with heteroarylstannanes.

Based on the results, it should be noted that, generally, when protected tributylstannylpyrrol (R = TMS or TIPS) was used in a temperature range of 70-75 °C for 8 or 24 h, a mixture of mono-coupling product **4c** (not isolated) and di-coupling product **5c** (61%), with removal of the protecting group, was observed by ^{1}H NMR spectroscopy.

Table 1. Stille reaction of 2-Bromoquinolizinium salt

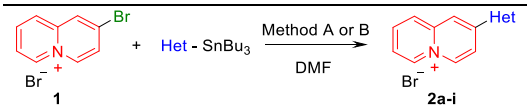

Table 2. Stille reaction of 2,7-Bromo quinolizinium salt

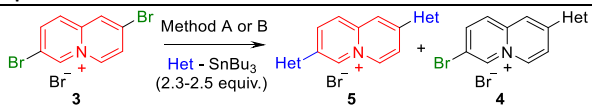

Entry	Het-SnBu₃	Mono-coupling Product 2	Reac. Conds. Meth/T(°C)/ t(h)	Yield (%)	Di-coupling product 5	Reac. Conds. T(°C)/t(h)/Meth/ equiv. Het-SnBu₃	Yield % 5	Yield % 4
1	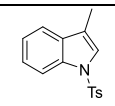	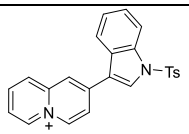 **2a**	**A**/70 /4	97				
2		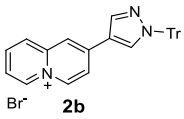 **2b**	**A**/65 /8	94[1]	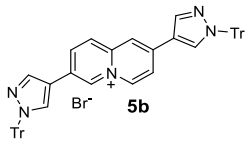 **5b**	70 /22/ **A**/1 70 /22/ **A**/2	69	52
3		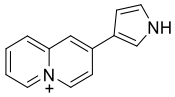 **2c**	**A**/70 /24	74[1]	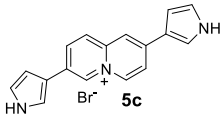 **5c**	70-75/8 or 24/**A**/2.3	61 (R=H))	
4	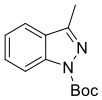	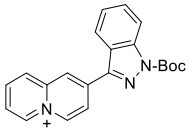 **2d**	**A**/r.t/24	70	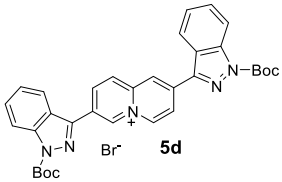 **5d**	70 /24/**A**/2.3 rt /7/**A**/2.3	15 30	13 25
5	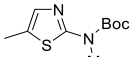	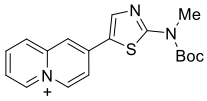 **2e**	**A**/r.t/24	93	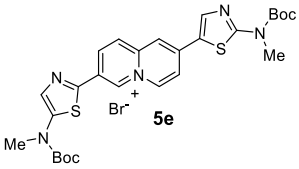 **5e**	70 /22/**A**/2.8	36	
6	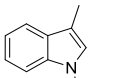	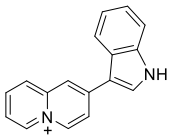 **2f**	**B**/75 /20	(X⁻= Br) 94	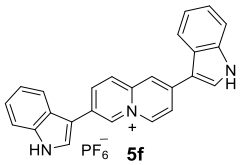 **5f**	70 /24/**B**/2.5	(X⁻= Br⁻) 60	

TMS: Trimethylsilyl; TIPS: Triisopropylsilyl; TBS: tert-Butyldimethylsilyl; Tr: Trityl; Boc: tert-Butoxycarbonyl; Ts: Tosyl.
Table 1. Method A: $Pd(PPh_3)_4$/CuI/rt or 70 °C/DMF; Method B: $Pd_2(dba)_3$/P(*o*-Tol)$_3$/70-75 °C/DMF.
Table 2. Method A: $Pd(PPh_3)_4$/CuI/rt or 70-75 °C/DMF; Method B: $Pd_2(dba)_3$/P(*o*-Tol)$_3$/75 °C/DMF.

The coupling reaction between **3** and stannylindazole at room temperature for 7 h afforded **5d** and **4d** (30% and 25%, respectively). This result is in agreement with the conditions applied for the coupling between **1** and tributylstannylindazole, for which the best results were obtained at room temperature (see Table 1, entry 5). Under standard conditions, the coupling of **3** with

the tributylstannylthiazole derivative (entry 4, Table 2) leads to the di-coupling compound **5e** in 36% yield as the only product.

The coupling of **3** with tributylstannylindole (entry 5, Table 2), protected as the TBDMS derivative, using the catalytic system [$Pd_2(dba)_3$/P(o-Tol)$_3$] in DMF at 70 °C for 24 h, gave **5f** (deprotected) in 60% yield (Table 2, entry 5). Under these reaction conditions, indole deprotection is observed as in the case for pyrrole.

In light of these results for the coupling reactions of 2-bromoquinolizinium **1** and 2,7-dibromoquinolizinium **3** with different stannanes (Table 1 and 2), we were unable to establish a relationship between the nature of the stannane and the reaction yields (medium or high) because of the low solubility of the coupling compounds in common organic solvents. Another obstacle was the difficulties encountered during the purification process as the mono- and di-coupled systems have similar *Rf* (retention factor) values, with both being lower than for the starting compound **3**.

Finally, having obtained unprotected quinolizinium derivatives D-A$^+$ (**2c, 2f**) and D-A$^+$-D (**5c**, **5f**) directly upon loss of the protecting group during Stille coupling with pyrrole and indole, we then investigated the reaction conditions for deprotection of chromophores **2b**(Tr), **2d**(Boc), **5b**(Tr) and **5d**(Boc) (Scheme 3 and SI), with the aim of analyzing the effect of the presence/absence of a protecting group on the linear and nonlinear optical properties of 1D and 2D chromophores (see Figure 5 and/or Figure 8).

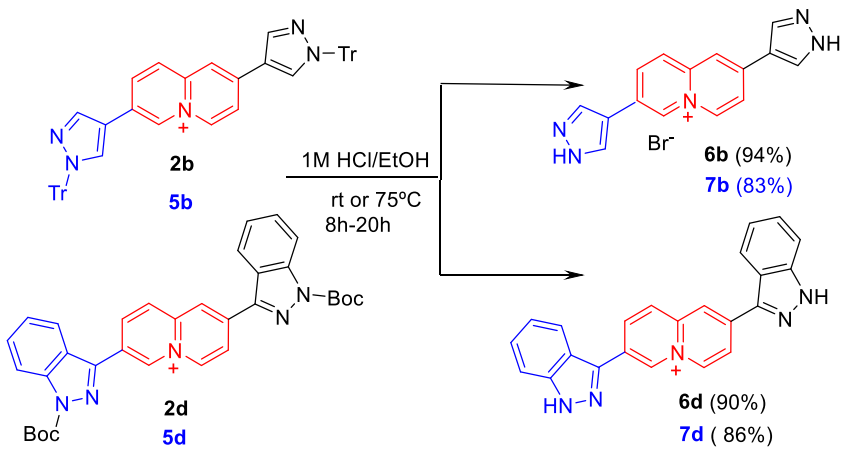

Scheme 3. Reaction conditions for unprotected chromophores

The isolation of functionalized unprotected quinolizinium systems will allow us to direct our research towards generating structures with high charge delocalization between the two rings upon abstraction of a proton from the donor group, thus generating a heterobetainic system as a new organic material. As mentioned above, most of the hyperpolarizability studies reported in the literature have involved traditional π-electron conjugated systems, with only a few unbridged D-A systems being reported as good alternatives [19a,b] for applications as nonlinear optical materials. A deeper understanding of their fundamental structure-property relationships must therefore be acquired by evaluating their linear and NLO properties.

2.2 Linear optical properties

The UV/Vis spectra (see Figure 3) for all 2-mono- and 2,7-disubstituted selected quinolizinium derivatives (see Figure 5) exhibit an absorption below 500 nm. The band with a maximum at the longest wavelength was assigned to the transition to a π–π* excited state prior to the formation of a stable intramolecular charge transfer (ICT) excited state from which emission occurs. Band position ($\lambda_{abs,max}$) is usually quite sensitive to the ring conjugation and the electron-donating character of the heterocycle substituted at the acceptor, in this case the

quinolizinium moiety. The ICT bands for all the derivatives studied exhibit a sharp cut-off, with no broadening of this absorption band to the red. A weak broadening, attributed to the n–π* transition due to the presence of N heteroatoms, was observed previously for some other cationic acceptors, such as pyridinium cations, containing the same substituents [19b,c]. A comparison of $\lambda_{abs,max}$ for the C-2 substituted quinolizinium acceptor derivatives with those containing pyridinium moieties with the same electron-donating substituents linked in the activated positions (C2/C4) [19b] revealed bathochromic shifts in the 10-45 nm range, which were attributed to an increase in the degree of conjugation for the quinolizinium derivatives. Similarly, a comparison of $\lambda_{abs,max}$ for the unprotected 2-mono substituted derivatives containing indole, pyrazole, indazole and pyrrole groups (**2f**, **6b**, **6d** and **2c** respectively) indicated that the compound containing the weakest donor pyrazole substituent (**6b**) absorbed at the shortest wavelength (354 nm). The $\lambda_{abs,max}$ for indole- and indazole-substituted compounds (good donors), as well as their pyrrole counterpart, appeared at 396, 366 and 370 nm, respectively. Similar findings were obtained when comparing the protected monosubstituted **2a** (364 nm) with **2b** (357 nm), the unprotected **2f** (396 nm) with **6b** (400 nm), as well as the disubstituted **5c** (395 nm) with **7b** (377 nm) derivatives. Those containing weak pyrazole donors (**2b, 6b** and **7b**) exhibited shorter $\lambda_{abs,max}$ than their counterparts (**2a**, **2f** and **5c**). The greater electron-withdrawing character of the tosyl group, compared to the trityl one, probably reduces the difference between $\lambda_{abs,max}$ for **2a** and **2b**. As expected, moving from mono- to disubstituted protected (**2b** to **5b**) or non-protected (**6b** to **7b**) compounds resulted in a shift of the absorption maxima to the red (357 to 378 nm and 354 to 377 nm). The addition of a second heterocyclic of even the weakest pyrazole donor to the quinolizinium acceptor moiety at C(7) contributes to extending the π-delocalization, thus inducing a bathochromic displacement in the π-π* transitions. Something similar could be inferred for mono- and

disubstituted **2c** and **5c** pyrrole derivatives, which showed $\lambda_{abs,max}$ at 370 and 395 nm, respectively.

The $\lambda_{abs,max}$ for derivative **2a** (364 nm) was shifted to the blue by 32 nm compared to the non-protected **2f** (396 nm). Adding an electron-withdrawing tosyl group to the indole donor decreases its electron donating ability resulting in a diminishing of the charge transfer efficiency and hence a higher energy is associated to the transition. However, no apparent correlation was found between $\lambda_{abs,max}$ for **2b** substituted at C-2 with a pyrazole ring protected with a trityl group, which exerts a slight electron-withdrawing effect, and unprotected **6b**, the maxima for which appear at 357 and 354 nm respectively. A similar situation was found for pyrazole-disubstituted compounds **5b** and **7b**, whose maxima appear at 378 and 377 nm. In general, molar absorptivities at $\lambda_{abs,max}$ (ε_{max}) for quinolizinium acceptor derivatives (Table 3) are larger than for their pyridinium-containing counterparts [19b], with values ranging from approximately 1.1×10^4 to 3.7×10^4 $M^{-1}cm^{-1}$. However, no correlation was found between the ε_{max} values and the number of substituents on the different derivatives, their electron-donating character, or whether they were protected or not.

The emission spectra for all compounds were structureless (see Figure 4), showing maxima whose locations can be explained in a very similar manner to those of the absorption spectra. Thus, the unprotected mono-substituted derivatives **2f**, **6b**, **6d** and **2c** exhibit $\lambda_{em,max}$ at 496, 400, 451 and 485 nm, respectively. The pyrazole-containing compound (**6b**, weakest donor) emits at 400 nm, with the indole (**2f**), indazole (**6d**) and pyrrole (**2c**) counterparts being significantly shifted to the red by 96, 51 and 85 nm, respectively.

The changes in $\lambda_{em,max}$ upon moving from the protected 2-monosubstituted **2a** (448 nm) to **2b** (398 nm) and from the unprotected **2f** (496 nm) to **6b** (354 nm) and from the disustituted unprotected **5c** (463 nm) to **7b** (412 nm) can also be explained in a similar manner. The pyrazole-containing derivatives exhibited the smallest $\lambda_{em,max}$. As was also the case for the

absorption maxima, a comparison of $\lambda_{em,max}$ for mono- and disubstituted pyrazole-containing derivatives protected **2b** (398 nm) and **5b** (409 nm) or unprotected **6b** (400 nm) and **7b** (412 nm) revealed a displacement to the red, in this case by about 12 nm. However, the opposite behavior was observed when comparing mono- and disubstituted **2c** (485 nm) and **5c** (463 nm) compounds with pyrrole donor groups. The high degree of electronic asymmetry of a good donor substituent and central accepting moiety in the monosubstituted derivatives compared to the disubstituted ones should increase the extent of ICT. As a result, the emission of **2c** is displaced to higher wavelengths relative to the disubstituted derivatives **5c**.

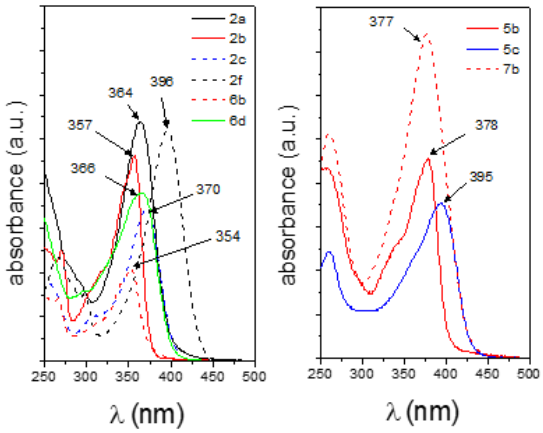

Figure 3. Electronic UV-Vis absorption spectra for 2-substituted quinolizinium derivatives 2a, 2b, 2c, 2f, 6b and 6d (left) and 2,7-disubstituted derivatives 5b, 5c and 7b in methanol at 25 °C (right). Values at the absorption maxima (depicted) are proportional to the molar absorptivities.

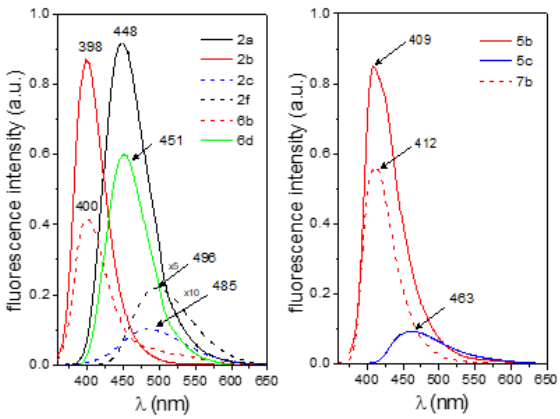

Figure 4. Emission spectra for 2-monosubstituted quinolizinium derivatives 2a, 2b, 2c, 2f, 6b and 6d (left) and 2,7-disubstituted derivatives 5b, 5c and 7b in methanol at 25 °C (right). Values at the emission maxima (depicted) are proportional to their fluorescence quantum yields.

The $\lambda_{em,max}$ for the electron-withdrawing tosyl protecting group at the indole ring of **2a** (448 nm) was, as expected, displaced to the blue compared to its unprotected counterpart **2f** (496 nm). This effect was smaller for pyrazole protected with a trityl group **5b** (409 nm) and its unprotected counterpart **7b** (412 nm) in the case of 2,7-quinolizinium derivatives. A similar situation was found for the C2-monosubstituted compounds **2b** (398 nm) and **6b** (400 nm), protected with a trityl group and unprotected, respectively.

An interesting observation was that the Stokes shifts ($\Delta\bar{\nu}$) for most derivatives were in the 5300-6575 cm^{-1} range. However, the series of mono- and disubstituted pyrazole derivatives **2b**, **6b**, **5b** and **7b** showed significantly smaller $\Delta\bar{\nu}$ values (2125-3435 nm) than the other compounds studied. Upon photoexcitation, the excited state reached quickly transfers its energy to the excited ICT state, from which emission occurs. As stated previously, the stability of ICT excited states depends strongly on the donating character of the substituent at the quinolizinium acceptor. Obviously, the small Stokes shifts observed for **2b**, **6b**, **5b** and **7b** are due to the low stabilization of the ICT complexes when the substituent was the weak donor pyrazole. In contrast, C-2 monosubstituted derivatives **2c**, **2f** and **6d**, which contain unprotected pyrrole, indole and indazole moieties, seemed to exhibit larger Stokes shifts as a consequence of a better ICT stabilization [27]. When comparing monosubstituted **2b**, **2c** and **6b** derivatives with their disubstituted **5b**, **5c** and **7b** partners, smaller Stokes shift were observed for the latter ones. As stated, pseudo-quadripolar structures (disubstituted derivatives), which hardly exhibit change in dipole moments upon electronic transition in polar solvents, usually exhibit smaller Stokes shifts than monosubstituted ones.

Table 3. Photophysical properties of selected quinolizinium derivatives (Fig. 5)

Comp	$\lambda_{abs,max}$ nm	λ_{exc} nm	$\lambda_{em,max}$ nm	$\Delta\bar{\nu}$ cm^{-1}	ϕ	$\varepsilon_{max}\times10^{-3}$ M^{-1} cm^{-1}	<τ> (ns)
2a	364	366	448	5300	0.59±0.10[a]	26.7±1.7	3.6(3.0)
2b	357	354	398	2885	0.88±0.03[a]	23.6±0.5	2.6(2.5)
2c	370	373	485	6575	0.01±0.01[a]	17.4±1.3	1.0(0.8)
2f	396	395	496	5450	0.04±0.0 [b]	26.1±0.5	3.6(3.5)
5b	378	373	409	2125	0.85±0.03[b]	21.5±0.1	2.0(1.9)
5c	395	373	463	3855	0.09±0.01[b]	17.6±0.1	1.7(1.7)
6b	354	354	400	3435	0.42±0.04[a]	2.10.5±0.04	3.4(3.4)
6d	366	366	451	5345	0.60±0.08[a]	19.0±2.1	3.0(3.4)
7b	377	373	412	2370	0.57±0.06[b]	37.0±1.7	2.8(2.9)

Maximum absorption wavelength (λ_{max}), excitation wavelength (λ_{exc}) used for fluorescence quantum yield (ϕ) measurements, maximum emission wavelength ($\lambda_{em,max}$), Stokes Shift ($\Delta\bar{\nu}$), molar absorptivity at $\lambda_{abs,max}$ (ε_{max}) and weighted average lifetimes upon excitation at 335 and 370 nm (in parentheses) by fixing the emission at $\lambda_{em,max}$. For fluorescence quantum yields: (a) using quinine sulfate in H_2SO_4 0.1M (ϕ=0.546) or (b) perylene in ethanol (ϕ=0.93) as standard [28].

Fluorescence quantum yields (ϕ) are shown in Table 3. In general, most of the quinolizinium-containing derivatives exhibit high quantum yields that are larger than for their counterparts containing pyridinium acceptors[19a,b]. Compounds **2b**, **6b**, **5b** and **7b**, which contain the weak donor pyrazole substituent with low ICT and exhibit the smallest Stokes shifts, present large ϕ values. The opposite was found for **2f**, **2c** and **5c** (with pyrrole or indazole donors), which exhibited the lowest ϕ values, $\lambda_{em,max}$ clearly displaced to the red, and relatively high Stokes shifts. In general, fluorescence quantum yields tend to decrease with the electron-donating ability of the substituent [19a].

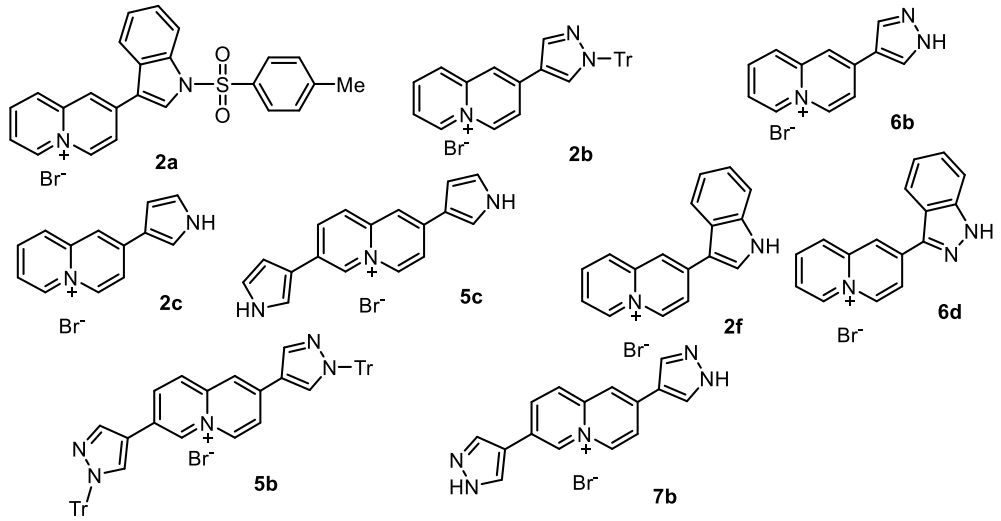

Figure 5. Selected chromophores for the study of linear optical properties and cyclic voltammetry (Tables 3 and 4). Tr: Trityl group

Fluorescence decay profiles were obtained upon excitation with monochromatic nanoleds emitting at 335 and 370 nm by fixing the fluorescence emission at $\lambda_{em,max}$. Irrespective of the excitation wavelength, all profiles could be reasonably fitted to double exponential decay functions. Weighted average lifetimes (<τ>), which depended slightly on the donor nature, exhibited similar values upon excitation at 335 or 370 nm, ranging from approximately 1.0 to 3.6 ns (Table 3 and Table S1). Rather low <τ> values were obtained for derivatives **2c** and **5c**, which contain pyrrole substituents; they also exhibited low fluorescence quantum yields. We

were unable to find any plausible correlation between the quantitative values for <τ> or lifetime component contributions and substituent donor features of the different derivatives.

2.3. Electrochemical properties

The electrochemical behaviour of selected quinolizinium salts (Figure 5) was studied by cyclic voltammetry (CV) (see Figure S1 in SI and Figure 6 in text) in dry acetonitrile/$LiClO_4$ (**5c** and **7b** in DMF-acetonitrile (1:1)/$LiClO_4$) as SSE (solvent-supporting electrolyte) system. The cathodic and anodic peak potentials, measured at a scan rate of 100 mV/s, and summarized in Table 4, are quoted relative to the Ag/Ag^+ ($AgCl_{sat}$) reference electrode.

The redox abilities of the above-mentioned quinolizinium salts were investigated, focusing on the first oxidation-reduction potentials, since these values correspond (tentatively) to the HOMO and LUMO energies, respectively. These cationic chromophores are electroactive at the cathode, to give the corresponding stabilized radicals, in the same potential range (E*pc* = -1.35 ± 0.15 V) due to the positive charge at the nitrogen atom in the quinolizinium ring. A similar electron-acceptor ability was recently described for aza-quinolizinium perchlorates [29].

The relationship between the energy of the highest occupied molecular orbital (HOMO) and the voltammetric oxidation potential values of a molecular organic semiconductor was described by Forrest *et al*. [30]. Table 4 includes the estimation of this energy (-IP, eV) and the energy gap (eV) for each compound.

Compound **2c**, which is substituted at the C2-position with a 3-pyrrolyl ring, has an Epa value of + 0.480 V, which correlates with the expected higher ability of this compound to be oxidized in comparision with the homologous 3-indolyl **2f** (Epa = +0.551 V). The loss of stability for **2c**, when oxidized to its cation radical, is energetically favoured compared with **2f** (Scheme 4). The same occurs for **6d** in comparison with **6b** (see Scheme S1 in SI).

Table 4. Experimental values of the peak potentials E (V, vs Ag/Ag+) (± 0.03V) of selected D-A$^+$ chromophores (Figure 5). *Epa* is the anodic peak potential, *Epc* is the cathodic peak potential. Scan rate: 100 mV/s. Ionization potentials (IP) and electron affinities (EA) and fundamental gap (Efund=IP – EA) (eV).

Comp.	*Epa1*	*Epa2*	*Epc*	-IP^1 (eV)^a	-IP^2 (eV)	-EA (eV)	Energy band gap (eV)
2a	+0.643	+0.834	-1.231	-5.50	-5.77	-2.88	2.62
2b	+0.737	+0.982	-1.351	-5.63	-5.97	-2.71	2.92
2c	+0.480	+0.798	-1.478	-5.27	-5.72	-2.53	2.74
2f	+0.551	+0.822	-1.440	-5.37	-5.75	-2.58	2.79
5b	+0.574	+0.99	-1.238	-5.40	-5.99	-2.87	2.53
5c	+0.610	+0.89	-1.407	-5.45	-5.85	-2.63	2.82
6b	+0.607	+0.836	-1.36	-5.45	-5.77	-2.70	2.75
6d	+0.726	+1.00	-1.292	-5.62	-6.0	-2.80	2.82
7b	+ 0.530	+0.96	-1.282	-5.34	-5.94	-2.79	2.55

IP and EA: Estimated from CV data (E*pa1* or E*pa2* values) by applying the relationship proposed by Forrest [30].

When comparing structures **6b** and **2c**, the latter is expected to be easier to oxidize (lower E*pa*) than **6b** as the pyrazole ring is less π-rich than the pyrrole ring. This argument can also be applied to the experimental E*pa* values for **2f** and **6d.** Thus, larger energy gaps are found for **2f** and **6d**, respectively, than for **2c** and **6b**, and the Epa values are also less positive compared with **2f** and **6d** (Figure S6 see SI).

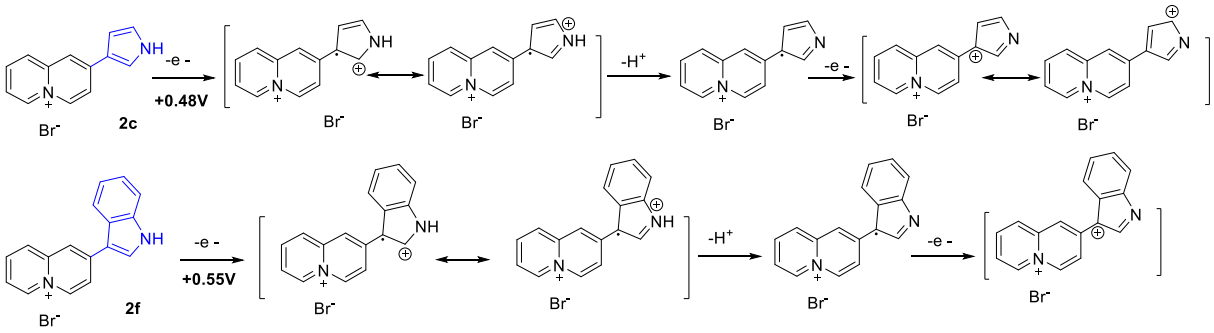

Scheme 4. Comparative Epa values for D-A$^+$ chromophores **2c** and **2f**.

For compounds **2a** and **2f**, a less negative E*pc* value can be expected for **2a** because the electron-withdrawing tosyl group increases the charge deficiency of the quinolizinium ring, which is therefore more easily reduced. However, when anodic potentials are compared for

2a and **2f**, the first E*pa* value for **2a** is more positive than that for **2f**, as expected due to the above-mentioned influence of the tosyl group.

Compound **2b**, which is substituted at C-2 with an *N*-triphenylmethyl (trityl) pyrazole ring, should be compared with its homologue **6b**. The trityl group (weak electron-withdrawing character) makes **2b** slightly more difficult to be oxidized than **6b**, as confirmed by the cyclic voltammetry data. The E*pa* value for **2b** is +0.737 V, compared with +0.607 V for **6b**, which correlates with the expected results.

When the E*pc* values of disubstituted compounds **5b**, **5c** and **7b** at the cathode are compared, it can be seen that the effect of two pyrazole rings in **7b**, instead of two pyrrole rings in **5c**, results in an easier reduction, similar to that already mentioned for **6b** compared to **2c.** However, for **5b** (*N*-substituted with a trityl group), the reduction potential is even less negative compared with unsubstituted **7b**, thus meaning that **5b** is easier to reduce.

With regard to the voltammetric oxidation scan of these two molecules, it is surprising that the E*pa* values for the first and second peaks are quite similar for **5b**, **5c** and **7b**, probably due to the compensation of electronic effects.

A final comparison of the pairs **2b/5b, 2c/5c** and **6b/7b** was performed (Figure 7). For 2,7-disubstituted quinolizinium bromides, the E*pc* values appear only to be affected by electronic effects. Thus, at the C2-position, both inductive and conjugative effects are important, whereas at the C7-position, only inductive effects are seen. As such, the cathodic discharge potentials (E*pc* values) are less negative when a second heterocyclic ring is introduced at the C7-position. i.e. the disubstituted compounds are reduced more easily than the monosubstituted ones.

The oxidation tendencies for C2- and C7-disubstituted quinolizinium salts, in comparison with their monosubstituted counterparts (Figure 7 SI), depend on the stability of cationic intermediates and oxidation products. Thus, the pyrazole ring at the C7-position in **5b** and

7b is easier to oxidize than that at the C2-position (Scheme 5) because the positive charge on quinolizinium cannot be delocalized by the C7-position, thus meaning that the C7-pyrazole ring has a higher electronic density. In **7b**, after losing $2e^-$ and $2H^+$ (or 2e- and $2Tr^+$ in **5b**), a stable, highly conjugated and symmetric new quinolizinium bromide is formed. For this reason, compounds **5b**/**7b** are more easily oxidized than their monosubstituted counterparts **2b**/**6b**, respectively. The oxidation proceeds as follows:

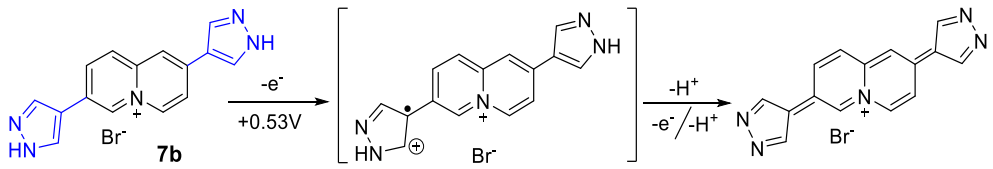

Scheme 5. Oxidation process for D-A+-D chromophore **7b**

However, in contrast to the former disubstituted salts, compound **5c** (Epa = +0.610 V) is slightly more difficult to oxidize than monosubstituted **2c** (Epa = +0.48 V). A plausible explanation is as follows.

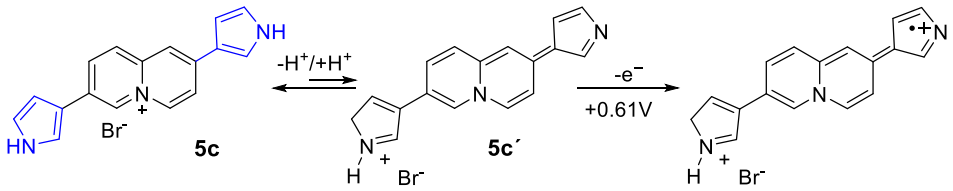

Scheme 6. Oxidation process for D-A+-D chromophore **5c**

Compound **5c** delocalizes the positive charge on the quinolizinium over the pyrrole ring at C2 but not that at C7 position. The latter heterocycle (at C7) is therefore more easily oxidized as it is more electron-rich. However, an internal acid-base equilibrium prior to the oxidative step can be proposed, as indicated in Scheme 6. When this occurs, the oxidation potential E*pa* of cation **5c´** increases as the heterocycle at C7 is protonated, which means that oxidation of the C2 ring is more difficult.

These electrochemical results show that double substitution at both the C2 and C7 positions in quinolizinium salts by weakly electron-donating heterocycles clearly decreases the HOMO-LUMO gap (in comparison to C2 monosubstitution).

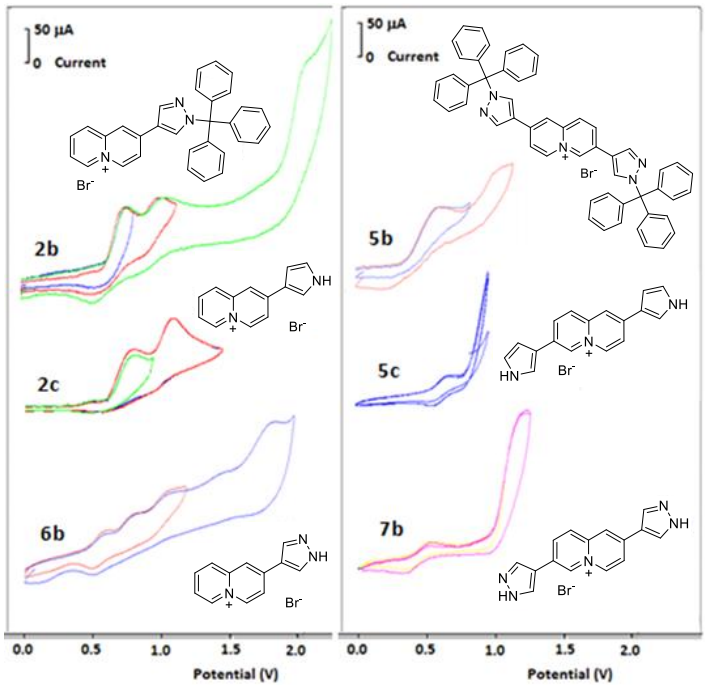

Figure 6. Cyclic voltammograms of **2b/5b**, **2c/5c** and **6b/7b** in dry acetonitrile/$LiClO_4$ (0.1M) (**2b**, **2c** and **6b**) or DMF/$LiClO_4$ (0.1M) (**5b**, **5c** and **7b**) as SSE, at Pt working and auxiliary electrodes. Ag/Ag^+ (sat) as reference electrode. Scan rate: 100 mV/s.

Another interesting conclusion is that, in contrast to electronic effects, steric hindrance does not seem to affect the electrochemical response (**7b**→**5b** or **6b**→**2b**).

Thus, the presence of a highly electrodonating ring at C7, where conjugation is blocked (**5c**), seems to cause destabilization in the D-A^+ system, which behaves as an amphoteric molecule before being oxidized.

2.4. Nonlinear optical properties: Hyper-Rayleigh Scattering (HRS) measurements

Femtosecond hyper-Rayleigh scattering (HRS) measurements were performed at a wavelength of 800 nm to study the potential of these relatively small ionic compounds for second-order nonlinear optical applications. The results of these HRS experiments are given in Table 5 both

in terms of dynamic hyperpolarizability (measured at 800 nm) and of static values, derived from the two-level model (TLM). The second-order nonlinear optical properties reflect the observations already made for linear optical properties as regards the nature of the conjugation at C-2 in relation to disubstitution at the C2 and C7 positions of the chromophores, thus confirming that the best conjugation and charge transfer from the donor to the acceptor is achieved at position C2.

The largest first hyperpolarizability values were found for protected indole-substituted compound **2a** (β_{HRS}= 674×10^{-30} esu), and **5b** (393x10^{-30} esu), followed by indazole derivatives **6d** (β_{HRS}=356×10^{-30} esu) and **2d** (β_{HRS}= 250×10^{-30} esu). In agreement with the greater influence of the donor substituent at the C2-position of the quinolizinium acceptor, the relative electron-donating strength characteristics, and better conjugation and stabilization, the largest β values correspond to indole and indazole derivatives (relatively good donors), which can be explained by a more efficient charge transfer between frontier orbitals in these non-bridged systems.

Table 5. Experimental nonlinear optical properties of D–A+ and D-A+-D

Comp.	λ_{max}	β_{HRS}	β_{zzz}	$\beta_{zzz,0}$	β_0	τ
2a	364	674±34	1629±83	222±11	33±1.6	4.21±0.73
2b	357	68±5	165±13	27±2	4±0.3	2.94±0.36
2c	370	91±6	220±15	25±2	3±0.2	0.92±0.18
2d	360	250±10	606±25	91±4	13.7±0.55	3.48±0.44
2f	399	129±52	312±127	1.1±0.5	0.16±0.06	----
5b	365	393±13	951±32	126±4	18.7±0.61	1.93±0.19
5c	392	49±17	120±42	25±2	0.49±0.17	1.91±0.70
5f	423	87±5	210±14	18±1.2	2.35±0.13	6.14±3.09
6b	350	45±2	109±6	21±1.1	3.16±0.14	3.41±0.51
6d	371	356±16	860±40	94±4	13.8±0.62	3.55±0.44
6e	416	95±11	231±28	14±1.7	1.82±0.21	----
7b	364	203±9	492±22	67±3	9.95±0.44	3.19±0.45
7d	397	171±17	415±43	5±05	0.64±0.06	2.18±0.37

Wavelength of maximum absorbance λmax (nm), resonance-enhanced HRS experimental first hyperpolarizability β_{HRS} (10^{-30} esu), resonance-enhanced diagonal component of the molecular first hyperpolarizability βzzz (10^{-30} esu), off-resonance diagonal component of the molecular first hyperpolarizability βzzz,0 (10 $^{-30}$ esu), dispersion-free hyperpolarizability β_0 (10^{-30} esu) .
The values of the fluorescence lifetime, τ (ns) are also included for molecules exhibiting demodulation.

The effects of the *N*-protecting groups were also evaluated. Thus, compound **2a**, which bears a strongly electron-withdrawing substituent that is expected to increase intramolecular charge transfer and, thus, the first hyperpolarizability, shows a higher β_{HRS} value. *N*-substitution stabilizes the ground and excited state upon *N*-*p*-toluensulfonyl substitution at indole [32]. The HOMO and LUMO energies are stabilized for the electron-withdrawing group due to the delocalization of π electrons from indole to the sustituent [32]. Compound **2a**, which bears a strongly electron-attracting substituent, exhibits higher charge transfer compared to **2f**.

N-Boc substitution in indazole **2d** (β_{HRS}=250×10^{-30} esu) was also studied and measured in the absence of the protecting group (**6d**, β_{HRS}=356×10^{-30} esu), exhibiting a large increase in β_{HRS}. In contrast, the *N*-Tr group is a slightly sigma-withdrawing (inductive -I effect) and therefore has less effect on delocalization onto the pyrazole ring, which is a less π-rich system. Interestingly, chromophores bearing an *N*-Tr protecting group give β values that are twice those for the corresponding unprotected C2 and C2/C7 quinolizinium derivatives.

Similar absorption maxima and first hyperpolarizabilities approximately 50% lower are observed for compounds with double substitution at the C2/C7 positions, (**2f**/**5f** and **6d/7d**). However, the absorption maxima for compounds **7b** and **5b** are similar (364/365 nm), whereas the chromophore substituted with a trityl protecting group (**5b**) exhibits a large β value (393 × 10^{-30} esu) that is nearly twice that measured for **7b**. A similar trend is observed for **6d**/**7d.**

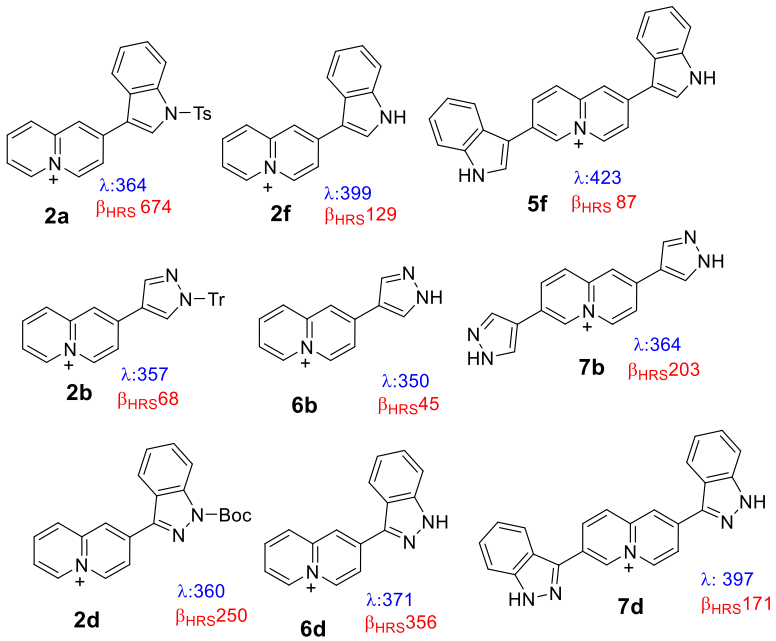

Figure 8. Selected chromophores for the study of nonlinear optical properties

A comparison of monosubstituted chromophores **2f** and **6d** and disubstituted compounds **5f** and **7d**, which contain indole and indazole moieties, respectively, lacking a protecting group, allows us to conclude that the disubstituted compounds exhibit a beta value half that of the C2-functionalized chromophore.

For the series of charged dipolar (D-A$^+$) and quadrupolar (D-A$^+$-D) chromophores, large first hyperpolarizabilities were obtained for compounds **2a**, **2d** and **6d**, as determined by HRS. The low transition energy and high degree of CT are the decisive factors resulting in a large first hyperpolarizability in compounds substituted at the C2 position of the quinolizinium system.

In comparison to previously reported (D–π-A$^+$) molecules [19c], the lack of a conjugated bridge in pyridinium-containing (D–A$^+$) chromophores [19b] results in higher β values. Consequently, the common assumption that β can be maximized by using a conjugated bridge to link D and A units does not hold in general [19b].

The experimental results reported here for quinolizinium chromophores (D-A$^+$) or (D-A$^{+\prime}$-D) reveal the highest hyperpolarizability for the unbridged geometry. Furthemore, the β value

obtained for D-A$^+$ chromophores with a quinolizinium acceptor are larger than for their pyridinium counterparts. These results for non-bridged azonia systems allow a remarkable degree of control by supression of the linker and N-substitution at the donor heterocycle unit.

2.5 Computational studies

To understand the electronic reorganizations that occur upon excitation and the microscopic NLO properties of the synthesized quinolizinium chromophores, theoretical (DFT and HF) calculations were performed using the Gaussian 09 program package [33]. As a first step, a geometry optimization of the molecular structures was performed at the B3LYP/6-31+G(d,p) level of theory for all cations studied, in the gas phase and in methanol, except the bulky compound **5b**, the geometry of which was optimized at the B3LYP/6-31G(d,p) level of theory. The gas phase optimized low-energy isomers for protected and deprotected 1D (compounds **2** and **6**) and 2D chromophores (compounds **5** and **7**) are shown in Figure S1 in the Supporting Information. Time-dependent density functional theory (TDDFT) calculations were used to probe the electronic reorganizations of the cationic systems studied upon excitation in methanol. The data reported in Table 6 show that the TDDFT method with a hybrid Perdew–Burke–Ernzerhof exchange-correlation functional (PBE0) is able to fully reproduce the linear optical properties, with the theoretically predicted wavelength values differing from the experimental ones by up to 7%. The TDDFT/PBE0/6-311+G(2d,p) absorption maxima, oscillator strengths and frontier orbital energies for the compounds studied (with/without protecting group) in methanol are reported in Table 6.

The band positions and intensities predicted by TDDFT are consistent with the experimentally observed values. For all compounds, the first excited states are determined by HOMO → LUMO transitions. The HOMO-LUMO gaps range from 3.44 (**5e**) to 4.46 eV (**6b**) for the compounds in methanol.

In all compounds shown in Figure 9, the HOMO orbitals were found to be populated over the entire molecular system, except for the protecting groups. Similarly, the LUMOs were found to be delocalized over the quinolizinium and, to a lesser extent, over the substituents (indole, pyrazole and indazole fragments). It is known that the gap, defined as the difference between the ionization potential (IP) and electron affinity (EA) (E_{fund} = IP - EA), is only approximately given by the difference between the calculated HOMO and LUMO energy levels [34]. The computational methodology we have adopted, more specifically the hybrid functional (PBE0) with 25% exact Hartree–Fock exchange, reproduces the experimental cyclic voltammetry-based ionization potentials relatively well (with errors of about 1 eV) and the electron affinities very well.

Table 6. Calculated TDDFT/PBE0/6-311+G(2d,p) absorption maxima λmax (nm), oscillator strengths (f), HOMO and LUMO energies, and difference between the calculated FMOs energies, HLG, (eV).

Comp.	λ_{max}	f	HOMO	LUMO	HLG
2a	373	0.61	-6.73	-2.76	3.98
2b	337	0.81	-7.00	-2.66	4.34
2c	357	0.32	-6.69	-2.55	4.14
2d	360	0.56	-7.08	-2.99	4.09
2e	384	0.87	-6.67	-2.87	3.80
2f	385	0.42	-6.42	-2.57	3.85
2g	372	0.97	-6.66	-2.80	3.86
2h	352	0.82	-6.88	-2.75	4.14
2i	376	0.75	-6.54	-2.68	3.86
5b	371	1.32	-6.49	-2.74	3.75
5c	388	0.46	-6.35	-2.50	3.85
5d	387	1.00	-6.97	-3.14	3.83
5e	432	1.38	-6.40	-2.96	3.44
5f	418	0.63	-6.14	-2.54	3.60
5g	412	1.49	-6.40	-2.86	3.54
5h	379	1.20	-6.68	-2.79	3.89
5i	404	1.14	-6.33	-2.69	3.65
6b	329	0.57	-7.13	-2.67	4.46
6d	367	0.60	-6.80	-2.81	3.98
7b	357	0.76	-6.83	-2.70	4.13
7d	397	0.94	-6.60	-2.88	3.72

The largest experimental β_{HRS} values were found for compounds **2a** (674 × 10^{-30} esu), **2d** (250 × 10^{-30} esu), **5b** (393 × 10^{-30} esu) and **6d** (356 × 10^{-30} esu). Both theoretical approaches (HF and MP2) predict higher β_{HRS} values for deprotected mono- and disubstituted quinolizinium cationic systems in comparison with the values calculated for the Ts- and Boc-protected ones. The calculated β_{HRS} values for Tr-protected systems (**2b** and **5b**) are higher than those calculated for the corresponding deprotected ones (**6b** and **7b**, respectively).

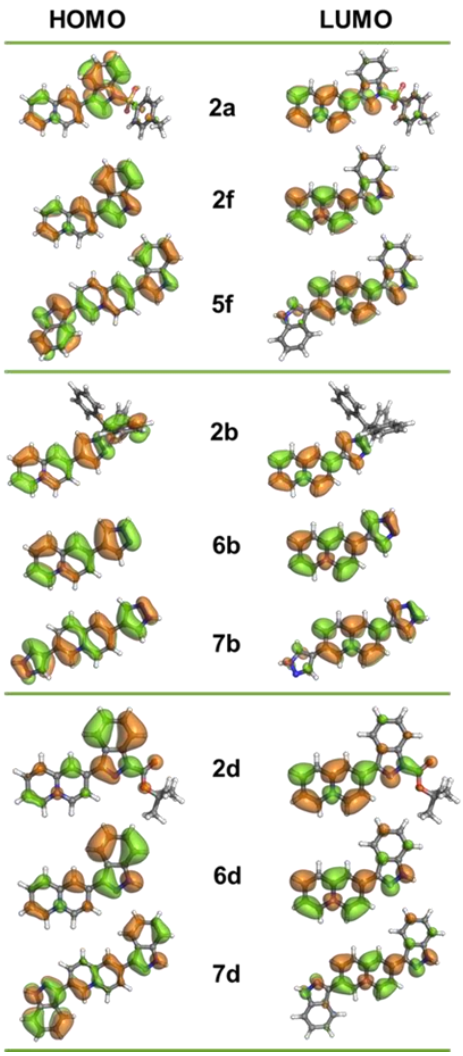

Figure 9. Graphical representation of the frontier orbitals (isodensity plot, isovalue = 0.02 a.u.) for the cationic fragments of the triads protected monosubstituted/deprotected monosubstituted/disubstituted cationic quinolizinium systems **2a/2f/5f**; **2b/6b/7b**; **2d/6d/7d**.

Disubstituted cationic quinolizinium systems are characterized by lower β_{HRS} values than their monosubstituted counterparts (**2f**/**5f**; **6b**/**7b**; **6d**/**7d**). Similar trends are observed for the static

($\beta_{HRS,0}$) and dynamic (evaluated at 800 nm, $\beta_{HRS,800}$) molecular first hyperpolarizabilities. It should be noted that the theory (both theoretical approaches - HF and MP2) did not fully succeed in predicting the experimental β_{HRS} values of the series of differently substituted protected/unprotected compounds (Table 7). Further investigations based on both representative and reliable experimental data and computational approaches are needed to address this issue.

Table 7. HF-calculated β_{HRS} values ($\beta_{HRS,0}$ and $\beta_{HRS,800}$) for selected compounds **2**, **5-7**. MP2-calculated β_{HRS} values are given in parentheses.

Comp.	$\boldsymbol{\beta_{HRS,0}}$ ($\times 10^{-30}$ esu)	$\boldsymbol{\beta_{HRS,800}}$ ($\times 10^{-30}$ esu)
2a	35 (70)	61 (122)
2b	38 (65)	59 (101)
2c	44 (71)	62(100)
2d	16 (35)	26 (57)
2f	48 (100)	93 (194)
5b*	11 (98)	10 (125)
5c	18 (35)	25 (47)
5f	28 (38)	58 (79)
6b	29 (44)	37 (56)
6d	37 (68)	58 (107)
7b	13 (24)	20 (35)
7d	19 (27)	34 (48)

In comparison with the previously investigated pyridinium systems [19b], the newly proposed cationic quinolizinium systems appear to perform better in terms of applications related to nonlinear optics. Indeed, the β_{HRS} values predicted at the MP2 level for a model pyrrole-substituted cationic quinolizinium system (**2c**, Table 7, Figure S3) are higher ($\beta_{HRS,800}$ = 100×10^{-30} esu) than those calculated for a model 2-methylpyridinium (**B**), 3-methylpyridinium (**C**) and 4-methylpyridinium cationic system (**D**) ($\beta_{HRS,800}$ values of 32×10^{-30}, 29×10^{-30} and 66×10^{-30} esu, respectively). The representatives with the smallest substituents in the methylpyridinium/quinolizinium cationic systems were compared and the electron densities for both substituted cations (quinolizinium and methylpyridinium) found to be quite similar (Figure S3).

3. Experimental section

3.1 Materials and Methods (See SI)

3.2. *Synthesis of D–A$^+$ and D-A$^+$-D Quinolizinium chromophores.*

The structures of all new chromophores were unambiguously confirmed by their analytical and spectral data. Details are provided in the supplementary information (ESI). Only General Procedures and selected chromophores are given here.

Synthesis of D–A+ quinolizinium salts (2). ***General procedure. Stille Reaction***. *A flame-dried flask was charged under argon with 1 equiv. of bromoquinolizinium bromide or hexafluorophosphate (1 mmol), 5 mol % $Pd(PPh_3)_4$ (**Method A**) or 5 mol % $Pd_2(dba)_3$ and 5 mol % $P(o\text{-}Tol)_3$ (**Method B**) in dry DMF (5 mL). The corresponding stannyl heterocycle (1.3-1.4 mmol or 1.1 mmol) was then added. After stirring at room temperature or heating at 65-75 °C for 15-20 h, the solution was filtered through a small pad of celite and washed with methanol. The solution was then concentrated and the solid purified by flash chromatography on silica gel using CH_2Cl_2/MeOH (9:1) as eluent.*

2-(*N*-Tosylindol-3'-yl)quinolizinium bromide (2a). General procedure A, from 2-bromoquinolizinium bromide **1** (0.10 g, 0.35 mmol) and 3-tributylstannyl-*N*-(toluen-4-sulfonyl)-1-*H*-indole (0.21 g, 0.38 mmol). Heating the reaction mixture for 4 h at 70 °C afforded **2a** (0.16 g, 97%) as a pale-brown solid: M.p. 265–266 °C (CH_3CN); IR (KBr) $\nu_{máx}$ (cm^{-1}): 1647, 1173, 1146, 1552; ^{1}H NMR (500 MHz, DMSO-d_6) δ (ppm): 9.41 (d, *J* = 7.2 Hz, 1H), 9.31 (d, *J* = 6.8 Hz, 1H), 8.99 (s, 1H), 8.92 (s, 1H), 8.67 (dd, *J* = 7.2, 2.2 Hz, 1H), 8.64 (d, *J* = 8.7 Hz, 1H), 8.37 (t, *J* = 8.0 Hz, 1H), 8.33 (d, *J* = 7.8 Hz, 1H), 8.08 (d, *J* = 8.1 Hz, 1H), 8.07 – 8.01 (m, 3H), 7.53 (t, *J* = 7.7 Hz, 1H), 7.49 (t, *J* = 7.5 Hz, 1H), 7.44 (d, *J* = 8.0 Hz, 2H), 2.33 (s, 3H); ^{13}C NMR (126 MHz, DMSO-d_6) δ (ppm): 146.3, 142.9, 140.4, 136.9, 136.6, 136.4, 134.8, 133.5, 130.5, 129.5, 127.1, 127.0, 126.6, 126.0, 124.7, 123.0, 122.1, 121.8, 121.0, 117.4, 113.6, 21.1.; MS (ESI$^+$, *m/z*): 399 (M$^+$). Anal. Calcd for $C_{24}H_{19}N_2SO_2Br$ (479 g/mol) C,

60.12; H, 3.97; N, 5.84 S, 6.68. Found: C, 60.52; H, 4.35; N, 6.16, S, 7.06. HRMS (ESI-TOF) m/z calcd for $C_{24}H_{19}N_2O_2S$ $[M + H]^+$ 399.11618, found: 399.11597.

2-(*N*-Trityl-1*H*-pyrazol-4-yl)quinolizinium bromide (2b). General procedure A, from 2-bromoquinolizinium bromide **1** (0.10 g, 0.35 mmol) and 4-tributylstannyl-1-tritylpyrazole (0.27 g, 0.45 mmol). Heating the reaction mixture for 8 h at 65 °C afforded **2b** (0.17 g, 94%) as a pale-brown solid: M.p. 256–258 °C (CH_3CN); IR (KBr) $\nu_{máx}$ (cm^{-1}): 1647, 1458, 1072, 1028. ^1H NMR (500 MHz, CD_3OD) δ 9.09 (d, *J* = 7.3 Hz, 1H), 9.06 (d, *J* = 6.5 Hz, 1H), 8.62 (d, *J* = 2.1 Hz, 1H), 8.43 (d, *J* = 0.8 Hz, 1H), 8.40 (d, *J* = 0.8 Hz, 1H), 8.31 (d, *J* = 8.5 Hz, 1H), 8.23 (dd, *J* = 7.2, 2.1 Hz, 1H), 8.19 (ddd, *J* = 8.6, 7.1, 1.2 Hz, 1H), 7.84 (td, *J* = 7.0, 1.5 Hz, 1H), 7.42 – 7.33 (m, 9H), 7.25 – 7.17 (m, 6H). ^{13}C NMR (75 MHz, CD_3OD) δ (ppm): 146.3, 145.0, 144.1, 141.2, 139.1, 138.8, 138.5, 135.3, 132.5, 130.5, 130.3, 129.1, 124.7, 123.6, 122.5, 120.0, 82.5. MS (ESI^+, *m/z*): 438 (M^+). Anal. Calcd for $C_{31}H_{24}N_3Br$ (518 g/mol) C, 71.82; H, 4.67; N, 8.10. Found: C, 71.67; H, 4.71; N, 8.32. HRMS (ESI-TOF) m/z calcd for $C_{31}H_{24}N_3$ $[M + H]^+$ 438.19647, found: 438.19668.

Synthesis of D-A⁺-D Quinolizinium Salts 5. General Procedure. Stille Reaction. *A flame-dried flask (two necks, 25 ml) was charged under argon with 1 equiv. of 2,7-dibromoquinolizinium bromide **3** (1 mol), 14 mol% of CuI in DMF (2ml), the corresponding stannyl heterocycle (2.3-2.5 mmol), then 7 mol% of $Pd(PPh_3)_4$ (**Method A**) or 5 mol % $Pd_2(dba)_3$ and 10 mol % $P(o\text{-}Tol)_3$ (**Method B**) in dry DMF (3-5 mL). The corresponding stannyl heterocycle (2.3-2.5 mmol) in DMF (3 ml) 1.1 mmol) was then added. After stirring at room temperature or heating at 70-75 °C for 18-24 h, the solution was filtered through a small pad of celite and washed with methanol. The solution was concentrated and the solid purified by flash chromatography on silica gel using CH_2Cl_2/MeOH (9:1) as eluent.*

2,7-*bis*-(*N*-Tritylpyrazol-4'-yl)quinolizinium bromide (5b). From 2,7-dibromoquinolizinium bromide **3** (0.1 g, 0.27 mmol) and 4-tributylstannyl-1-trityl-1*H*-

pyrazole (0.38 g, 0.63 mmol) following the general procedure A , heating the mixture at 70 °C for 22 h. The solution was concentrated and treated with CH_2Cl_2, then the precipitate was isolated by filtration and washed with CH_2Cl_2 and MeOH to afford **5b** (0.116 g, 52%) as a pale-brown solid. M.p. 331–335 °C (d) (CH_3CN/EtOH). IR (KBr) $\nu_{máx}$ (cm^{-1}): 1641, 1555, 1489, 1442, 746. ^{1}H NMR (300 MHz, DMSO-d_6) δ (ppm): 9.50 (s, 1H), 8.97 (d, *J* = 7.3 Hz, 1H), 8.69 (s, 1H), 8.55 (dd, *J* = 8.9, 1.7 Hz, 1H), 8.48 (s, 1H), 8.46 (s, 1H), 8.41 – 8.32 (m, 2H), 8.28 (s, 1H), 8.23 (d, *J* = 9.1 Hz, 1H), 7.48 – 7.34 (m, 18H), 7.22 – 7.06 (m, 12H). ^{13}C NMR (75 MHz, DMSO) δ 142.1 (3C), 142.0 (3C), 140.6, 138.8, 138.4, 137.4, 135.8, 134.1, 132.4, 130.8, 130.7, 129.3, 127.7, 127.7, 126.5, 126.0, 120.9, 119.5, 117.2, 115.3. EM $(ESI)^+$ (*m/z)* 746 $(M)^+$. Anal. Calcd for $C_{53}H_{40}N_5Br$ (826 g/mol) C, 77.0; H, 4.84; N, 8.47. Found: C, 77.38; H, 5.25; N, 8.17. HRMS (ESI-TOF) m/z calcd for $C_{53}H_{40}N_5$ $[M + H]^+$ 746.32782, found: 746.32753.

2,7-bis-(1'*H*-Indol-3'-yl)-quinolizinium bromide (5f.Br$^-$). From 2,7-dibromoquinolizinium bromide **3** (0.05 g, 0.14 mmol) and 3-tributylstannyl indole (0.13 g, 0.34 mmol), following general procedure B, and heating the mixture at 70 °C for 24 h. The resulting solid was treated with AcOEt to afford **5f.Br$^-$** (0.036 g, 60%) as a brown solid: mp 249-251 °C (CH_3CN) .IR (KBr) ν_{max} 3102, 1636, 1524, 1430, 1256 cm^{-1}.^{1}H-NMR (DMSO, 300 MHz) δ (ppm) 12.25 (s, 1H, NH), 11.94 (s, 1H, NH), 9.38-9.34 (m, 2H), 8.72-8.24 (m, 8H), 7.59-7.46 (m, 2H), 7.4-7.12 (m, 4H).^{13}C-NMR (DMSO, 75 MHz) δ (ppm) 141.7, 140.1, 137.0, 136.5, 135.1, 134.1, 129.8, 128.9, 128.3, 126.8, 125.5, 123.5, 123.1, 122.3, 121.9, 120.9, 120.4, 120.1, 119.4, 119.0, 116.9, 112.2, 111.8, 110.6, 108.6. MS $(ESI)^+$ *m/z*(relative intensity) 360 $(M)^+$. Anal. Calcd for $C_{25}H_{18}BrN_3$ (440 g/mol) C, 68.18; H, 4.12; N, 9.54. Found: C, 68.59; H, 4.43; N, 9.36.

Deprotection reaction. General procedure. HCl 1M (2-7 mmol) was added to a suspension of starting salt (1 mol equiv.) in EtOH (5-8 ml) in several portions at different times. The reaction

mixture was then stirred at room temperature or heated at 75 °C for 18-30 h. It was then concentrated to dryness and the residue obtained was purified as indicated for each compound.

2-(1'*H*-Pyrazol-4'-yl)quinolizinium (6b). Following the general procedure, from **2b** (0.17 g, 0.33 mmol) and HCl 1M (0.5 ml, 0.5 mmol). After stirring at room temperature for 8 h, the solution was concentrated and the residue treated with Et_2O. The solid was filtered off to afford **6b** (0.11 g, 94%) as a pale solid: mp 230–231 °C (EtOH). IR (KBr) $\nu_{máx}$ (cm^{-1}): 3416, 1650, 1456, 1151, 839. ^1H NMR (500 MHz, CD_3OD) δ (ppm): 9.17 (d, *J* = 7.1 Hz, 1H), 9.11 (dd, *J* = 6.8, 1.1 Hz, 1H), 8.77 (bs, 2H), 8.72 (d, *J* = 2.0 Hz, 1H), 8.38 (dd, *J* = 9.0, 1.4 Hz, 1H), 8.34 (dd, *J* = 7.2, 2.0 Hz, 1H), 8.24 (ddd, *J* = 8.6, 7.1, 1.2 Hz, 1H), 7.88 (td, *J* = 7.0, 1.4 Hz, 1H). ^{13}C NMR (125 MHz, DMSO-d_6) δ (ppm): 143.0, 141.2, 136.9, 136.3, 136.1, 134.4 (2C), 126.2, 121.9, 120.7, 119.3, 117.7. MS (ESI^+, *m/z*): 196 $(M)^+$. Anal. Calcd for $C_{12}H_{10}BrN_3$ (276 g/mol) C, 52.20; H, 3.65; N, 15.22. Found: C, 52.63, H, 3.12, N, 15.90. HRMS (ESI-TOF) m/z calcd for $C_{12}H_{10}N_3$ $[M + H]^+$ 196.08692, found: 196.08707.

2,7-*bis*(1'*H*-Pyrazol-4'-yl)quinolizinium bromide (7b). . Following the general procedure, from **5b** (0.038 g, 0.046 mmol) and HCl 1M (0.17 ml, 0.17 mmol). Heating the mixture for 24 h afforded a crude residue, which was treated with a mixture of CH_2Cl_2:AcOEt (95:5). The solid was then filtered off and washed twice with EtOH:AcOEt to give **8b** (0.013 g, 83%) as a pale-brown solid. M.p. 312–313 °C (MeOH:EtOH). IR (KBr) $\nu_{máx}$ (cm^{-1}): 3089, 1641, 1561, 1438. ^1H NMR (500 MHz, DMSO-d_6, 80 °C) δ (ppm):9.49 (s, 1H), 9.42 – 8.73 (m, 5H), 8.64 (s, 1H), 8.51 (d, *J* = 8.6 Hz, 1H), 8.36 – 8.25 (m, 2H). MS (ESI^+, *m/z*) 262 $(M)^+$. Anal. Calcd. for $C_{15}H_{12}N_5Br$ (342 g/mol) C, 52.65; H, 3.53; N, 20.47. Found: C, 52.95, H, 3.88, N, 20.19. HRMS (ESI-TOF) m/z calcd for $C_{15}H_{12}N_5$ $[M + H]^+$ 262.10872, found: 262.10858.

4. Conclusions

A series of azonia cation derivatives has been synthesized and investigated for the first time as D-A^+ and D-A^+-D chromophores. The structure–property relationship of the studied chromophores may contribute to the recent interest in β enhancement strategies and to be used as an alternative to traditional azinium π-conjugated chromophores in nonlinear optics. We attribute this cooperative enhancement to the cationic strong acceptor, along with the increasing electron-donating ability of the donor, thus revealing the crucial role played by inherent polarization between both fragments to modulate NLO properties.

The photophysical and electrochemical properties of dipolar D-A^+ chromophores were investigated and compared with the corresponding D-A^+-D chromophores on the basis of UV–vis absorption/fluorescence spectroscopy and cyclic voltammetry to evaluate the intramolecular electronic interactions between the donor and acceptor and *N*-substitution at the donor unit.

The first hyperpolarizabilities of charged chromophores (D-A^+) and (D-A^+-D) were determined by HRS. Candidates with high β values were identified and the key factors governing the enhancement of the NLO responses determined. The low transition energy and high degree of CT are the decisive factors that confer a large first hyperpolarizability on compounds substituted at C2 of the quinolizinium system. The NLO response depends on the nature of the protecting group: β_{HRS} increases when removing the Ts and Boc protecting groups, whereas Tr-protected systems have higher values than their unprotected counterparts. It can therefore be concluded that Tr group deprotection does not result in quinolizinium systems with improved NLO properties.

The experimental linear/nonlinear optical and electrochemical measurements are compared with values calculated by the electronic structure methods (DFT and/or *ab initio*). The comparison sheds light on the structure-property relationship for these new D-A^+(D)

chromophores, although the theory did not fully succeed in predicting the experimental NLO properties. The structure-property relationships obtained will be used in ongoing studies focused on heterobetaines based on quinolizinium as cation for D-A- building blocks in organic–based materials. Overall, this study provides an insight into the promising D-A^+ and D-A^+-D architectures based on quinolizinium cation as an acceptor fragment. Our results suggest that materials based on this quinolizinium system have a great potential for application in integrated NLO devices. These findings also provide an intriguing area for future research into quinolizinuim building blocks and structure-directing constituents that may help to tune the NLO properties of these systems. It is expected that the present study that demonstrates the synthesis and properties of quinolizinium based D-A^+ and D-A^+-D architectures paves the way for the development of new organic NLO materials.

Acknowledgements

Financial support from the Spanish Ministerio de Ciencia y Competitividad (MINECO/ CTQ2017- 85263- R), Instituto de Salud Carlos III (MINEC0/ RD16/0009/0015). J.R gratefully acknowledges the funding of the FEDER funds and Comunidad de Madrid (CAM, project B2017/BMD-3688 MULTI-TARGET&VIEW-CM FEDER FUNDS). E.S-P and M.A.R.M are gratefully acknowledged for CONACYT grants 93389 and 144234/192425. S. A. gratefully acknowledges support from the “GINER DE LOS RIOS” program of the Universidad de Alcalá and B. B. gratefully acknowledges financial support from the Universidad de Alcala (project CCG19/CC-033).

Author information

Corresponding Author

*E-mail for AMC: ana.cuadro@uah.es.

ORCID https://orcid.org/0000-0002-8077-6938

Conflicts of interest

The authors declare no competing interest.

References

[1] (a) Popczyk A, Grabarz A, Cheret Y, El-Ghayoury A, Myśliwiec J, Sahraoui B. Tailoring the acceptor moiety of novel thiophene-based chromophores: Conjoined experimental and theoretical study on the nonlinear optical properties. Dyes Pigments 2021; 196: 109789. https://doi.org/10.1016/j.dyepig.2021.109789.
(b) Rajeshirke M, Sekar N. Multi-stimuli responsive emissive NLOphoric colorants – A recent trend in research, Dyes Pigments 2019; 163: 675-683. https://doi.org/10.1016/j.dyepig.2018.12.063.
(c) Gao W, Liu J, Kityk IV. The Progress in the Field Auxiliary Donors and their Application in Novel Organic Second-Order Nonlinear Optical Chromophores, Mini-Rev. Org. Chem 2019; 16: 228-235. https://doi.org/10.2174/1570193X15666180627150155.
(d) Dini D, Calvete MJF, Hanack M. Nonlinear Optical Materials for the Smart Filtering of Optical Radiation. Chem. Rev. 2016; 116: 13043-13233. ttps://doi.org/10.1021/acs.chemrev.6b00033.
(e) Cambre S, Campo J, Beirnaert C, Verlackt C, Cool P, Wenseleers W. Asymmetric dyes align inside carbon nanotubes to yield a large nonlinear optical response. Nat. Nanotechnol. 2015; 10: 248-252. https://doi.org/10.1038/nnano.2015.1.
(f) Taboukhat S, Akdas-Kilig H, Fillaut JL, Karpierz M, Sahraoui B. Tuning the nonlinear optical properties of BODIPYs by functionalization with dimethylaminostyryl substituents. Dyes Pigments 2017; 137: 507-511. https://doi.org/10.1016/j.dyepig.2016.10.045.
(g) Szukalski A, Parafiniuk K, Haupa K, Goldeman W, Sahraoui B, Kajzar F, Mysliwiec J. Synthesis and nonlinear optical properties of push-pull type stilbene and pyrazoline based chromophores. Dyes Pigments 2017; 142: 507-515. https://doi.org/10.1016/j.dyepig.2017.04.009.
(h) Kulyk B, Taboukhat S, Akdas-Kilig H, Fillaut J-L, Karpierz M, Sahraoui B. Tuning the nonlinear optical properties of BODIPYs by functionalization with dimethylaminostyryl substituents. Dyes Pigments 2017; 137:507-511. https://doi.org/10.1016/j.dyepig.2016.10.045
(i) Spiridon MC, Iliopoulos K, Jerca FA, Jerca VV, Vuluga DM, Vasilescu DS, Gindre D, Sahraoui B. Novel pendant azobenzene/polymer systems for second harmonic generation and optical data storage. Dyes Pigments 2015; 114:2-32. https://doi.org/10.1016/j.dyepig.2014.10.010

[2] (a) Yang X, Lin X, Zhao YS, Yan D. Recent Advances in Micro- /Nanostructured Metal–Organic Frameworks towards Photonic and Electronic Applications. Chem. Eur. J. 2018; 24: 6484-6493. https://doi.org/10.1002/chem.201704650.
(b) Xin H, Ge C, Jiao X, Yang X, Rundel K, McNeill CR, Gao X. Incorporation of 2,6-Connected Azulene Units into the Backbone of Conjugated Polymers: Towards High-Performance Organic Optoelectronic Materials. Angew. Chem. Int. Ed. 2018; 57: 1322-1326. https://doi.org/10.1002/anie.201711802.
(c) Kalinin AA, Smirnov MA, Islamova LN, Fazleeva GM, Vakhonina TA, Levitskaya AI, Fominykh OD, Ivanova NV, Khamatgalimov AR, Nizameev IR, Balakina MY. Synthesis and characterization of new second-order NLO chromophores containing the isomeric indolizine moiety for electro-optical materials. Dyes Pigments 2017; 147: 444-454. https://doi.org/10.1016/j.dyepig.2017.08.047.
(d) Ostroverkhova O. Organic Optoelectronic Materials: Mechanisms and Applications. Chem. Rev. 2016; 116: 13279- 13412. https://doi.org/10.1021/acs.chemrev.6b00127.
(e) Dalton LR, Sullivan PA, Bale DH. Electric Field Poled Organic Electro-optic Materials: State of the Art and Future Prospects. Chem. Rev. 2010; 110: 25-55. https://doi.org/10.1021/cr9000429.

[3] (a) Yu S, Wu X, Wang Y, Guo X, Tong L. 2D Materials for Optical Modulation: Challenges and Opportunities. Adv. Mater. 2017; 29: 1606128. https://doi.org/10.1002/adma.201606128.
(b) Hales JM, Barlow S, Kim H, Mukhopadhyay S, Bredas J, Perry JW, Marder SR. Design of Organic Chromophores for All-Optical Signal Processing Applications. Chem. Mater. 2014; 26; 549-560. https://doi.org/10.1021/cm402893s.

(c) Gieseking RL, Mukhopadhyay S, Risko C, Marder SR, Bredas J. 25th Anniversary Article: Design of Polymethine Dyes for All- Optical Switching Applications: Guidance from Theoretical and Computational Studies. Adv. Mater. 2014; 26: 68-84.
https://doi.org/10.1002/adma.201302676.
(d) He GS, Zhu J, Baev A, Samoc M, Frattarelli DL, Watanabe N, Facchetti A, Agren H, Marks TJ, Prasad PN. Twisted π-System Chromophores for All-Optical Switching. J. Am. Chem. Soc. 2011; 133: 6675-6680.
https://doi.org/10.1021/ja1113112.

[4] (a) Fu Q, Zhu R, Song J, Yang H, Chen X. Photoacoustic Imaging: Contrast Agents and Their Biomedical Applications. Adv. Mater. 2019; 31: 1805875.
https://doi.org/10.1002/adma.201805875.
(b) Mei J, Huang Y, Tian H. Progress and Trends in AIE-Based Bioprobes: A Brief Overview. ACS Appl. Mater. Interfaces 2018; 10: 12217-12261.
https://doi.org/10.1021/acsami.7b14343.
(c) Klymchenko AS. Solvatochromic and Fluorogenic Dyes as Environment-Sensitive Probes: Design and Biological Applications. Acc. Chem. Res. 2017; 50: 366-375.
https://doi.org/10.1021/acs.accounts.6b00517.
(d) Qi J, Qiao W, Wang ZY. Advances in Organic Near- Infrared Materials and Emerging Applications. Chem. Rec. 2016; 16: 1531-1548.
https://doi.org/10.1002/tcr.201600013.

[5] (a) Ding L, Ou Y, Sun A, Li H, Wu T, Zhang D, Xu P, Zhao R, Zhu L, Wang R, Xu B, Hua Y. Developing D-π-D hole-transport materials for perovskite solar cells: The effect of π-bridge on device performance. Mater. Chem. Front. 2021; 5: 876-884.
https://doi.org/10.1039/D0QM00719F.
(b) Chen F. Emerging Organic and Organic/Inorganic Hybrid Photovoltaic Devices for Specialty Applications: Low- Level- Lighting Energy Conversion and Biomedical Treatment. Adv. Opt. Mater. 2019; 7: 1800662 (24p).
https://doi.org/10.1002/adom.201800662.
(c) Benesperi I, Michaels H, Freitag M. The researcher's guide to solid-state dye-sensitized solar cells. J. Mater. Chem. C 2018; 6: 11903-11942.
https://doi.org/10.1039/C8TC03542C.
(d) Prachumrak N, Sudyoadsuk T, Thangthong A, Nalaoh P, Jungsuttiwong S, Daengngern R, Namuangruk S, Pattanasattayavong P, Promarak V. Improvement of D–π–A organic dye-based dye-sensitized solar cell performance by simple triphenylamine donor substitutions on the π-linker of the dye. Mater. Chem. Front. 2017; 1: 1059-1072.
https://doi.org/10.1039/C6QM00271D.
(e) Eom YK, Kang SH, Choi IT, Yoo Y, Kim J, Kim HK. Significant light absorption enhancement by a single heterocyclic unit change in the π-bridge moiety from thieno[3,2-b]benzothiophene to thieno[3,2-b]indole for high performance dye-sensitized and tandem solar cells. J. Mater. Chem. A 2017; 5: 2297-2308.
https://doi.org/10.1039/C6TA09836C.
(f) Lee CP, Lin RY, Lin L, Li C, Chu T, Sun S, Lin JT, Ho K. Recent progress in organic sensitizers for dye-sensitized solar cells. RSC Adv. 2015; 5: 23810-23825.
https://doi.org/10.1039/C4RA16493H.
(g) Malytskyi V, Simon J, Patrone L, Raimundo J. Thiophene-based push–pull chromophores for small molecule organic solar cells (SMOSCs). RSC Adv. 2015; 5: 354-397.
https://doi.org/10.1039/C4RA11664J.

[6] (a) Beharry AA. Next-Generation Photodynamic Therapy: New Probes for Cancer Imaging and Treatment. Biochemistry 2018; 57: 173-174.
https://doi.org/10.1021/acs.biochem.7b01037.
(b) Zhao J, Chen K, Hou Y, Che Y, Liu L, Jia D. Recent progress in heavy atom-free organic compounds showing unexpected intersystem crossing (ISC) ability. Org. Biomol. Chem. 2018; 16: 3692-3701.
https://doi.org/10.1039/C8OB00421H.
(c) Lucky SS, Soo KC, Zhang Y, Nanoparticles in Photodynamic Therapy. Chem Rev. 2015; 115: 1990-2042.
https://doi.org/10.1021/cr5004198.
(d) Ji S, Ge J, Escudero D, Wang Z, Zhao J, Jacquemin D. Molecular Structure–Intersystem Crossing Relationship of Heavy-Atom-Free BODIPY Triplet Photosensitizers. J. Org. Chem. 2015; 80: 5958-5963.
https://doi.org/10.1021/acs.joc.5b00691.

[7] (a) Wu K, Pan S. A review on structure-performance relationship toward the optimal design of infrared nonlinear optical materials with balanced performances. Coord. Chem. Rev. 2018; 377: 191-208.
https://doi.org/10.1016/j.ccr.2018.09.002.
(b) Lv X, Li W, Ouyang M, Zhang Y, Wright DS, Zhang C. Polymeric electrochromic materials with donor–acceptor structures. J. Mater. Chem. C 2017; 5: 12-28.
https://doi.org/10.1039/C6TC04002K.
(c) Ok KM. Toward the Rational Design of Novel Noncentrosymmetric Materials: Factors Influencing the Framework Structures. Acc. Chem. Res. 2016; 49: 2774-2785.
https://doi.org/10.1021/acs.accounts.6b00452.

(d) Wu J, Wilson BA, Smith DW, Nielsen SO. Towards an understanding of structure-nonlinearity relationships in triarylamine-based push-pull electro-optic chromophores: the influence of substituent and molecular conformation on molecular hyperpolarizabilities. J. Mater. Chem. C 2014; 2: 2591-2599. https://doi.org/10.1039/C3TC32510E.

[8] (a) Wang L, Ye JT, Wang H, Xie H, Qiu Y. Self-Assembled Donor–Acceptor Chromophores: Evident Layer Effect on the First Hyperpolarizability and Two-Dimensional Charge Transfer Character. J. Phys. Chem. C 2017; 121: 21616-21626. https://doi.org/10.1021/acs.jpcc.7b07053.

(b) Vijayalakshmi S, Kalyanaraman S. Role of charge transfer on the nonlinear optical properties of donor-π- acceptor (D- π- a) conjugated schiffbases with DFT approach. J. Phys. Org. Chem. 2016; 29: 436-442. https://doi.org/10.1002/poc.3556.

(c) List NH, Zalesny R, Murugan NA, Kongsted J, Bartkowiak W, Aagren H. Relation between Nonlinear Optical Properties of Push–Pull Molecules and Metric of Charge Transfer Excitations. J. Chem. Theory Comput. 2015; 11: 4182-4188. https://doi.org/10.1021/acs.jctc.5b00538.

(d) Mallia AR, Salini PS, Hariharan M. Nonparallel Stacks of Donor and Acceptor Chromophores Evade Geminate Charge Recombination. J. Am. Chem. Soc. 2015; 137: 15604-15607. https://doi.org/10.1021/jacs.5b08257.

[9] (a) Xu H, Zhou Z, Wang J, Zhang X, Li Z, Deng G, Liu F. Synthesis, characterization and comparative studies of nonlinear optical chromophores with rod-like, Y-shaped and X-shaped configurations. Dyes Pigments 2019; 164: 54-61. https://doi.org/10.1016/j.dyepig.2019.01.008.

(b) Chen P, Zhang H, Han M, Cheng Z, Peng Q, Li Q, Li Z. Janus molecules: large second-order nonlinear optical performance, good temporal stability, excellent thermal stability and spherical structure with optimized dendrimer structure. Mater. Chem. Front. 2018; 2: 1374-1382. https://doi.org/10.1039/C8QM00128F.

(c) Hu C, Chen Z, Xiao H, Zhen Z, Liu X, Bo S. Synthesis and characterization of a novel indoline based nonlinear optical chromophore with excellent electro-optic activity and high thermal stability by modifying the π-conjugated bridges. J. Mater. Chem. C 2017; 5: 5111-5118. DOI https://doi.org/10.1039/C7TC00735C.

(d) Yang Y, Liu J, Xiao H, Zhen Z, Bo S. The important role of the isolation group (TBDPS) in designing efficient organic nonlinear optical FTC type chromophores, Dyes Pigments 2017; 139: 239-246. https://doi.org/10.1016/j.dyepig.2016.12.003.

(e) Chen P, Yin X, Xie Y, Li S, Luo S, Zeng H, Guo G, Li Q, Li Z. FTC-containing molecules: large second-order nonlinear optical performance and excellent thermal stability, and the key development of the "Isolation Chromophore" concept. J. Mater. Chem. C 2016; 4: 11474-11481. https://doi.org/10.1039/C6TC04282A.

[10] Bures F. Fundamental aspects of property tuning in push–pull molecules. RSC Adv. 2014; 4: 58826-58851. https://doi.org/10.1039/C4RA11264D.

[11] (a) Sulatskaya AI, Sulatsky MI, Povarova OI, Rodina NP, Kuznetsova IM, Lugovskii AA, Voropay ES, Lavysh AV, Maskevich AA, Turoverov KK. Trans-2-[4-(dimethylamino) styryl]-3-ethyl-1,3-benzothiazolium perchlorate - New fluorescent dye for testing of amyloid fibrils and study of their structure. Dyes Pigments. 2018; 157: 385-395. https://doi.org/10.1016/j.dyepig.2018.05.006.

(b) Wen L, Fang Y, Yang J, Han Y, Song Y. Third-order nonlinear optical properties and ultrafast excited-state dynamics of benzothiazolium salts: Transition in absorption and refraction under different time regimes. Dyes Pigments 2018; 156: 26-32. https://doi.org/10.1016/j.dyepig.2018.03.065.

(c) Cigan M, Gaplovsky A, Sigmundova I, Zahradnik P, Dedic R, Hromadova M. Photostability of D–π–A nonlinear optical chromophores containing a benzothiazolium acceptor. J. Phys. Org. Chem. 2011; 24: 450-459. https://doi.org/10.1002/poc.1782.

(d) Coe BJ, Harris JA, Hall JJ, Brunschwig BS, Hung S, Libaers W, Clays K, Coles SJ, Horton PN, Light ME, Hursthouse MB, Garin J, Orduna J. Syntheses and Quadratic Nonlinear Optical Properties of Salts Containing Benzothiazolium Electron-Acceptor Groups. Chem. Mater. 2006; 18: 5907-5918. https://doi.org/10.1021/cm061594t.

[12] (a) Tang Y, Liu H, Zhang H, Li D, Su J, Zhang S, Zhou H, Li S, Wu J, Tian Y. A series of stilbazolium salts with A-π-A model and their third-order nonlinear optical response in the near-IR region. Spectrochim. Acta Part A 2017; 175: 92-99. https://doi.org/10.1016/j.saa.2016.12.017.

(b) Bures F, Cvejn D, Melanova K, Benes L, Svoboda J, Zima V, Pytela O, Mikysek T, Ruzickova Z, Kityk IV, Wojciechowski A, AlZayed N. Effect of intercalation and chromophore arrangement on the linear and nonlinear optical properties of model aminopyridine push–pull molecules. J. Mater. Chem. C 2016; 4: 468-478. https://doi.org/10.1039/C5TC03499J.

(c) Hao WH, Yan P, Li G, Wang ZY. Short-conjugated zwitterionic cyanopyridinium chromophores: Synthesis, crystal structure, and linear/nonlinear optical properties. Dyes Pigments 2014; 111: 145-155. https://doi.org/10.1016/j.dyepig.2014.06.005.

(d) Li L, Cui H, Yang Z, Tao X, Lin X, Ye N, Yang H. Synthesis and characterization of thienyl-substituted pyridinium salts for second-order nonlinear optics. CrystEngComm 2012; 14: 1031-1037. https://doi.org/10.1039/C1CE06177A.
(d) Coe BJ, Fielden J, Foxon SP, Harris JA, Helliwell M, Brunschwig BS, Asselberghs I, Clays K, Garin J, Orduna J. Diquat Derivatives: Highly Active, Two-Dimensional Nonlinear Optical Chromophores with Potential Redox Switchability. J. Am. Chem. Soc. 2010; 132: 10498-10512. https://doi.org/10.1021/ja103289a.
(e) Coe BJ, Harper CE, Clays K, Franz E. The synthesis of chiral, cationic nonlinear optical dyes based on the 1,1′-binaphthalenyl unit. Dyes Pigments 2010; 87: 22-29. https://doi.org/10.1016/j.dyepig.2010.01.018.
[13] (a) Somma C, Folpini G, Gupta J, Reimann K, Woerner M, Elsaesser T. Ultra-broadband terahertz pulses generated in the organic crystal DSTMS, Opt Lett 2015; 40: 3404-3407. https://doi.org/10.1364/OL.40.003404.
(b) Teng B, Wang S, Feng K, Cao L, Zhong D, You F, Jiang X, Hao L, Sun Q. Crystal growth, quality characterization and THz properties of DAST crystals. Cryst. Res. Technol. 2014; 49: 943-947. https://doi.org/10.1002/crat.201400147.
[14] (a) Jeong C, Kang BJ, Lee S, Lee S, Kim WT, Jazbinsek M, Yoon W, Yun H, Kim D, Rotermund F, Kwon O. Yellow- Colored Electro- Optic Crystals as Intense Terahertz Wave Sources. Adv. Funct. Mater. 2018; 28: 1801143. https://doi.org/10.1002/adfm.201801143.
(b) Lee S, Kang BJ, Shin M, Lee S, Lee S, Jazbinsek M, Yun H, Kim D, Rotermund F, Kwon O. Efficient Optical- to- THz Conversion Organic Crystals with Simultaneous Electron Withdrawing and Donating Halogen Substituents. Adv. Opt. Mater. 2017; 6; 1700930 (12p). https://doi.org/10.1002/adom.201700930.
(c) Dhillon SS, Vitiello MS, Linfield EH, Davies AG, Hoffmann MC, Booske J, Paoloni C et al. The 2017 terahertz science and technology roadmap. J. Phys. D: Appl. Phys. 2017; 50: 043001 (49p). https://doi.org/10.1088/1361-6463/50/4/043001.
[15] (a) Huang J, Yang Z, Murugesan V, Walter E. Spatially Constrained Organic Diquat Anolyte for Stable Aqueous Flow Batteries. ACS Energy Letters 2018; 3: 2533-2538. https://doi.org/10.1021/acsenergylett.8b01550.
(b) Yang NN, Fang JJ, Sui Q, Gao EQ. Incorporating Electron-Deficient Bipyridinium Chromorphores to Make Multiresponsive Metal–organic Frameworks. ACS Appl. Mater. Interfaces 2018; 10: 2735-2744. https://doi.org/10.1021/acsami.7b17381.
(c) Buckley LE, Coe BJ, Rusanova D, Sanchez S, Jirasek M. Joshi VD, Vavra J, Khobragade D, Pospisil L, Ramesova S, Cisarova I, Saman D, Pohl R, Clays K, Van Steerteghem N, Brunschwig BS, Teply F. Ferrocenyl helquats: unusual chiral organometallic nonlinear optical chromophores, Dalton Trans. 2017; 46: 1052-1064. https://doi.org/10.1039/C6DT04347J.
(d) Coe BJ, Rusanova D, Joshi VD, Sanchez S, Vavra J, Khobragade D, Severa L, Cisarova I, Saman D, Pohl R, Clays K, Depotter G, Brunschwig BS, Teply F. Helquat Dyes: Helicene-like Push–Pull Systems with Large Second-Order Nonlinear Optical Responses. J. Org. Chem. 2016; 81: 1912-1920. https://doi.org/10.1021/acs.joc.5b02692.
[16] Sucunza D, Cuadro AM, Alvarez-Builla J, Vaquero JJ. Recent Advances in the Synthesis of Azonia Aromatic Heterocycles. J. Org. Chem. 2016; 81: 10126-10135. https://doi.org/10.1021/acs.joc.6b01092.
[17] (a) Marcelo G, Pinto S, Caneque T, Mariz IFA, Cuadro AM, Vaquero JJ, Martinho JMG, Maçôas E. Nonlinear Emission of Quinolizinium-Based Dyes with Application in Fluorescence Lifetime Imaging. J. Phys. Chem. A 2015; 119: 2351-2362. https://doi.org/10.1021/jp507095b.
(b) Maçôas E, Marcelo G, Pinto S, Cañeque T, Cuadro AM, Vaquero JJ, Martinho JMG. A V-shaped cationic dye for nonlinear optical bioimaging. Chem. Commun. 2011; 47: 7374-7376. https://doi.org/10.1039/C1CC12163D.
(c) Caneque T, Cuadro AM, Alvarez-Builla J, Perez-Moreno J, Clays K, Castano O, Andres JL, Vaquero JJ. Novel charged NLO chromophores based on quinolizinium acceptor units. Dyes Pigments 2014; 101: 116-121. https://doi.org/10.1016/j.dyepig.2013.09.031.
[18] (a) Zacharioudakis E, Caneque T, Custodio R, Muller S, Cuadro AM, Vaquero JJ, Rodriguez R. Quinolizinium as a new fluorescent lysosomotropic probe. Bioorg. Med. Chem. Lett. 2017; 27: 203-207. https://doi.org/10.1016/j.bmcl.2016.11.074.
(b) Suarez RM, Bosch P, Sucunza D, Cuadro AM, Domingo A, Mendicuti F, Vaquero JJ. Targeting DNA with small molecules: a comparative study of a library of azonia aromatic chromophores. Org. Biomol. Chem. 2015; 13: 527-538. https://doi.org/10.1039/C4OB01465K.
(c) Mariz IFA, Pinto SN, Santiago AM, Martinho JMG, Recio J, Vaquero JJ, Cuadro AM, Maçôas E. Two-photon activated precision molecular photosensitizer targeting mitocondria, Commun. Chem. 2021; 4: 142. https://doi.org/10.1038/s42004-021-00581-4.
[19] (a) Cañeque T, Cuadro AM, Custodio R, Alvarez-Builla J, Batanero B, Gómez-Sal P, Pérez-Moreno J, Clays K, Castaño O, Andrés JL, Carmona T, Mendicuti F, Vaquero JJ. Azonia aromatic heterocycles as

a new acceptor unit in D-π-A+ vs D-A+ nonlinear optical chromophores. Dyes Pigments 2017; 144: 17-31.
https://doi.org/10.1016/j.dyepig.2017.05.005.
(b) Ramirez MA, Custodio R, Cuadro AM, Alvarez-Builla J, Clays K, Asselberghs I, Mendicuti F, Castaño O, Andrés JL, Vaquero JJ. Synthesis of charged bis-heteroaryl donor–acceptor (D–A+) NLO-phores coupling (π-deficient–π-excessive) hetero aromatic rings. Org Biomol Chem. 2013; 11: 7145-7154.
https://doi.org/10.1039/C3OB41159A
(c) Ramirez MA, Cuadro AM, Alvarez-Builla J, Castano O, Andres JL, Mendicuti F, Clays K, Asselbergh I, Vaquero JJ. Donor-(π-bridge)-azinium as D-π-A+ one-dimensional and D-π-A+-π-D multidimensional V-shaped chromophores, Biomol Chem. 2012; 10: 1659-1669.
https://doi.org/10.1039/C2OB06427H.
(d) M. A. Ramirez, T. Caneque, A. M. Cuadro, F. Mendicuti, K. Clays ,I. Asselbergh and J. J. Vaquero, Novel linear and V-shaped D-pi-A+-pi-D chromophores by Sonogashira reaction, *ARKIVOC*. 2011, 140-155.
(e) Caneque T, Cuadro AM, Alvarez-Builla J, Perez-Moreno J, Clays K, Marcelo G, Mendicuti F, Castaño O, Andrés JL, Vaquero JJ. Heteroaromatic Cation- Based Chromophores: Synthesis and Nonlinear Optical Properties of Alkynylazinium Salts. Eur. J. Org. Chem. 2010; 33: 6323-6330.
https://doi.org/10.1002/ejoc.201000816.
[20] (a) Chen X, Zhang N, Cai L, Li P, Wang M, Guo G. N- Methyl- 4- pyridinium Tetrazolate Zwitterion-Based Photochromic Materials. Chem. Eur. J. 2017; 23: 7414-7417.
https://doi.org/10.1002/chem.201700677.
(b) Beverina L, Sanguineti A, Battagliarin G, Ruffo R, Roberto D, Righetto S, Soave R, Lo Presti L, Ugo R Pagani G. A. UV absorbing zwitterionic pyridinium-tetrazolate: exceptional transparency/optical nonlinearity trade-off. Chem. Commun. 2011; 47: 292-294.
https://doi.org/10.1039/C0CC01652G.
(c) Marder SR. Themed issue: nonlinear optics. The evolving field of nonlinear optics—a personal perspective. J. Mater. Chem. 2009; 19: 7392-7393.
https://doi.org/10.1039/B916810A.
(d) Nerenz H, Meier M, Grahn W, Reisner A, Schmälzlin E, Stadler S, Meerholtz K, Bräuchle C, Jones PG. Nonlinear optical chromophores with isoquinolines, thieno[2,3-c]-pyridines and 2-(2'-thienyl)pyridines as inherently polarized π-electron bridges. J. Chem. Soc., Perkin Trans. 2 1998; 2: 437–448.
https://doi.org/10.1039/A703325G.
[21] (a) Jeong JH, Kim J, Campo J, Lee SH, Jeon WY, Wenseleers W, Jazbinsek M, Yun H, Kwon OP. N-Methyl quinolinium derivatives for photonic applications: Enhancement of electron-withdrawing character beyond that of the widely-used N-methylpyridinium. Dyes Pigments 2015; 113: 8-17.
https://doi.org/10.1016/j.dyepig.2014.07.016.
(b) Lee SH, Jazbinsek M, Yun H, Kim JT, Lee YS, Kwon OP. New quiolinium polymorph with optimal packing for maximal off-diagonal nonlinear optical response. Dyes Pigments 2013; 96: 435-439.
https://doi.org/10.1016/j.dyepig.2012.08.022
(c) Coe BJ, Beljonne D, Vogel H, Garin J, Orduna J. Theoretical Analyses of the Effects on the Linear and Quadratic Nonlinear Optical Properties of N-Arylation of Pyridinium Groups in Stilbazolium Dyes. J. Phys. Chem. A. 2005; 109: 10052-10057.
https://doi.org/10.1021/jp053721z.
[22] (a) Hrobarik P, Sigmundova I, Zahradnik P, Kasak P, Arion V, Franz E, Clays K. Molecular Engineering of Benzothiazolium Salts with Large Quadratic Hyperpolarizabilities: Can Auxiliary Electron-Withdrawing Groups Enhance Nonlinear Optical Responses? J. Phys. Chem. C. 2010; 114: 22289-22302.
https://doi.org/10.1021/jp108623d.
(b) Quist F, Vande Velde CML, Didier D, Teshome A, Asselberghs I, Clays K, Sergeyev S. Push–pull chromophores comprising benzothiazolium acceptor and thiophene auxiliary donor moieties: Synthesis, structure, linear and quadratic nonlinear optical properties. Dyes Pigments 2009; 81: 203-210.
https://doi.org/10.1016/j.dyepig.2008.10.004.
(c) Coe BJ, Harris JA, Hall JJ, Brunschwig BS, Hung S, Libaers W, Clays K, Coles SJ, Horton PN, Light ME, Hursthouse MB, Garin J, Orduna J. Syntheses and Quadratic Nonlinear Optical Properties of Salts Containing Benzothiazolium Electron-Acceptor Groups. Chem. Mater. 2006; 18: 5907-5918.
https://doi.org/10.1021/cm061594t.
[23] (a) Cheng Q, Shi X, Li C, Jiang Y, Shi Z, Zou J, Wang X, Wang X, Cui Z. Chromophores with side isolate groups and applications in improving the poling efficiency of second nonlinear optical (NLO) materials. Dyes Pigments 2019; 162: 721-727.
https://doi.org/10.1016/j.dyepig.2018.11.001.
(b) Li M, Li Y, Zhang H, Wang S, Ao Y, Cui Z. Molecular engineering of organic chromophores and polymers for enhanced bulk second-order optical nonlinearity. J. Mater. Chem. C 2017; 5: 4111-4122.
https://doi.org/10.1039/C7TC00713B.
(c) Jia J, Li Y, Gao J. A series of novel ferrocenyl derivatives: Schiff bases-like push-pull systems with large third-order optical responses. Dyes Pigments 2017; 137: 342-351.
https://doi.org/10.1016/j.dyepig.2016.11.008.

(d) Zhang X, Yu G, Huang X, Chen W. Introducing the triangular BN nanodot or its cooperation with the edge-modification via the electron-donating/withdrawing group to achieve the large first hyperpolarizability in a carbon nanotube system. Phys. Chem. Chem. Phys. 2017; 19: 17834-17844. https://doi.org/10.1039/C7CP02327H.
(e) Ziemann EA, Freudenreich N, Speil N, Stein T, Van Steerteghem N, Clays K, Heck J. Synthesis, structure and NLO properties of a 1,3,5-substituted tricationic cobaltocenium benzene complex. J. Organomet Chem. 2016; 820: 125-129. https://doi.org/10.1016/j.jorganchem.2016.07.021
(f) Yang Y, Wang H, Liu F, Yang D, Bo S, Qiu L, Zhen Z, Liu X. The synthesis of new double-donor chromophores with excellent electro-optic activity by introducing modified bridges. Phys. Chem. Chem. Phys. 2015; 17: 5776-5784. https://doi.org/10.1039/C4CP05829A.
(g) Zhang Y, Blau WJ. Dipoles align inside a nanotube. Nat. Nanotechnol. 2015; 10: 205-206. https://doi.org/10.1038/nnano.2015.9.
(h) Beverina L, Pagani GA. π-Conjugated Zwitterions as Paradigm of Donor–Acceptor Building Blocks in Organic-Based Materials. Acc. Chem. Res. 2014; 47: 319-329. https://doi.org/10.1021/ar4000967.
[24] For Stille reaction see: (a) Heravi MM, Mohammadkhani L. Recent applications of Stille reaction in total synthesis of natural products: An update. J. Organomet. Chem. 2018; 869: 106-200. https://doi.org/10.1016/j.jorganchem.2018.05.018.
(b) Cordovilla C, Bartolome C, Martinez-Ilarduya JM, Espinet P, The Stille Reaction, 38 Years Later. ACS Catal. 2015; 5: 3040-3053. https://doi.org/10.1021/acscatal.5b00448.
[25] (a) Cañeque T, Cuadro AM, Alvarez-Builla J, Vaquero JJ, Efficient functionalization of quinolizinium cations with organotrifluorobrates in water. Tetrahedron Lett. 2009; 50: 1419-1422. https://doi.org/10.1016/j.tetlet.2009.01.040.
(b) Nuñez A, Abarca B, Cuadro AM, Alvarez-Builla J, Vaquero JJ. Ring-Closing Metathesis Reactions on Azinium Salts: Straightforward Access to Quinolizinium Cations and Their Dihydro Derivatives. J. Org. Chem. 2009; 74: 4166-4176. https://doi.org/10.1021/jo900292b.
(c) Nuñez A, Cuadro AM, Alvarez-Builla J, Vaquero JJ. A New Approach to Polycyclic Azonia Cations by Ring-Closing Metathesis. Org. Lett. 2007; 9: 2977-2980. https://doi.org/10.1021/ol070773t.
(d) García-Cuadrado D, Cuadro AM, Barchín BM, Nuñez A, Cañeque T, Alvarez-Builla J, Vaquero JJ. Palladium-Mediated Functionaliza tion of Heteroaromatic Cations: Comparative Study on Quinolizinium Cation. J. Org. Chem. 2006; 71: 7989-7995. https://doi.org/10.1021/jo060634+.
(e) García-Cuadrado D, Cuadro AM, Alvarez-Builla J, Sancho U, Castaño O, Vaquero JJ. First Synthesis of Biquinolizinium Salts: Novel Example of a Chiral Azonia Dication. *Org. Lett.* 2006; **8**: 5955-5958. https://doi.org/10.1021/ol062314i.
(f) Garcia-Cuadrado D, Cuadro AM, Alvarez-Builla J, Vaquero JJ. Sonogashira Reaction on Quinolizium Cations. Org. Lett. 2004; 6: 4175-4178. https://doi.org/10.1021/ol048368e.
[26] (a) Liu C, Zhai J, Ma Y, Liang Y. A Simple Way for the Preparation of 3-Ferrocenyl-6,8-disubstituted Quinoline. Synth. Commun. 1998; 28: 2731-2735. https://doi.org/10.1080/00397919808004844.
(b) Liu CM, Chen BH, Liu WY, Wu XL, Ma YX. Conversion of tributylstannylferrocene to a variety of heteroaryl ferrocenes. J. Organomet. Chem. 2000; 598: 348-352. https://doi.org/10.1016/S0022-328X(99)00733-0.
[27] Misra R, Bhattachraryya SP , Intramolecular Charge Transfer (ICT): Theory and Applications. 2018 Wiley- VCH Verlag GmbH & Co. KGaA.
[28] Brouver AM. Standards for photoluminescence quantum yield measurements in solution (IUPAC Technical Report). Pure Appl. Chem. 2011; 83: 2213-2228. https://doi.org/10.1351/PAC-REP-10-09-31.
[29] Toriumi N, Asano N, Miyamoto K, Muranaka A, Uchiyama M. Alkynylpyridinium Salts: Highly Electrophilic Alkyne–Pyridine Conjugates as Precursors of Cationic Nitrogen-Embedded Polycyclic Aromatic Hydrocarbons. J. Am. Chem. Soc. 2018; 140: 3858−3862. https://doi.org/10.1021/jacs.8b00356.
[30] D'Andrade BW, Datta S, Forrest SR, Djurovich P, Polikarpov E, Thompson ME. Relationship between the ionization and oxidation potentials of molecular organic semiconductors. Org. Electron. 2005; 6: 11-20. https://doi.org/10.1016/j.orgel.2005.01.002.
[31]Okamoto K, Chiba K. Electrochemical Total Synthesis of Pyrrolophenanthridone Alkaloids: Controlling the Anodically Initiated Electron Transfer Process, Organic Letters 2020; 22: 3613-3617. https://doi.org/10.1021/acs.orglett.0c01082.
[32] Kumar J, Kumar N, Kumar P. Hota, Optical properties of 3-substituted índoles. RSC Adv. 2020; 10: 28213-28224. https://doi.org/10.1039/D0RA05405D.

[33] **Gaussian 09**, Revision A.1, Frisch MJ, Trucks GW, Schlegel HB, Scuseria GE, Robb MA, Cheeseman JR, Scalmani G, Barone V, Mennucci B, Petersson GA, Nakatsuji H, Caricato M, Li X, Normand HPJ, Raghavachari K, Rendell A, Burant JC, Iyengar SS, Tomasi J, Cossi M, Rega N, Millam JM, Klene M, Knox JE, Cross JB, Bakken V, Adamo C, Jaramillo J, Gomperts R, Stratmann RE, Yazyev O, Austin AJ, Cammi R, Pomelli C, Ochterski JW, Martin RL, Morokuma K, Zakrzewski VG, Voth GA, Salvador P, Dannenberg JJ, Dapprich S, Daniels AD, Farkas Ö, Foresman JB, Ortiz JV, Cioslowski J, Fox DJ. Gaussian, Inc., Wallingford CT, 2009.

[34] Bredas JL. Mind the gap! Mater. Horiz. 2014; 1: 17–19. https://doi.org/10.1039/C3MH00098B.